EFFECTS OF DIFFERENT CURING METHODS AND AGGREGATE SALT TREATMENT ON CONCRETE FREEZE-THAW DURABILITY AND HOW THESE METHODS CAN BE USED TO ACCELERATE KDOT AGGREGATE QUALIFICATION PROCEDURES

by

CALE ARMSTRONG

B.S., Kansas State University, 2014

A THESIS

submitted in partial fulfillment of the requirements for the degree

MASTER OF SCIENCE IN CIVIL ENGINEERING

Department of Civil Engineering
College of Engineering

KANSAS STATE UNIVERSITY
Manhattan, Kansas

2016

Approved by:

Major Professor
Dr. Kyle Riding

Copyright

CALE ARMSTRONG

2016

Abstract

The Kansas Department of Transportation (KDOT) currently practices a six-month procedure for determining freeze-thaw durability of coarse aggregate intended for use in concrete pavement. In addition to the excessive amount of time required to conduct this procedure, the testing conditions fail to replicate the accelerated rate of concrete deterioration commonly caused by deicer salt exposure in freeze-thaw environments. An experimental study was conducted in an attempt to reduce the duration of this aggregate qualification procedure. Limestone course aggregates from different quarries were used to batch concrete specimens. These specimens were subjected to curing regimes of different durations before being exposed to repeated cycles of freezing and thawing. The effects of the curing methods on freeze-thaw durability were then investigated. Another segment of this study entailed the immersion of coarse aggregate in salt brine solution prior to concrete batching. Salt-treated and non-salt-treated specimens were subjected to two different methods of freeze-thaw cycling to determine if the presence of salt could differentiate between aggregates with high and low performance. This study found that shorter curing methods, along with adjusted performance requirements, could be used to develop a shorter aggregate qualification procedure. It also found that shorter periods of time in more severe freeze-thaw conditions produced comparable concrete durability results to those of the current test method. Salt treatment of aggregates could indicate a difference in performance of aggregates when exposed to salts in freeze-thaw conditions. It could also be useful in determining frost resistance of hardened cement paste.

Table of Contents

List of Figures

List of Tables

Acknowledgements

Chapter 1 - Introduction

1.1 Background

D-cracking has caused damage in several million dollars' worth of Kansas concrete pavements over the last 80 years. Between 1981 and 2000, approximately one-third of the state's concrete roadways exhibited D-cracking before reaching their 20-year service life (McLeod, Welge, & Henthorne, 2014). Limestone aggregates, which are commonly used in Kansas concrete pavements, generally have high susceptibility to D-cracking when subjected to repeated cycles of freezing and thawing. In order to mitigate this damage, the Kansas Department of Transportation (KDOT) follows a rigorous procedure to predict freeze-thaw performance in the field. This test method, known as KTMR-22, consists of a 21-day drying period as part of a 90-day concrete curing regime (KDOT, 2006). The drying period removes a significant amount of moisture that would normally cause damage during freezing (Riding, Blackwell, Momeni, & McLeod, 2013). The lower degree of saturation causes less deterioration during the three months of freeze-thaw cycling required by KTMR-22 than would be experienced at a higher degree of saturation. The combined durations of KTMR-22 curing and freeze-thaw testing yield a six-month aggregate qualification procedure.

An earlier study conducted by KDOT and Kansas State University (KSU) showed that some shorter curing regimes yielded freeze-thaw durability results that were comparable to or slightly more severe than those of the KTMR-22 curing method. These accelerated cure methods could be used to reduce the standard aggregate qualification procedure by at least two months (Riding et al., 2013).

1.2 Problem Statement

During the extensive six-month testing period required by KTMR-22, time constraints often lead to the use of large quantities of nondurable aggregate in concrete pavements. Additionally, the KTMR-22 testing environment does not fully represent the conditions experienced by in-service pavement. During the winter, Kansas roadways are exposed to high concentrations of deicing salt. These salts absorb water at low relative humidity levels and lose

moisture slowly during periods of drying. This yields a high degree of saturation and makes concrete and aggregate more susceptible to freeze-thaw damage (Spragg, et al., 2011).

1.3 Objectives

The primary objectives of this study were as follows:

- Determine if the standard 90-day curing period of KTMR-22 can be shortened by correlating its durability results with those of samples subjected to an accelerated cure method
- Determine if different combinations of aggregate salt treatment and freeze-thaw testing conditions can differentiate good from poor performing aggregates
- Determine if aggregate salt treatment in freeze-thaw specimens can be used to accelerate aggregate qualification procedures

1.4 Study Method

This study was divided into two phases. The first of which, denoted as the "accelerated cure study", consists of tasks developed to meet the first two listed objectives. For the accelerated cure study, KDOT provided KSU with limestone coarse aggregate from seven different sources. These aggregates were used to batch seven different concrete mixes. Three sets of prisms were cast for each mix and subjected to a different curing method. The first two sets underwent experimental 30-day curing methods. One of these sets was placed in a 100% moist room until 28 days. The second set was cured in a 100% moist room until 7 days followed by immersion in a saturated lime-water bath at 100°F for 21 days. KDOT's standard 90-day curing regime outlined in KTMR-22 was used for the third set of prisms as a benchmark test. This entailed 67 days in the 100% moist room followed by drying in a 73°F room at 50% relative humidity for 21 days (KDOT, 2006). Each curing regime ended with 24 hours of immersion in 70˚F water followed by 24 hours in 40 ˚F water. Upon completion of curing, all samples were subjected to cycles of freezing in air and thawing in water in accordance with ASTM C666 Procedure B (2008a). Durability was monitored through multiple measurements of each sample's mass, resonant transverse frequency, and expansion. The durability results of the two accelerated cure methods were then compared to those of the KTMR-22 method.

The second phase will be referred to as the "salt brine study". During the salt brine study, KDOT obtained twelve sets of limestone coarse aggregates. KDOT batched two concrete mixes

for each set; one contained aggregate treated with salt brine and the other did not. Prisms were cast for each mix and subsequently subjected to the KTMR-22 cure method. At some point during curing, half of the prisms from each mix were transferred to KSU where KTMR-22 curing continued until the end of the specified time period. KSU then tested these samples by subjecting them to freezing and thawing in water in accordance with ASTM C666 Procedure A (2008a). KDOT conducted Procedure B testing for the remaining half. The durability results of different combinations of aggregate salt treatment and freeze-thaw test procedure were compared.

Figure 1.1 illustrates the general organization of experimental procedures conducted for the accelerated cure and salt brine studies.
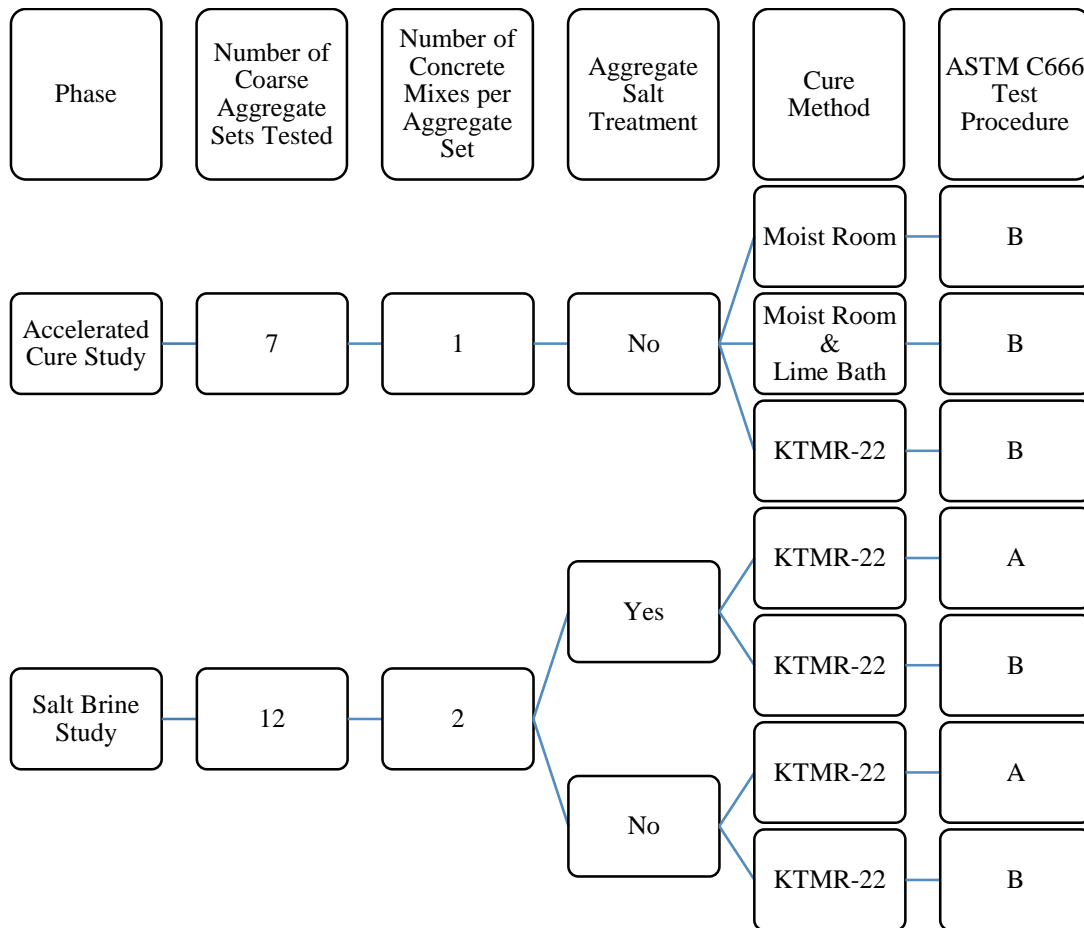
Figure 1.1: Experimental Method Flow Chart

1.5 Thesis Outline

Chapter 2 consists of a literature review with information regarding freeze-thaw damage in aggregates and concrete, standard procedures for identifying durable aggregates, and modified versions of standard curing and freeze-thaw testing methods. The materials used for concrete batching in the accelerated cure and salt brine studies are then discussed in Chapter 3. Chapter 4 provides detailed explanations of experimental methods that were followed in both studies. Chapters 5 and 6 summarize the results of the accelerated cure and salt brine studies, respectively. A discussion of all results is provided in Chapter 7, followed by conclusions and recommendations in Chapter 8.

Chapter 2 - Literature Review

2.1 D-Cracking of Coarse Aggregate

D-cracking is a distress that occurs in coarse aggregate subject to frequent cycles of freezing and thawing. The "D" in "D-cracking" has historically been referred to as "distress", "discoloration", "deterioration" (O'Doherty, 1987), "disintegration" (Whitehurst, 1980), and "durability" (Miller & Bellinger, 2003). This term has also been used to describe the geometry of concrete pieces separated by the cracks (O'Doherty, 1987). In general, D-cracking refers to a series of closely spaced cracks that run parallel to longitudinal and transverse joints as well as existing cracks in concrete. It also commonly runs along free edges of pavement slabs (Whitehurst, 1980).

2.1.1 Mechanism of D-Cracking

D-cracking occurs in the presence of moisture. Coarse aggregate in the concrete absorbs water and becomes susceptible to D-cracking if it reaches or exceeds its critical degree of saturation. A study conducted by the Michigan Department of Transportation suggests that the critical level occurs when approximately 91% of aggregate pores contain moisture since water expands an additional 10% of its original volume when it freezes (Vogler & Grove, 1989). Once all of the pore space is occupied, expansive internal pressures are induced within pore walls. Cracks form within the aggregate if the pore walls cannot adequately resist these expansive forces. These cracks can then propagate into the surrounding mortar (Schwartz, 1987), (Vogler & Grove, 1989).

2.1.2 Appearance and Progression of D-Cracking

D-cracking typically first appears in locations where water is initially absorbed in concrete pavement. In many cases, D-cracking will begin at the base of the pavement due to the availability of moisture in underlying soil. Under this condition, the slab may already have significant deterioration before cracks appear on the top surface (Schwartz, 1987). D-cracking can also begin where water infiltrates from multiple directions such as intersections of longitudinal and transverse joints, exterior slab faces and corners, and existing surface cracks. As concrete is subject to freeze-thaw cycles, a distinct, continuous network of D-cracks develops in these areas. Water also begins to saturate aggregates near the center or interior areas of the slab. D-cracking progresses into these locations as well (Whitehurst, 1980). It often takes five to ten years before D-cracking becomes

apparent (Janssen & Snyder, 1994). With some aggregates, it can take longer than ten years to appear. D-cracks that are visible on the pavement surface may appear different colors such as black, blue, white, or gray due to deposits of calcium carbonate and dirt (Schwartz, 1987).

2.1.3 Influential Conditions for D-Cracking

As discussed in Section 2.1.1, aggregates will be susceptible to D-cracking in environments where freezing and thawing occurs regularly and where moisture is available. More damage will occur in pavements under these conditions compared to those that exist in climates where the temperature stays below freezing most of the time. Concrete that undergoes occasional drying will also be less susceptible to D-cracking due to the removal of moisture which may create internal aggregate pressure during freezing (Schwartz, 1987).

Coarse aggregate composition, size, and pore structure can have significant influence on D-cracking resistance as well. Sedimentary materials such as limestone, dolomite, shale, sandstone, and greywacke have historically been associated with D-cracking (Schwartz, 1987). Argillaceous, or clayey, carbonate aggregates are also susceptible to freeze-thaw damage. Clay constituents typically have high absorption capacities which can increase an aggregate's degree of saturation. These aggregates have shown poor performance when 20-45% of their insoluble residues consist of silty clays. (Shakoor, West, & Scholer, 1982). A smaller maximum aggregate size has been found to improve freeze-thaw performance. The final report for a study conducted by researchers at PCA Laboratories suggests that water must travel a shorter distance within a smaller aggregate particle. Under this condition, water has a higher probability of escaping aggregate pores before excessive internal pressures develop during freezing. However, this idea also relies heavily on aggregate permeability. If an aggregate with low permeability becomes critically saturated and is subjected to freezing, minimal water expulsion will occur. Consequently, expansive pressures will develop and cracking may occur (Whitehurst, 1980). Low permeability combined with high porosity and small pore size further increases an aggregate's susceptibility to D-cracking (Schwartz, 1987).

2.1.4 Non-influential Factors

Multiple studies have found that varying quantities and compositions of fine aggregate and cement have little effect on D-cracking compared to coarse aggregate (Whitehurst, 1980), (Schwartz, 1987). The use of an air-entraining admixture protects the cement paste from

deterioration, but it does not significantly prevent damage to saturated coarse aggregate (Whitehurst, 1980). Traffic alone also has little effect on D-cracking in concrete pavement (Schwartz, 1987).

2.1.5 Prevention

The most effective way to prevent D-cracking in concrete pavement is to avoid using nondurable aggregates. Intrusive rocks such as granite, diorite, and gabbro are not typically associated with D-cracking. Some metamorphic rocks such as marble and quartzite are also known to provide freeze-thaw resistance (Stark, 1975). Most transportation organizations identify reliable aggregate sources through testing and field performance and will only use aggregate from these sources. In some cases, only certain ledges or beds of these quarries are used. Reducing the maximum size of coarse aggregate particles to 1" or ½" can improve freeze-thaw resistance as well (Schwartz, 1987). Kansas uses crushed aggregate sizes smaller than ¾" (KDOT, 2006).

It is difficult to minimize damage if D-cracking-susceptible aggregates are used. Blending poor-performing aggregates with durable ones can sometimes decrease the rate of deterioration. Removing harmful particles from nondurable aggregate by heavy media separation is another method that has been used. This process involves using heavy liquids to float off materials with low specific gravity. It has been effective in some cases, but specific gravity does not always correlate well with D-cracking. An efficient drainage system beneath pavement may also decrease the rate of deterioration (Schwartz, 1987).

2.2 Freeze-Thaw Resistance of Concrete

Concrete specimens with adequate freeze-thaw performance require more than just durable aggregate. A durable cement paste matrix is needed as well. The mechanisms of internal and surface damage to hardened cement paste are discussed in this section. The effects of characteristics such as air void structure, moisture content, and permeability on freeze-thaw durability of concrete are also discussed.

2.2.1 Mechanisms of Internal Frost Damage

Four widely accepted theories have been used to explain the source of freeze-thaw damage in concrete. Each of them discusses pressures developed by internal moisture, but with different insight on the direction in which the pressures act (Janssen & Snyder, 1994).

The hydraulic pressure theory was developed by Powers in 1945. It states that water is displaced within concrete pores due to advancing ice formation, and destructive stresses develop as a result. Water in critically saturated pores will be forced to flow in order to make room for increased ice volume. This level of saturation occurs when more than 86-88% of concrete pores are filled with water (Li, Pour-Ghaz, Castro, & Weiss, 2012). The magnitude of pressure developed depends on the rate of freezing, concrete permeability, and water viscosity (Janssen & Snyder, 1994).

Powers and Helmuth further developed the hydraulic pressure theory into the osmotic pressure theory in 1953. The osmotic pressure theory accounts for dilation and shrinkage of concrete specimens at constant temperatures. It also states that a concentrated alkali solution develops as ice is produced. Unfrozen water travels toward the freezing site due to differences in solute concentrations. This action is similar to the process of osmosis. (Janssen & Snyder, 1994).

The third theory, developed by Larson and Cady, is also similar to the hydraulic pressure theory. This theory states that concrete continues to dilate after the end of freezing. These dilations occur due to hydraulic pressures generated by an increase in specific volume of water during phase change (Janssen & Snyder, 1994).

In 1972, Litvan introduced the desorption theory. It states that as relative humidity decreases in aggregate pores, vapor differentials force water to expel from aggregate pores into concrete pores (Janssen & Snyder, 1994).

2.2.2 Surface Scaling

Concrete can also be subjected to more apparent damage in the form of surface scaling. Scaling is the loss of surface layers of cement mortar from concrete due to freezing and thawing (Afrani & Rogers, 1994). Scaling is more likely to occur when concrete freezes in water and it is often amplified by the presence of deicing chemicals (Pigeon, Pleau, & Aitcin, 1986). When deicer salt particles come into contact with water, the freezing point of the solution is lowered (Kimbrough, 2006). Therefore, an increase in amount of deicing chemicals corresponds to a reduction in ice formation pressures. However, chloride ions in deicing salts can become physically or chemically bound by cement hydration products and can cause concrete expansion (Zemei, Caijun, Peiwei, Wang, & Cao, 2015). These salts also lose moisture slowly during periods of drying. This yields a high degree of saturation and makes concrete and aggregate more

susceptible to freeze-thaw damage (Spragg, et al., 2011). Pieces of surface mortar may break off as a result of this damage. Due to the combination of positive and negative effects of deicing salts, low-to-medium concentrations (3-5% by mass) typically lead to the most deterioration (Zemei et al., 2015).

Scaling susceptibility can also be attributed to improper or excessive finishing of concrete. This leads to air loss in the surface layer (Zemei et al., 2015), which will remove space for water to expand during freezing. However, entrained air does not completely protect concrete against scaling in most cases (Pigeon et al., 1986). Zemei et al. (2015) also states that use of a low water-to-cement ratio and silica fume has demonstrated good scaling resistance.

2.2.3 Effect of Air Void Structure

The concrete air void structure plays an important role in resistance of freeze-thaw damage. As discussed in Section 2.2.1, frost damage to concrete can develop from different forms of hydraulic pressure induced by expanding ice. Concrete usually requires an air content between 4% and 8% by volume to adequately resist these pressures (Distlehorst & Kurgan, 2007). In most concrete mix designs, only air content is specified. However, air void size and distribution are just as influential on freeze-thaw resistance (Du & Folliard, 2005). Water must be able to efficiently migrate through concrete pores in order to prevent the development of excessive hydraulic pressures. To accommodate water migration, air voids should be small and closely spaced. The air void spacing factor is a good representation of air bubble geometry and configuration. This value can be determined by finding the average maximum distance from any point in the cement paste to the boundary of the nearest air void (Distlehorst & Kurgan, 2007). ASTM C457 (2012b) states that an ideal spacing factor value should fall between 0.004 and 0.008 inches.

Air bubbles in fresh concrete are naturally unstable due to the free surface energy that exists between dispersed air and the cement paste matrix. This energy has tendency to reduce the surface areas that separate the air bubbles from the surrounding matrix (Du & Folliard, 2005). An extended period of setting or use of a retarding agent gives this energy more time to eliminate small air pockets. Additionally, physical agitations such as mixing and vibration can be detrimental to the air void structure. The mechanism of air bubble collapse varies under different conditions. In some situations, air diffuses from a small bubble with high internal pressure to either a larger one with

low pressure or into the bulk solution surrounding the bubble. Another form of collapse is when the lamellar films between two bubbles rupture as they coalesce (Du & Folliard, 2005).

Air-entraining admixtures (AEAs) can be used to protect air bubbles in fresh concrete. The process of chemical entrainment of air can be described as an emulsion of air in the cement paste matrix or as foam formation retained by the solid network. AEAs are most commonly composed of surfactants which have two general chemical components. The hydrophilic head is attracted to water while its counterpart, the hydrophobic tail, has little attraction to water. Surfactants adsorb onto the surface of air bubbles in an orientation that protects them from collapse. The hydrophobic tail embeds into the air bubble while the hydrophilic head sits on the outside surface. If the hydrophobic tail came in contact with the liquid phase of the matrix, it would distort surrounding molecules. By sticking out of the solution, it lowers the free energy of the system. Additionally, the mutual repulsion of the two components reduces the attraction of the liquid phase to the air bubble, which results in a lower surface tension (Du & Folliard, 2005).

2.2.4 Effect of Drying

Periods of drying during concrete curing can be beneficial for freeze-thaw durability. By removing moisture from the concrete pore structure, drying eliminates the threat of internal damage caused by the expansive pressures of freezing water. However, if concrete is re-exposed to water for an extended period of time after drying, the beneficial effects may be minimal. Drying causes pores to expand and interconnect, which increases the permeability of the concrete. Water can then enter pores quickly, and the concrete becomes more susceptible to freeze-thaw damage (Riding et al., 2013).

2.2.5 Effect of Water-to-Cement Ratio

Researchers at Iowa State University began a freeze-thaw durability investigation with the idea that high-strength concrete (HSC) and concrete with low water-to-binder (w/b) ratios have low permeability. Since little water can penetrate into these types of concrete, they do not typically reach critical saturation in the field. The water that does manage to percolate into the fine capillary voids of HSC rarely freezes due to pore surface tension. Additionally, almost all of the mixing water in low w/b concrete is utilized during cement hydration. This leaves the hardened concrete with almost no extra water to cause damage during freezing. Theoretically, air-entraining

admixtures (AEA) are not necessary for providing freeze-thaw durability in these types of concrete (Wang, Lomboy, & Steffes, 2009).

The objective of this study was to investigate the effects of different combinations of w/b ratios, cement types, and the use of AEA on concrete freeze-thaw durability. The researchers experimented with four different w/b ratios: 0.25, 0.35, 0.45, and 0.55. They also used two different types of binders. One consisted of type I cement with Class C fly ash; the other was type IP cement. Two sets of samples were batched for each combination of w/b and binder type; one had AEA and the other did not (Wang et al., 2009).

All samples underwent ASTM C666 Procedure A testing after 28 days of curing in a fog room (2008a). The samples with air entrainment each completed 300 freeze-thaw cycles with RDME values above 90. Testing was terminated for most of the non-air-entrained samples before 300 cycles due to excessive damage. However, researchers observed a trend that the terminal RDME was higher for samples with lower w/b ratios. The non-air-entrained sample with a 0.25 w/b ratio and type IP cement finished 300 cycles with a RDME of 94. This performed almost as well as the same sample with AEA, which had a RDME of 95 after 300 cycles (Wang et al., 2009).

The comparable performance confirmed the authors' belief that air entrainment was not needed in samples with a low w/b ratio. However, a 0.25 w/b ratio is very low and may not always be practical in the field. The authors concluded that a combination of low permeability and high strength is needed to yield durable concrete without air entrainment. They suggest that this can be achieved by increasing the degree of hydration through longer moist-curing periods or by using a lower water-to-cement ratio if placement and finishing operations can accommodate it (Wang et al., 2009).

2.3 Durable Aggregate and Concrete Identification Procedures

Many standard test procedures have been developed by ASTM International (ASTM) and other organizations to either predict or measure freeze-thaw resistance of aggregate and concrete.

2.3.1 ASTM C666: Rapid Freezing and Thawing of Concrete

This standard, titled *Standard Test Method for Resistance of Concrete to Rapid Freezing and Thawing* (ASTM, 2008a), is used by many transportation organizations. It provides procedures for subjecting concrete specimens to frequent cycles of freezing and thawing as well as for determining specimen durability levels. Two different procedures may be used within ASTM

C666. Procedure A requires samples to be immersed in water during freezing and thawing. Procedure B involves freezing samples in air followed by thawing in water. Each freeze-thaw cycle must last between two and five hours. The temperature at the center of concrete specimens must be 40±3°F at the beginning of each cycle. This temperature is then lowered to 0±3°F and elevated back to 40±3°F at the end of the cycle.

Durability readings must be recorded for concrete specimens once every 36 cycles or less. ASTM C666 requires mass and resonant frequency of vibration to be measured after each of these intervals. Mass loss generally indicates that the exterior surfaces of a concrete specimen are deteriorating. This often occurs in the form of scaling, but can also occur due to severe internal cracking (Pigeon et al., 1986). Mass gain suggests that a sample is absorbing more water into its pores or that its cement is still hydrating. The resonant vibration of a concrete specimen is the frequency at which the maximum amplitude of an induced mechanical wave occurs (Tanesi & Meininger, 2006). The initial frequency is measured at the beginning of freeze-thaw testing and is continuously compared to new readings through calculation of a concrete specimen's relative dynamic modulus of elasticity (RDME). A specimen's RDME will decrease as the resonant frequency decreases. Resonant frequency decreases in response to increasing internal damage because mechanical waves take longer to travel through concrete specimens with excess cracking (Tanesi & Meininger, 2006). Mass and frequency readings must be recorded until the requisite number of freeze-thaw cycles are complete or until the RDME drops below 60%. However, ASTM C666 allows other failure limits to be specified. More detailed explanations on obtaining a concrete sample's resonant frequency and calculating its RDME are provided in Chapter 4.

ASTM C666 also provides an optional length change measuring procedure which may be conducted every 36 cycles to determine durability of concrete specimens. When internal cracking occurs in aggregate or cement paste, more volume is created and the specimen expands as a result. ASTM C666 suggests using an expansion of 0.10% of a specimen's original length as a failure limit. The procedure for determining concrete specimen expansion will be discussed in Chapter 4.

2.3.2 ASTM C88: Aggregate Sulfate Soundness

The objective of this test is to estimate the soundness of aggregates when subjected to weathering. This test is useful when aggregate has no field performance records or when little information is available. A sample of aggregate is repeatedly immersed in saturated solutions of

sodium or magnesium sulfate. It is then oven-dried to a level of partial or complete dehydration of salt precipitated in permeable pore spaces. A simulated internal expansive force caused by water expansion during freezing can be determined from the rehydration of salt when the aggregate is re-immersed in water. However, this test has poor precision and should not be used for outright aggregate rejection without supporting data from other tests (ASTM, 2013).

2.3.3 ASTM C295: Petrographic Analysis of Aggregates

ASTM C295 (2012a) outlines procedures for petrographic examination of materials proposed for use as aggregates. These procedures must be conducted by an experienced petrographer and may involve optical microscopy, x-ray diffraction analysis, differential thermal analysis, and infrared spectroscopy. Identifying mineral components of an aggregate sample using these procedures is typically a necessary step in predicting its behavior for its intended use. Petrographic examination has the capability of identifying the amount and severity of weathering within aggregate particles. This test can therefore predict poor freeze-thaw performance if it classifies an aggregate as finely porous and highly weathered or altered. However, the identification of these characteristics is only useful if accurate information regarding the material's source and proposed use is provided for the petrographer. The petrographer must also be able to correlate this information with findings of the analysis (ASTM, 2012a).

2.3.4 Washington Hydraulic Fracture Test

The Washington Hydraulic Fracture Test (WHFT) is used to predict aggregate freeze-thaw performance by rapidly inducing pressure in aggregate pore walls to simulate the expansion of water caused by freezing and thawing. This is done by forcing water in and out of the pore structure of dry aggregate particles in a water-filled pressure vessel. Pressurized nitrogen is used to force water into the aggregate pores. The pressure is then rapidly released to allow compressed air in the pores to expand. This expels water from the aggregates and induces internal stresses in pore walls similar to those produced during freezing and thawing. Aggregate fracture occurs when the pore structure cannot rapidly dissipate the pressure. The severity of this fracturing can be used to predict aggregate freeze-thaw resistance (Embacher & Snyder, 2003). Results from the WHFT have been found to match those of freeze-thaw tests conducted on unconfined aggregates. However, multiple studies have been unable to establish direct correlations between results of the WHFT and ASTM C666 (Hossain & Zurbey, 1996), (Issa, Issa, & Bendok, 1999).

2.3.5 PCA Absorption-Adsorption

As discussed in Section 2.1.3, aggregate pore structure can play a significant role in freeze-thaw resistance. The Portland Cement Association (PCA) developed an aggregate absorption and adsorption test based on this concept (Schwartz, 1987). Absorption is the measure of how much water can occupy aggregate pore volume when the aggregate is in saturated-surface dry (SSD) condition. This occurs when all of an aggregate's pore space is filled with water; but no excess water exists on its surface (Mamlouk & Zaniewski, 2011). An aggregate's adsorption is a rough measure of its internal and external surface area. The PCA identified aggregates with an absorption higher than 0.3% or an adsorption higher than 0.1% as susceptible to D-cracking (Koubaa & Snyder, 1996). Although conducting the absorption-adsorption test requires minimal amount of time, preparation, and equipment (Whitehurst, 1980), the results are often too restrictive. This test commonly identifies good-performing aggregates as nondurable and should therefore be used in conjunction with more reliable freezing and thawing tests (Schwartz, 1987).

2.4 Modified Versions of ASTM C666 Testing

Multiple state DOT's and transportation agencies use ASTM C666 to identify durable aggregate and concrete. However, some of these organizations have modified test characteristics such as curing and freeze-thaw cycling duration in order to obtain results that correlate well with field service records.

2.4.1 Kansas Department of Transportation Practices

KDOT's standard test method for determination of aggregate durability, KTMR-22, outlines the curing and testing procedures for concrete specimens subject to ASTM C666 Procedure B testing. Specimens undergo a 90-day curing method, which entails more than two months in a 100% moist room followed by three weeks in a room at 50% relative humidity (KDOT, 2006). The two-month period in the moist room accommodates extensive cement hydration. This leads to a more durable cement paste matrix, provided that an adequately entrained air void system is present as well. The extensive moist curing period is used so that freeze-thaw damage primarily occurs in the coarse aggregate. The three-week drying period then removes some of the excess moisture from aggregate pores, which can reduce the expansive pressures caused by freezing water. This drying period is also intended to represent field conditions in which concrete is allowed to dry before reabsorbing water (Riding et al., 2013). KDOT adopted this curing method in

response to the results obtained from a 1980 study on D-cracking. From these results, KDOT concluded that the durability of lab specimens subjected to 90-day curing periods correlated well with pavement field service records (Clowers, 1999).

KDOT has also modified the total number of freeze-thaw cycles for ASTM C666 testing from 300 to 660. When tests were only conducted through 300 cycles, the results were not adequately predicting field performance. Increasing the number of cycles was a convenient option for solving this problem as it would not require new equipment or test methodology. KDOT selected 660 as the final test cycle based on weather data showing that Kansas averages 33 hard freeze-thaw cycles per year. When multiplying this number by KDOT's desired pavement service life of 20 years, 660 is obtained (McLeod et al., 2014). KTMR-22 classifies coarse aggregate as durable if concrete samples maintain a RDME $\geq$ 95% and an expansion $\leq$ 0.025% after the completion of 660 cycles (KDOT, 2006).

2.4.2 Progression of ASTM C666 Testing in Iowa

From 1966 to 1968, the Iowa State Highway Commission examined the effects of three different curing methods on freeze-thaw durability of concrete. These methods included 90 days in a moist room (the standard procedure at the time), 14 days in a moist room, and 7 days in a moist room followed by 7 days in a 50% humidity environment. The results of the shorter curing durations yielded invaluable information. The 90-day curing method generally resulted in aggregate durability that matched field performance records, although some exceptions did exist. The authors concluded that the 90-day curing duration should remain the standard method (Marks & Grubb, 1969).

Moussalli (1986) conducted a study for the Iowa Department of Transportation in 1986 involving freeze-thaw testing of concrete specimens in accordance with ASTM C666 Procedure B. The 90-day moist curing period was used in lieu of the standard 14-day method specified by ASTM C666. However, the study followed other ASTM C666 requirements by testing concrete specimens until the completion of 300 cycles or until the RDME dropped below 60% (2008a).

During the study on low-permeability concrete discussed in Section 2.2.5, Wang et al. (2009) used the 28-day moist curing method specified by ASTM C192 (2015a) for freeze-thaw specimens. These samples underwent freezing and thawing for 300 cycles and were classified as nondurable if the RDME fell below 50% (Wang et al., 2009).

2.4.3 Other ASTM C666 Procedure B Test Methods

The Illinois, Michigan, and Ohio DOT's use Procedure B for concrete durability testing. Illinois (IDOT) requires a 14-day fog room curing period for freeze-thaw specimens. After curing, IDOT subjects samples to freezing and thawing until the completion of 350 cycles or until sample expansion exceeds 0.06%. IDOT does not have minimum requirements for RDME or mass change (Woodhouse, 2005).

Michigan (MDOT) also uses a 14-day curing period. MDOT samples are covered with wet burlap for the first 24 hours after placement. They are then demolded and immersed in saturated lime water for 12 days before spending approximately 16 hours in 40°F water. Freeze-thaw testing is conducted for 300 cycles or until expansion reaches 0.10% (Michigan Department of Transportation, 2015). Similarly to IDOT, MDOT does not require measurement of mass or RDME (Woodhouse, 2005).

Ohio (ODOT) cures freeze-thaw specimens by placing them in a fog room for 24 hours while they are still in their molds. The samples are then demolded and immersed in water for 14 days (Woodhouse, 2005). ODOT maintains a list of approved aggregate sources, but requires ASTM C666 to be performed for all ¾" and 1" nominal aggregate sizes. Aggregate durability is determined through calculation of the area under the curve obtained by plotting expansion versus the number of freeze-thaw cycles for a given test specimen. For aggregate sources that are approved by ODOT within a year of testing, this area may not exceed 2.05 after a maximum of 350 cycles. Between one and two years after approval, this area may not exceed 1.00 after 350 cycles (Ohio Department of Transportation, 2013).

2.4.4 Nebraska Department of Roads Practices

The Nebraska Department of Roads utilizes ASTM C666 Procedure A for 300 cycles to measure freeze-thaw durability of concrete mixes (Nebraska Department of Roads, 2008). The acceptable performance criteria at the completion of testing entails a minimum durability factor of 70% and a maximum mass loss of 5% (Hanna, Morcous, & Tadros, 2014).

2.5 Concrete Curing Methods for Freeze-Thaw Testing

Effective concrete curing processes create closer porous structures and higher resistance to physical and chemical deterioration. In laboratory environments, curing methods typically involve placing samples in a saturated lime-water bath or in a fog room (Al-Assadi, Casati, Fernandez, &

Galvez, 2010). The studies discussed in this section investigate the effects of unconventional curing methods and durations on freeze-thaw performance of concrete specimens.

2.5.1 Steam and Microwave Curing

Researchers at Chaoyang University of Technology experimented with steam- and microwave-curing of concrete freeze-thaw specimens. Three sets of samples were batched and cured under different conditions. The first two sets were cured in water for 28 days. They were then subjected to seven hours of steam curing at 65°C before being placed in water again for 17 hours. Following this, one of the sets was microwave-cured for 40 minutes. The third set was cured for 28 days in water without any steam or microwave exposure (Lee, 2007).

After curing, samples were cooled to room temperature and placed in a saturated lime-water bath. The samples were then subjected to freeze-thaw cycling at a rate of one cycle every 185 minutes. Each cycle included 90 minutes of freezing in air at -18°C (0°F) and 90 minutes of thawing in wet air at 4.4°C (40°F). The researchers intended for the freeze-thaw conditions to closely match those of ASTM C666 Procedure B (Lee, 2007).

The average RDME was provided for all sample sets after 100 cycles, 300 cycles, and 600 cycles. The water-cured samples of each mix design yielded equivalent or slightly higher durability values than those of the steam- and microwave-cured samples at all freeze-thaw cycling durations (Lee, 2007).

2.5.2 Climatic Curing

The primary objective of a study conducted at the Technical University of Madrid was to observe effects of curing on internal and external concrete freeze-thaw damage when poured under summer conditions. Researchers batched four sets of concrete samples with crushed limestone coarse aggregate. Each set had a different combination of a 0.4 or 0.5 water-to-cement (w/c) ratio and the use or absence of an air-entraining admixture (AEA). The samples were demolded after 24 hours and placed in a chamber at 30°C with 37% relative humidity for 28 days. These conditions were selected to simulate typical summer climate in central Spain. During the first week in the climatic chamber, half of each set's samples were wetted daily. The other samples were "dry-cured" and were not exposed to additional water while in the chamber (Al-Assadi et al., 2010).

After 28 days of curing, all specimens were immersed in water for four days to ensure saturation. They were then subjected to 300 freeze-thaw cycles. The temperature during each cycle

started at 10°C, dropped to approximately -18°C, and raised back to 10°C in four hours (Al-Assadi et al., 2010).

The average RDME for each set was monitored throughout testing. All of the 0.4 w/c mixes performed well, with a final RDME at or near 100%. The worst-performing mix was wet cured with a 0.5 w/c and no AEA. It finished with an average RDME of less than 60%, which was used as the failure criterion. The second-worst performing samples in this experiment occurred with the same mix under dry curing. These samples finished with an average RDME of less than 90% (Al-Assadi et al., 2010). In general, these results show that samples with high mixing water content and no AEA will perform poorly in freeze-thaw environments. Adding water during curing further stimulates this deterioration.

The authors investigated porosity and cement hydration throughout testing. They found that lower porosity was observed in all specimens after freeze-thaw cycling, regardless of the use of an AEA. The authors also concluded that both curing conditions accommodated continuous cement hydration throughout freeze-thaw testing. Since the wet-cured samples had a higher rate of hydration before testing, they had a more closed pore structure than the dry-cured samples. This allowed internal pressures to develop during freezing and resulted in more deterioration (Al-Assadi et al., 2010).

2.5.3 Temperature-Match-Curing

High-strength concrete (HSC) in large structures typically has high cement content and may develop high internal temperatures due to cement hydration. Jon A. Jonsson and Jan Olek (2004) created an experiment in which concrete freeze-thaw specimens were cured under temperature conditions that matched those of in situ concrete. This technique, called temperature-match-curing (TMC), ensures that concrete test samples experience the same temperature history as the concrete member they represent (Jonsson & Olek, 2004).

Preparation for this study involved batching four different mix designs. Each contained type I cement, a 0.33 water-cement ratio, and no AEA. 5.5 liters of each mix were placed in separate polystyrene blocks which were meant to simulate actual temperature profiles induced in HSC structural members. Researchers also batched four freeze-thaw prisms per mix. These were placed in a special enclosure equipped with adjustable heaters to match the temperature history with that of the concrete in the polystyrene blocks. During the first two days after batching, two

prisms of each mix were temperature-match-cured while the other two served as control blocks and were cured at room temperature. At the end of the two days, all freeze-thaw samples were placed in a fog room (Jonsson & Olek, 2004).

Researchers found that the control specimens for all mixes had a maximum temperature of less than 30°C during curing while the maximum TMC temperatures reached between 59°C and 69°C. For all four mixes, the TMC samples had better ASTM C666 performance than that of the control blocks. The RDME for all control samples dropped below 60% before or at approximately 100 freeze-thaw cycles. The TMC samples maintained a RDME above 60% until approximately 100 cycles, but they all eventually failed before reaching 200 cycles (Jonsson & Olek, 2004). The higher freeze-thaw resistance of the TMC samples can likely be attributed to a lower degree of saturation caused by drying action of heat curing.

2.6 Summary

Internal concrete freeze-thaw damage occurs due to the development of hydraulic pressures in the pores of cement paste. Concrete may also be susceptible to surface scaling when exposed to water and deicing chemicals during freezing. Air void structure, moisture content, and concrete permeability affect concrete resistance as well. Many standard test procedures have been developed to predict and measure durability of aggregate and concrete. KDOT's standard method for determining aggregate durability consists of an extended curing period and more freeze-thaw cycles than specified by ASTM C666 Procedure B. Due to the longer curing period, higher number of cycles, and higher RDME acceptance criteria, KDOT has more stringent aggregate durability requirements than those of ASTM C666. Other state DOT's have implemented modified curing methods, freeze-thaw test durations, and performance criteria as part of their ASTM C666 testing. Curing studies have shown that elevated curing temperatures can accelerate deterioration of aggregates and concrete. This information supports experimentation with high cure temperatures to develop a shorter qualification test. These studies have also showed that exposing concrete specimens to drying periods during curing can yield high durability after several freeze-thaw cycles. Although these dry cure methods are often used to simulate field conditions, they may prolong the freeze-thaw testing process.

Chapter 3 - Materials

3.1 Coarse Aggregate

KDOT provided limestone coarse aggregate from seven different sources in Kansas and Missouri to determine the effects of accelerated curing methods on sample freeze-thaw durability using ASTM C666 Procedure B. Table 3-1 provides the quarry information for each of these aggregates.

Table 3-1: Accelerated Cure Coarse Aggregate Sources

Producer	Quarry ID	Bed(s)	Location
Bayer Construction	2-031-04-LS	1,2	Junction City, KS
Cornejo Stone	4-025-03-LS	1,2,3	Moline, KS
Hamm WB	2-021-16-LS	2,3	Abilene, KS
Jasper Stone	MO-043-LS	1	Jasper, MO
Martin Marietta Materials	MO-044-LS	Cooper-Callaway	Randolph, MO
Midwest Minerals	4-006-03-LS	6,7,8	Fort Scott, KS
Midwest Minerals	4-050-06-LS	1,2	Parsons, KS

Some of these aggregates were tested during the salt brine study as well. Table 3-2 lists the twelve limestone coarse aggregates used to examine the ability of salt treating aggregates and ASTM C666 Procedure A and B to better differentiate aggregate performance in freeze-thaw testing.

Table 3-2: Salt Brine Coarse Aggregate Sources

Producer	Quarry ID	Bed(s)	Location
Bayer Construction	2-031-04-LS	1,2	Junction City, KS
Cornejo Stone	4-025-03-LS	1,2,3	Moline, KS
Eastern Colorado Aggregates	CO-001-SG	Pit	Prowers County, CO
Florence Rock	2-057-05-LS	1,2	Marion County, KS
Hamm WB	2-021-16-LS	2,3	Abilene, KS
Jasper Stone	MO-043-LS	1	Jasper, MO
Mid-States Materials	1-046-04-LS	9	Edgerton, KS
Mid-States Materials	1-070-11-LS	3	Osage County, KS
Mid-States Materials	1-070-11-LS	4	Osage County, KS
Midwest Minerals	4-006-03-LS	6,7,8	Fort Scott, KS
Midwest Minerals	4-050-06-LS	1,2	Parsons, KS
Penny's Aggregates	4-030-05-LS	8,9,10,11	Franklin County, KS

Aggregate properties such as SSD bulk specific gravity and absorption were needed for concrete mix proportioning. These values were obtained in accordance with ASTM C127: Standard Test Method for Density, Relative Density (Specific Gravity), and Absorption of Coarse Aggregate (ASTM, 2012c). Aggregate was immersed in water for 24 hours in order to saturate the pores. The coarse aggregates were then towel-dried and weighed in SSD condition. The SSD aggregate's apparent mass in water was then obtained before recording its mass after oven-drying for 24 hours. The SSD bulk specific gravity was determined through comparison of the SSD and apparent masses. Absorption was found by comparing the SSD and oven-dry masses (ASTM, 2012c). Aggregate properties for the accelerated cure and salt brine studies are displayed in Table 3-3 and Table 3-4, respectively.

Table 3-3: Accelerated Cure Coarse Aggregate Properties

Producer	SSD Bulk Specific Gravity	Absorption (%)
Bayer Construction	2.61	2.2
Cornejo Stone	2.59	3.2
Hamm WB	2.53	3.6
Jasper Stone	2.66	0.8
Martin Marietta Materials	2.69	0.8
Midwest Minerals - Ft. Scott	2.58	2.3
Midwest Minerals - Parsons	2.64	1.7

Table 3-4: Salt Brine Coarse Aggregate Properties

Producer	SSD Bulk Specific Gravity	Absorption (%)
Bayer Construction	2.62	2.0
Cornejo Stone	2.57	2.8
Eastern Colorado Aggregates	2.60	1.4
Florence Rock	2.28	8.8
Hamm WB	2.45	2.6
Jasper Stone	2.65	1.0
Mid-States Materials - Edgerton	2.61	2.1
Mid-States Materials - Osage (Bed 3)	2.66	1.2
Mid-States Materials - Osage (Bed 4)	2.64	3.1
Midwest Minerals - Ft. Scott	2.59	1.8
Midwest Minerals - Parsons	2.65	1.5
Penny's Aggregates	2.58	3.0

The aggregate properties provided in Table 3-3 and Table 3-4 were obtained by Kansas State University and KDOT, respectively. As a result, slight variations in specific gravity and absorption were found for the aggregate sources that were used in both studies.

3.2 Fine Aggregate

Kaw River sand was obtained from Kansas Sand & Concrete, Inc. in Topeka, Kansas. Concrete mixes that are batched in accordance with KTMR-22 require the use of this sand as fine aggregate (KDOT, 2006). These properties were obtained using the gravimetric procedure outlined in ASTM C128: Standard Test Method for Density, Relative Density (Specific Gravity), and Absorption of Fine Aggregate (ASTM, 2012d). Sand was immersed in water for 24 hours and then dried to SSD condition using a hair dryer. KSU tested the sand for surface moisture by placing it in a cone-shaped mold with two open ends. A tamper was used to lightly consolidate the sand. The sand was considered SSD when it deformed slightly upon removal of the mold. KDOT used the procedure outlined in KT-6: Specific Gravity and Absorption of Aggregates (KDOT, 2007) to bring sand to SSD condition. This procedure involved transferring sand between two drying pans with rusted bottoms which indicated the presence of surface moisture (KDOT, 2007). The SSD bulk specific gravity was determined using a series of mass measurements involving the sand in

SSD and oven-dry conditions, water, and a pycnometer. Absorption was measured by comparing SSD and oven-dry mass values (ASTM, 2012d).

The measured SSD bulk specific gravity and absorption values for the accelerated cure study were 2.63 and 0.8%, respectively. Table 3-5 provides fine aggregate values used for each salt brine study mixture based on the fine aggregate sample taken, along with the name of the corresponding coarse aggregate used in the same concrete mix.

Table 3-5: Salt Brine Fine Aggregate Properties

Fine Aggregate		Coarse Aggregate Used
SSD Bulk Specific Gravity	Absorption (%)	
2.602	0.7	Bayer Construction
2.598	0.7	Cornejo Stone
2.602	0.7	Eastern Colorado Aggregates
2.598	0.7	Florence Rock
2.602	0.7	Hamm WB
2.602	0.7	Jasper Stone
2.602	0.7	Mid-States Materials - Edgerton
2.598	0.7	Mid-States Materials - Osage (Bed 3)
2.598	0.7	Mid-States Materials - Osage (Bed 4)
2.598	0.7	Midwest Minerals - Ft. Scott
2.598	0.7	Midwest Minerals - Parsons
2.614	0.5	Penny's Aggregates

3.3 Cement

Monarch type I/II cement was used in all concrete mixes in accordance with KTMR-22 specifications (KDOT, 2006). The average physical and chemical compositions of the cement used for the accelerated cure study are shown in Table 3-6.

Table 3-6: Mill Test Results for Cement used in Accelerated Cure Study

Property		Reported Value	Spec Limit
325 Sieve, % Passing		95.8	None
Blaine fineness, specific surface – Air Permeability (cm^2/g)		3790	2600 min
Time of Setting, Gilmore test:	Initial (hrs:min)	2:00	60 min
	Final (hrs:min)	3:00	600 max
Air Content of Mortar (volume %)		8.2	12.0 max
Autoclave Expansion (%)		0.013	0.80 max
Compressive Strength (psi)	1 Day	2155	None
	3 Days	3295	1740 min
	7 Days	4223	2760 min
C_3S – Tricalcium silicate (%)		52.3	None
C_2S – Dicalcium silicate (%)		22.7	None
C_3A – Tricalcium aluminate (%)		7.1	8 max
C_4AF – Tetracalcium aluminoferrite (%)		9.3	None
SiO_2 – Silicon dioxide (%)		21.68	None
Fe_2O_3 – Ferric oxide (%)		3.06	6.0 max
Al_2O_3 – Aluminum oxide (%)		4.63	6.0 max
CaO – Calcium oxide (%)		63.92	None
MgO – Magnesium oxide (%)		1.90	6.0 max
SO_3 – Sulphur trioxide (%)		2.70	3.0 max
Loss on ignition (%)		1.39	3.0 max
Insoluble residue (%)		0.47	0.75 max
Free lime (%)		1.22	None
Na_2O – Sodium oxide (%)		0.17	None
K_2O – Potassium oxide (%)		0.52	None
Equivalent Alkalies (%0		0.51	0.60 max
Inorganic Processing Addition (%)		2.09	5.0 max
Inorganic Process Addition (C150)	Process Dust (%)	2.09	N/A
	SiO_2 (%)	10.5	N/A
	Fe_2O_3 (%)	2.28	N/A
	Al_2O_3 (%)	4.42	N/A
	CaO (%)	43.7	N/A
	SO_3 (%)	0.50	N/A

3.4 Air-Entrainment

Daravair® 1400 from W.R. Grace & Co. was used as an air-entraining agent for all accelerated cure mixtures. Daravair® 1000 was used for salt brine mixtures.

Chapter 4 - Methods

4.1 Concrete Mix Design

All concrete mixes were designed based on the requirements outlined in KTMR-22. The water-to-cement (w/c) ratio for each mix ranged between 0.40 and 0.42. As per KTMR-22 requirements, 50% of the coarse aggregate gradation contained -3/4" +1/2" aggregate and the remaining 50% consisted of -1/2" +3/8" aggregate (KDOT, 2006). Mixture proportions for each aggregate set in the accelerated cure and salt brine studies are summarized in Table 4-1 and Table 4-2, respectively.

Table 4-1: Accelerated Cure Concrete Mixture Proportions

Aggregate Source	Material Weight (lbs./yd^3)				Air-Entraining Admixture (mL/yd^3)
	Cement	Water	Fine Aggregate (SSD)	Coarse Aggregate (SSD)	
Bayer Construction	601.6	246.7	1495.8	1495.8	138
Cornejo Stone	601.6	252.7	1469.5	1469.5	144
Hamm WB	601.6	246.7	1470.4	1470.4	138
Jasper Stone	601.6	249.7	1493.0	1493.0	144
Martin Marietta Materials	601.6	249.7	1503.0	1503.0	144
Midwest Minerals - Ft. Scott	601.6	249.7	1470.6	1470.6	144
Midwest Minerals - Parsons	601.6	249.7	1489.3	1489.3	144

Table 4-2: Salt Brine Concrete Mixture Proportions

Aggregate Source	Material Weight (lbs./yd^3)				Air-Entraining Admixture (mL/yd^3)
	Cement	Water	Fine Aggregate (oven-dry)	Coarse Aggregate (SSD)	
Bayer Construction	601.60	240.8	1507.5	1507.5	138
Cornejo Stone	601.60	240.8	1489.3	1489.3	138
Eastern Colorado Aggregates	601.60	240.8	1501.4	1501.4	138
Florence Rock	601.60	240.8	1405.7	1405.7	138
Hamm WB	601.60	240.8	1458.7	1458.7	138
Jasper Stone	601.60	240.8	1516.1	1516.1	138
Mid-States Materials - Edgerton	601.60	240.8	1506.3	1506.3	138
Mid-States Materials - Osage (Bed 3)	601.60	240.8	1516.7	1516.7	138
Mid-States Materials - Osage (Bed 4)	601.60	240.8	1509.5	1509.5	138
Midwest Minerals - Ft. Scott	601.60	240.8	1497.1	1497.1	138
Midwest Minerals - Parsons	601.60	240.8	1513.5	1513.5	138
Penny's Aggregates	601.60	240.8	1498.8	1498.8	209

4.2 Preparation of Salt-Treated Aggregate

Two concrete mixes were batched for each of the twelve aggregate sets used in the salt brine study. In one of the two mixes, the coarse aggregate was treated with salt brine solution containing a 23.6% concentration of rock salt in water. The salt-treatment procedure began with oven-drying aggregate at 230°F for 24 hours. The aggregates were then immersed in the salt solution for another 24 hours. This process was repeated five times before towel-drying the aggregate to SSD condition (K. Larson, personal communication, February 8, 2016).

4.3 Concrete Batching

Materials were prepared in accordance with KTMR-22 before mixtures were batched. Non-salt-treated coarse aggregate was immersed in water for 24 hours and towel-dried to SSD condition. Moisture corrections were incorporated into mix designs to account for the water that would be absorbed by the dry sand during batching. All materials were batched in a 2 ft^3 pan mixer using the procedure provided in ASTM C192: Standard Practice for Making and Curing Concrete Test Specimens in the Laboratory (ASTM, 2015a):

1. Place coarse aggregate in mixer
2. Add approximately half of the mixing water
3. Add air-entraining admixture
4. Start mixer
5. Add fine aggregate
6. Add cement
7. Add remaining half of mixing water
8. Start timer and mix for 3 minutes with lid open
9. Stop mixer and let concrete sit still for 3 minutes with lid closed
10. Start mixer and mix for additional 2 minutes with lid open

4.4 Fresh Concrete Tests

Each mix was required to pass KTMR-22 slump and fresh concrete air content test specifications. Target slump values were between 1-1/2" and 2-1/2". Target air contents were 5-7% of the total concrete volume (KDOT, 2006). Slump and air content values were measured using the procedures outlined in ASTM C143 (2015b) and ASTM C231 (2014b), respectively. Unit weight and temperature were measured for each concrete mixture using ASTM C138 (ASTM, 2014a) and ASTM C1064 (ASTM, 2012e), respectively.

4.5 Preparation of Concrete Prisms

Concrete prisms with dimensions of 3 in. x 4 in. x 16 in. were made upon completion of slump and air content testing. The prisms were made in accordance with ASTM C192 (2015a). Approximately half of the prism height was filled with fresh concrete and rodded 25 times. All faces of the prism mold were then struck with a mallet several times before spading the concrete

along the prism edges. This process was repeated after filling the second half of the mold. A wood trowel was used to smooth the exposed face of the prism.

Two mixtures were batched for each of the twelve aggregates in the salt brine study. One mix contained salt-treated aggregate and the other contained non-salt treated aggregates from the same source. Six prisms were cast from each mix, which yielded a total of 144 prisms.

For the accelerated cure study mixtures, nine prisms were cast for each of the seven aggregates. The nine prisms were divided into three sets of three prisms. Each set was subjected to a different curing method.

4.5.1 Curing Method 1: 100% Moist Room

The first set of accelerated cure prisms experienced a 30-day curing period. They were first placed in a 100% moist room for 28 days. They were then immersed in water at approximately 70°F for 24 hours followed by another 24-hour period of being submerged in 40°F water. The soaking period in 40°F water lowered the sample temperatures to the level at which they must begin freeze-thaw testing.

4.5.2 Curing Method 2: 100% Moist Room and Lime Water Bath

The second set of prisms also underwent 30 days of curing. They spent seven days in a 100% moist room followed by 21 days in a 100°F saturated lime-water bath. Lime water is commonly incorporated into lab curing environments in order to prevent concrete moisture loss and provide consistent internal and external concrete temperatures (Akhavan & Malik, 1999). The elevated temperature of the lime bath was used to accelerate cement hydration. These samples then spent two consecutive 24-hour soaking periods in 70°F and 40°F water after they were removed from the lime water.

4.5.3 Curing Method 3: KTMR-22

The KTMR-22 curing method was used for the third set of accelerated cure prisms. KTMR-22 (KDOT, 2006) outlines KDOT's standard 90-day curing procedure used for samples subjected to freezing and thawing. These samples were placed in a 100% moist room for 67 days. They were then transferred into a 73°F room at approximately 50% relative humidity for 21 days before spending two consecutive 24-hour soaking periods in 70°F and 40°F water. This curing method was also used for all prisms batched for the salt brine study.

4.6 ASTM C666 Testing

Freeze-thaw testing for accelerated cure samples was conducted in accordance with ASTM C666 Procedure B (2008a). A freeze-thaw machine developed by Scientemp Corporation was used to automatically cycle concrete specimens through temperatures specified by ASTM C666. The chamber in this machine has a capacity of 20 concrete prisms. Two of the slots contained control prisms which were used to monitor internal concrete temperatures through thermocouple wires. Test specimens occupied the remaining 18 slots. The freeze-thaw machine was programmed to complete one cycle every three hours (8 cycles/day). Specimen temperatures were $40\pm3°F$ at the beginning of each cycle. They were subjected to freezing in air for 110 minutes until they reached $0\pm3°F$. The chamber then filled with tempered water, which allowed the samples to thaw.

ASTM C666 Procedures A and B were both used to test prisms in the salt brine study. Different combinations of testing conditions for each of the twelve aggregates are summarized in Table 4-3.

Table 4-3: Salt Brine Concrete Testing Conditions for Each Aggregate Set

Aggregate Condition	ASTM C666 Test Method	Number of Concrete Prisms
Salt-Treated	A	3
Salt-Treated	B	3
No Salt Treatment	A	3
No Salt Treatment	B	3

Procedure A samples were tested in an 80-slot freeze-thaw machine. Under this method, the samples were required to be surrounded by a water depth between 1/32 in. and 1/8 in. throughout freezing and thawing (ASTM, 2008a). To meet this requirement, samples were placed in prism-shaped plastic sleeves filled with water before being placed in the chamber. Similarly to Procedure B, Procedure A requires concrete temperatures to start at $40\pm3°F$, drop to $0\pm3°F$, and elevate back to $40\pm3°F$ within 2-5 hours (ASTM, 2008a). This was accomplished by programming the freeze-thaw machine to complete one cycle every 4.75 hours (~5 cycles/day). A full cycle consisted of 200 minutes of freezing, 70 minutes of thawing, and 15 minutes of water draining from the chamber.

Mass, resonant frequency, and expansion readings were recorded for all prisms before the beginning of the first freeze-thaw cycle. These values were then recorded in intervals of no more

than 36 cycles. Testing generally continued until samples completed 660 cycles as specified by KTMR-22 (KDOT, 2006) or until freeze-thaw deterioration prevented measurements from being taken.

4.6.1 Mass Measurements

Mass was recorded using a scale with a capacity of 30 kg. This capacity met ASTM C666 requirements as it was more than 50% of the specimens' mass (ASTM, 2008a), which ranged between 7 and 8 kg. Surface water was removed from concrete prisms by towel-drying in order to maintain consistent moisture conditions for recording mass.

Change in mass was calculated using Equation 1.

$$Change\ in\ Mass\ (\%) = \frac{(m_x - m_0)}{(m_0)} * 100$$

Equation 1

Where: m_x =   Mass reading at freeze-thaw cycle x (kg)

            m_0 =   Initial mass reading (kg)

4.6.2 Resonant Frequency Measurements

The concrete prism transverse resonant frequency was obtained using a modified version of the impact resonance method in ASTM C215 specified by KTMR-22. A James E-Meter™ Mk II, equipped with an impactor and an accelerometer, was used to measure frequency values. Prism mass and dimensions were first entered into the James E-Meter™. The impactor was then used to strike the prism approximately 25 mm from one end. The accelerometer was placed 25 mm away from the opposite end to receive and measure the resulting vibration. The frequency spectrum was then computed by the meter (NDT James Instruments Inc., n.d.).

Equation 2 shows how resonant transverse frequency values were used to calculate each sample's relative dynamic modulus of elasticity (RDME).

$$RDME\ (\%) = \frac{(n_x{}^2)}{(n_0{}^2)} * 100$$

Equation 2

Where: n_x =   Transverse frequency at freeze-thaw cycle x (Hz.)

            n_0 =   Initial transverse frequency (Hz.)

4.6.3 Expansion Measurements

In order to monitor length change, or expansion, of concrete prisms, stainless steel gauge studs were installed in both prism ends during mixing. The initial length of a prism was measured with a caliper before subjecting it to its first freeze-thaw cycle. The difference in length between the prism and a steel invar reference bar was also measured at this time. This was accomplished by placing the invar bar in a length comparator equipped with a digital deflection indicator. The indicator value was set to zero in order to establish a reference point from which prism length could be measured. The invar bar was then removed and replaced by the prism, which was secured in the comparator using its gauge studs. The indicator displayed the difference in length with a precision of 0.00001 inches. The increase in length difference was continuously monitored throughout freeze-thaw cycling.

Expansion was calculated using Equation 3.

$$Expansion \ (\%) = \frac{(l_x - l_0)}{(l_i)} * 100$$ **Equation 3**

Where: l_x =   Indicator reading at freeze-thaw cycle x (in.)

                        l_0 =   Initial indicator reading (in.)

                        l_i =   Initial prism length (in.)

Chapter 5 - Accelerated Cure Study Results

Mass change, RDME, and expansion were measured for each sample until the completion of 660 freeze-thaw cycles or until excessive deterioration prevented recording of such measurements. Averages of these properties were then calculated for each of the three curing methods discussed in Section 4.5. This chapter provides a summary, as well as examples, of the ASTM C666 results for the accelerated curing portion of this study. Graphical representations of mass change, RDME, and expansion during freeze-thaw testing can be found for all seven sample sets in Appendix A. All prisms subjected to the KTMR-22 90-day curing period completed 660 freeze-thaw cycles.

5.1 Change in Mass

A summary of change in mass for all samples at their terminal freeze-thaw cycle is summarized in Table 5-1.

Table 5-1: Summary of Accelerated Cure Mass Change Results

Sample Set	30-Day Curing				90-Day Curing	
	Moist Room		Moist Room and Lime Bath		KTMR-22	
	Average Final Mass Change (%)	Final Cycle	Average Final Mass Change (%)	Final Cycle	Average Final Mass Change (%)	Final Cycle
Bayer	-0.05	660	0.15	660	0.08	660
Cornejo	1.52	437	1.19	416	0.59	660
Hamm	0.21	588	0.32	397	0.39	660
Jasper	0.32	660	0.26	660	0.25	660
Martin Marietta	0.04	660	0.08	660	0.33	660
Midwest Minerals Ft. Scott	0.67	358	0.60	358	0.79	660
Midwest Minerals Parsons	0.85	660	0.66	660	0.38	660

With the exception of one sample set, increases in mass were observed with increasing exposure to freezing and thawing. This likely occurred as a result of water absorption in aggregates. As the D-cracking progressed, more internal volume became accessible for water. In order to confirm the presence of cracking in the aggregates typically seen with D-cracking, one-inch-thick prism cross-sections were sawcut and polished. An example of one of these samples is shown in Figure 5.1.

Figure 5.1: D-Cracking of Sawcut Prism

In samples that experienced high increases in mass, such as the 30-day-cured Cornejo samples, D-cracking progressed from the aggregate into the surrounding hardened cement paste. This provided even more accessible space for water. Figure 5.2 shows an example of one of these prisms.

Figure 5.2: Cracking Progression into Hardened Cement Paste

5.2 Relative Dynamic Modulus of Elasticity

Three of these sample sets passed KTMR-22 requirements by maintaining an average RDME ≥ 95% (KDOT, 2006). Only one sample set met this requirement after just 30 days of curing. Table 5-2 summarizes the final RDME results for each sample set and curing method.

Table 5-2: Summary of Accelerated Cure RDME Results

Sample Set	90-Day Curing		30-Day Curing			
	KTMR-22		Moist Room		Moist Room and Lime Bath	
	Average Final RDME (%)	Final Cycle	Average Final RDME (%)	Final Cycle	Average Final RDME (%)	Final Cycle
Bayer	96	660	74	660	29	620
Cornejo	76	660	28	150	26	119
Hamm	93	660	33	446	22	325
Jasper	93	660	75	660	80	660
Martin Marietta	97	660	97	660	92	660
Midwest Minerals Ft. Scott	54	660	23	358	39	358
Midwest Minerals Parsons	98	660	21	660	26	660

The RDME data is also organized in a manner such that the durability results of the KTMR-22-cured samples can be correlated with those of the two 30-day curing methods. Upon completion of 660 freeze-thaw cycles, the average RDME for each KTMR-22-cured sample set was calculated and recorded. This value was then compared to the average RDME of the 30-day-cured samples at 300 cycles. This cycle was selected based on the ASTM C666 (2008a) performance criterion which classifies aggregate as durable in concrete samples that maintain a RDME ≥ 60% after 300 cycles. The objective of the comparison was to find possible relationships between the 30-day-cured samples meeting ASTM C666 requirements and the KTMR-22-cured samples of the same aggregate set that have a RDME greater than 95% after 660 cycles. RDME values at 300 cycles

were calculated through linear interpolation between the RDME readings at the two cycles above and below 300. This comparison is presented in Table 5-3.

Table 5-3: Comparison of RDME Results under Different Curing Methods and Freeze-Thaw Durations

Sample Set	Average RDME (%) at 660 Cycles	Average RDME (%) at 300 Cycles	
	KTMR-22 Curing	Moist Room Curing	Moist Room and Lime Bath Curing
Bayer	96	92	70
Cornejo	76	*	*
Hamm	93	57	25
Jasper	93	91	90
Martin Marietta	97	98	94
Midwest Minerals Ft. Scott	54	34	47
Midwest Minerals Parsons	98	86	79

* Excessive deterioration prevented measurement of RDME at 300 cycles

Another analysis was conducted to compare results of the different curing methods. Upon completion of 660 cycles, the average KTMR-22 RDME was calculated and recorded for each aggregate set. For the 30-day-cured samples, the cycle at which the equivalent average RDME values occurred was then identified. This cycle was determined by interpolation between the 30-day-cure RDME values that were larger and smaller than the final KTMR-22 RDME. An illustration of this concept is provided in Figure 5.3.
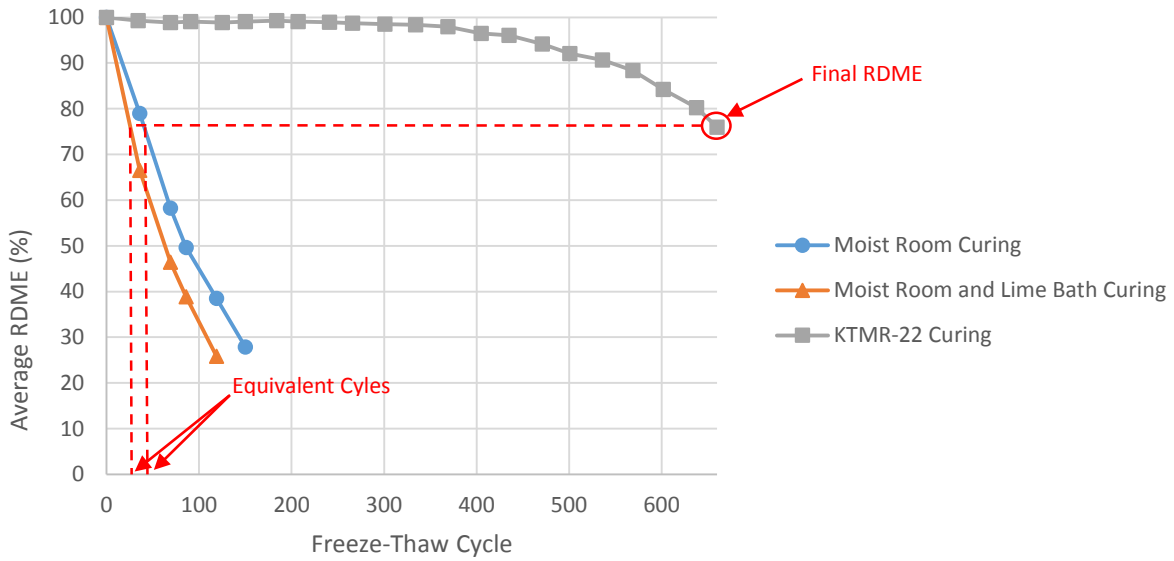
Figure 5.3: Determination of Equivalent Freeze-Thaw Cycles

This procedure was conducted for all seven sample sets. The calculated equivalent freeze-thaw cycles for each are displayed in Table 5-4.

Table 5-4: Summary of Equivalent Freeze-Thaw Cycles based on Final RDME

Sample Set	Average RDME (%) at 660 Cycles	Cycle with Equivalent Average RDME	
	KTMR-22 Curing	Moist Room Curing	Moist Room and Lime Bath Curing
Bayer	96	25	21
Cornejo	76	41	26
Hamm	93	37	21
Jasper	93	181	134
Martin Marietta	97	578	27
Midwest Minerals Ft. Scott	54	247	271
Midwest Minerals Parsons	98	26	18

5.3 Expansion

A summary of length change for all samples at their terminal freeze-thaw cycle is summarized in Table 5-5.

Table 5-5: Summary of Accelerated Cure Expansion Results

| Sample Set | 90-Day Curing | | 30-Day Curing | | | |
| | KTMR-22 | | Moist Room | | Moist Room and Lime Bath | |
	Average Final Expansion (%)	Final Cycle	Average Final Expansion (%)	Final Cycle	Average Final Expansion (%)	Final Cycle
Bayer	0.02	660	0.06	660	0.25	660
Cornejo	0.08	660	0.91	437	0.97	416
Hamm	0.02	660	0.24	588	0.29	397
Jasper	0.05	660	0.11	660	0.10	660
Martin Marietta	0.05	660	0.03	660	0.05	660
Midwest Minerals Ft. Scott	0.12	660	0.23	358	0.23	358
Midwest Minerals Parsons	0.02	660	0.36	660	0.28	660

Three of seven sample sets passed KTMR-22 requirements by maintaining an average expansion ≥ 0.10% after 660 freeze-thaw cycles (KDOT, 2006). None of the 30-day-cured samples met this requirement.

The comparisons made for the RDME results were also made for expansion results. After finding the average final expansion of KTMR-22-cured samples, the average expansion of the 30-day-cured samples at 300 cycles was calculated. These values are provided in Table 5-6. An equivalent cycle analysis was also conducted in order to determine the cycle at which the average expansion for 30-day-cured samples was equivalent to that of the KTMR-22 samples at 660 cycles. This comparison is presented in Table 5-7.

Table 5-6: Comparison of Expansion Results under Different Curing Methods and Freeze-Thaw Durations

Sample Set	Average Expansion (%) at 660 Cycles	Average Expansion (%) at 300 Cycles	
	KTMR-22 Curing	Moist Room Curing	Moist Room and Lime Bath Curing
Bayer	0.02	0.01	0.07
Cornejo	0.08	0.51	0.56
Hamm	0.02	0.07	0.19
Jasper	0.05	0.05	0.04
Martin Marietta	0.05	0.02	0.03
Midwest Minerals Ft. Scott	0.12	0.16	0.17
Midwest Minerals Parsons	0.02	0.06	0.08

Table 5-7: Summary of Equivalent Freeze-Thaw Cycles based on Final Expansion

Sample Set	Average Expansion (%) at 660 Cycles	Cycle with Equivalent Average Final Expansion (%)	
	KTMR-22 Curing Method	Moist Room Curing	Moist Room and Lime Bath Curing
Bayer	0.02	391	113
Cornejo	0.08	48	43
Hamm	0.02	160	65
Jasper	0.05	363	393
Martin Marietta	0.05	*	*
Midwest Minerals Ft. Scott	0.12	264	234
Midwest Minerals Parsons	0.02	133	64

* Average expansion for 30-day-cured samples never that of the KTMR-22-cured samples at 660 cycles

Chapter 6 - Salt Brine Study Results

Mass change, RDME, and expansion were measured for each sample. Averages of these properties were then calculated for each combination of aggregate salt treatment and freeze-thaw test method. This chapter provides a summary, as well as examples, of the ASTM C666 results for the salt brine study. Graphical representations of all results can be found in Appendix B.

6.1 Change in Mass

Most of the non-salt-treated samples experienced small changes in mass. Some of the salt-treated prisms maintained a relatively constant mass until their terminal cycle, such as the ones for the mix shown in Figure 6.1. However, most of salt-treated samples experienced mass loss immediately after the beginning of freeze-thaw cycling. Figure 6.2 shows an example of this trend.
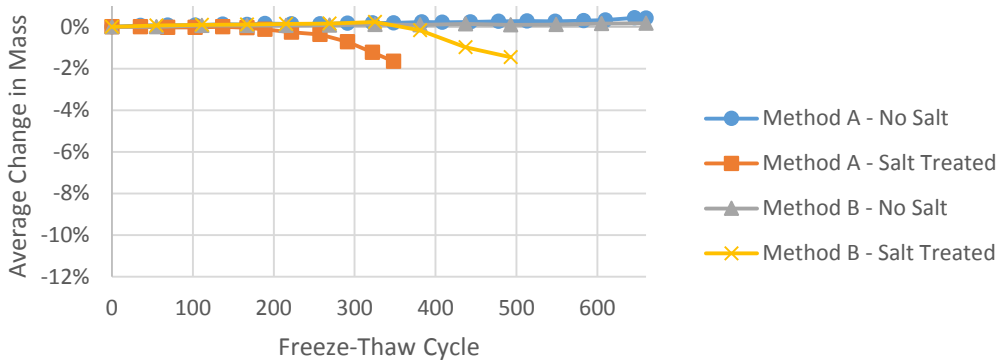
Figure 6.1: Average Change in Mass: Midwest Minerals - Parsons Samples
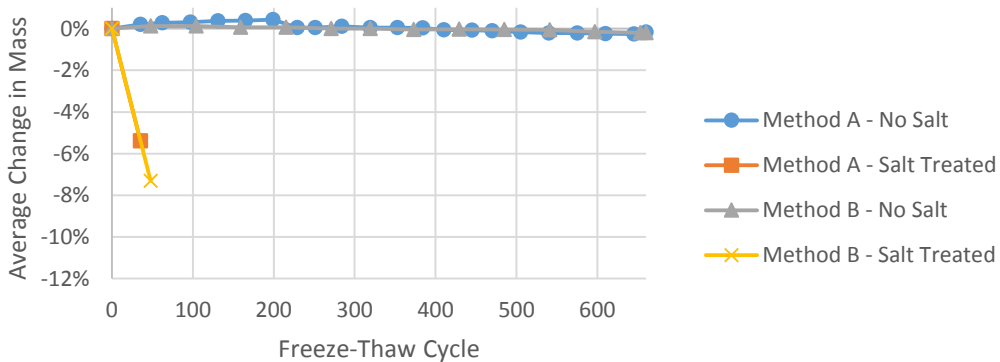
Figure 6.2: Average Change in Mass: Florence Rock Samples

Most salt-treated samples, including the ones depicted by the data in Figure 6.2, experienced severe surface scaling during the early stages of freeze-thaw testing. Figure 6.3 illustrates the deterioration of one of these samples after its final cycle of ASTM C666 Method A testing. Another prism with the same mix design and testing conditions, but without salt-treated aggregate, is displayed in Figure 6.4.

Figure 6.3: Salt Scaling of Florence Prism after 35 Cycles of Method A Testing

Figure 6.4: Non-salt-treated Florence Prism after 660 Cycles of Method A Testing

This extreme contrast in mass change and visible damage between salt-treated and non-salt-treated samples can be observed quantitatively for most of the salt brine mixes. Table 6-1 provides a summary of average change in mass for each combination of mix design, salt treatment, and freeze-thaw test method.

Table 6-1: Average Mass Change after Final Freeze-Thaw Cycle

Sample Set	ASTM C666 Test Method	Salt Treatment			
		Yes		No	
		Final Change in Mass (%)	Final Cycle	Final Change in Mass (%)	Final Cycle
Bayer	A	-2.26	105	-0.04	660
	B	-11.58	656	0.16	660
Cornejo	A	-0.43	34	0.24	660
	B	-0.62	48	0.33	660
Eastern Colorado	A	-0.29	263	0.13	300[a]
	B	-0.11	660	0.10	660
Florence	A	-5.39	35	-0.16	660
	B	-7.30	48	-0.19	660
Hamm	A	-2.33	63	0.17	541[b]
	B	-4.82	496	0.41	660
Jasper	A	-0.05	105	-0.40	660
	B	-1.75	260	0.16	660
Mid-States Edgerton	A	-1.26	63	0.08	660
	B	-3.50	104	0.18	660
Mid-States Osage (Bed 3)	A	0.35	236	-1.12	660
	B	-0.62	327	0.36	660
Mid-States Osage (Bed 4)	A	-2.81	167	0.32	270
	B	-6.45	272	-0.40	327
Midwest Minerals Ft. Scott	A	-4.85	69	0.06	660
	B	-8.62	111	0.14	660
Midwest Minerals Parsons	A	-1.65	348	0.43	660
	B	-1.46	493	0.18	660
Penny's	A	0.41	235	-0.50	300[a]
	B	-1.35	660	-0.36	660

[a] Testing terminated at 300 cycles in accordance with ASTM C666 requirements
[b] Samples removed from chamber early to make room for new samples

Table 6-1 shows that only one non-salt-treated sample set had an average mass loss exceeding 1% of its initial measurement by the completion of its final freeze-thaw cycle. The remaining 23 finished with an average mass change of 0.5% or less. Mass change for the salt-treated samples ranged between -12% and +0.5%.

Method A testing was originally only conducted until the completion of 300 cycles, as mandated by ASTM C666 (2008a). However, Method A testing was later extended to 660 cycles

in accordance with KTMR-22 (KDOT, 2006) requirements for Method B after a discussion with the KDOT project sponsor, Kyle Larson (personal communication, March 23, 2015).

6.2 Relative Dynamic Modulus of Elasticity

A summary of average RDME values for all sample sets at their terminal freeze-thaw cycle is summarized in Table 6-2.

Table 6-2: Average RDME after Final Freeze-Thaw Cycle

Sample Set	ASTM C666 Test Method	Salt Treatment			
		Yes		No	
		Final RDME (%)	Final Cycle	Final RDME (%)	Final Cycle
Bayer	A	43	105	90	660
	B	86	656	99	660
Cornejo	A	41	34	49	660
	B	72	48	90	660
Eastern Colorado	A	43	263	97	300[a]
	B	86	660	97	660
Florence	A	21	35	92	660
	B	86	48	99	660
Hamm	A	69	63	73	541[b]
	B	95	496[c]	86	660
Jasper	A	22	105	76	660
	B	66	260	93	660
Mid-States Edgerton	A	55	63	71	660
	B	79	104	95	660
Mid-States Osage (Bed 3)	A	25	236	42	660
	B	31	327	60	660
Mid-States Osage (Bed 4)	A	43	167	25	270
	B	48	272	34	327
Midwest Minerals Ft. Scott	A	27	69	47	660
	B	69	111	88	660
Midwest Minerals Parsons	A	16	348	85	660
	B	70	493	98	660
Penny's	A	64	235	94	300[a]
	B	45	660	83	660

[a] Testing terminated at 300 cycles in accordance with ASTM C666 requirements
[b] Samples removed from chamber early to make room for new samples
[c] Testing discontinued due to pins falling out of one of the samples

42

Table 6-3 lists the aggregate sets that achieved a final RDME larger than the minimum specified by KTMR-22. None of the prims that were subjected to salt treatment or ASTM C666 Method A testing met KTMR-22 final RDME requirements at 660 cycles.

Table 6-3: Qualified Aggregate Sets for KTMR-22 RDME

ASTM C666 Test Method	Salt-Treated Aggregate Sets	Non-Salt-Treated Aggregate Sets
A	None	None
B	None	Eastern Colorado Bayer Mid-States - Edgerton Florence Midwest Minerals - Parsons

An analysis was conducted to correlate the results of Method A and Method B testing for the aggregates without salt treatment. For each aggregate set, the final cycle during which all three Method B RDME readings could be obtained was identified. The average RDME at this cycle was calculated and recorded. The cycle at which the equivalent average Method A RDME occurred was then identified. This cycle was calculated through linear interpolation between the two Method A RDME values which were larger and smaller than the final Method B RDME. The difference between the final Method B cycle and the equivalent Method A cycle was then calculated. The results of this analysis are displayed in Table 6-4.

Table 6-4: Equivalent Cycle Determination for Non-Salt-Treated Aggregates

Sample Set	Method B Average RDME at Final Cycle	Method B Final Cycle	Method A Cycle with Equivalent Average RDME	Difference between Final and Equivalent Cycles
Bayer	98.6	660	28	632
Cornejo	89.6	660	418	242
Eastern Colorado	97.0	660	*	*
Florence	98.7	660	11	649
Hamm	86.3	660	395	265
Jasper	93.0	660	122	538
Mid-States Edgerton	95.3	660	253	407
Mid-States Osage (Bed 3)	59.8	660	511	149
Mid-States Osage (Bed 4)	34.3	327	236	91
Midwest Minerals Ft. Scott	88.4	660	389	271
Midwest Minerals Parsons	98.0	660	55	605
Penny's	82.8	660	*	*

* Method A RDME was not recorded long enough to drop below final Method B RDME

Another comparison was made between the non-salt-treated RDME results of Method A and Method B testing. Figure 6.5 shows a plot of the average Method B RDME for each aggregate set at 660 cycles versus the average Method A RDME at 300 cycles.
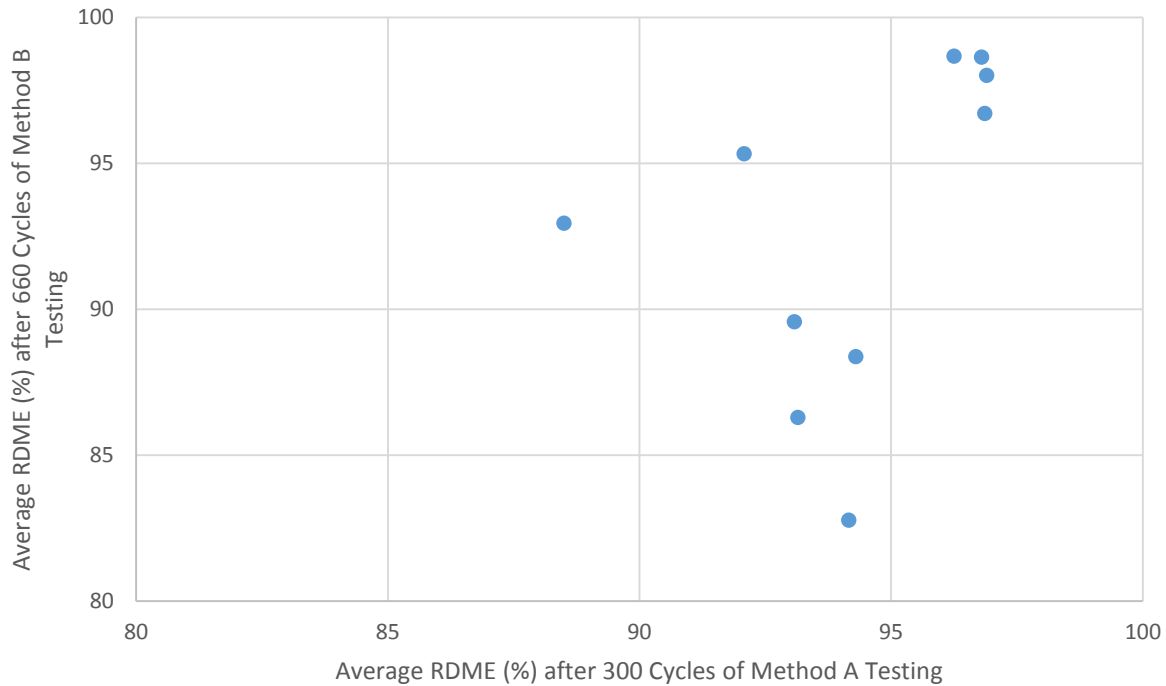
Figure 6.5: Comparison of Method A RDME at 300 Cycles with Method B RDME at 660 Cycles for Non-Salt-Treated Aggregate Sets

This plot suggests that a final RDME ≥ 95% could be used a valid acceptance requirement for Method A testing at 300 cycles. Only one aggregate set's RDME fell below 95% after 300 cycles of Method A testing and exceeded it after 660 cycles of Method B. The Method A and Method B RDME of the remaining nine aggregate sets either both stayed above or fell below 95%. Two aggregate sets were not included in the plot due to excessive deterioration.

The procedure that was used for non-salt treated aggregates to calculate the number of freeze-thaw cycles needed with Method A to reach an equivalent RDME with method B at 660 cycles was also used to calculate the equivalent Method A cycles for salt-treated aggregate sets. These results are summarized in Table 6-5.

45

Table 6-5: Equivalent Cycle Determination for Salt-Treated Aggregates

Sample Set	Method B Average RDME at Final Cycle	Method B Final Cycle	Method A Cycle with Equivalent Average RDME	Difference between Final and Equivalent Cycles
Bayer	86.3	656	20	636
Cornejo	71.7	104	16	88
Eastern Colorado	86.3	660	153	507
Florence	86	48	6	42
Hamm	95	496	6	490
Jasper	66	260	81	179
Mid-States Edgerton	79	104	25	79
Mid-States Osage (Bed 3)	31.3	327	217	110
Mid-States Osage (Bed 4)	48	272	159	113
Midwest Minerals Ft. Scott	69.3	111	25	86
Midwest Minerals Parsons	69.7	493	235	258
Penny's	45.4	660	*	*

* Method A RDME was not recorded long enough to drop below final Method B RDME

No significant correlations in freeze-thaw performance were observed between salt-treated and non-salt-treated samples. However, the results could be used to predict the performance of these aggregates in the field when exposed to deicing salts. The salt-treated aggregate sets subjected to Method A always showed lower RDME values and failed quicker than those tested under Method B. This likely occurred because of the higher degree of saturation in Method A samples caused by freezing in water. Additionally, the hygroscopic characteristics of salt can lead to more water retention, which also increases the concrete degree of saturation.

6.3 Expansion

A summary of average expansion values for all sample sets at their terminal freeze-thaw cycle is summarized in Table 6-6.

Table 6-6: Average Expansion after Final Freeze-Thaw Cycle

Sample Set	ASTM C666 Test Method	Salt Treatment			
		Yes		No	
		Final Expansion (%)	Final Cycle	Final Expansion (%)	Final Cycle
Penny's	A	0.73[c]	235	0.53[c]	300[a]
	B	0.34	660	0.07	660
Eastern Colorado	A	0.08	263	0.02	300[a]
	B	0.05	660	0.01	660
Jasper	A	0.11	105	0.08	660
	B	0.39	260	0.04	660
Bayer	A	0.09	105	0.05	660
	B	0.13	656	0.01	660
Hamm	A	0.08	63	0.06	541[b]
	B	0.09	496	0.02	660
Mid-States Edgerton	A	0.13	63	0.08	660
	B	0.04	104	0.02	660
Mid-States Osage (Bed 3)	A	0.20	236	0.13	660
	B	0.24	327	0.11	660
Mid-States Osage (Bed 4)	A	0.20	167	0.25	270
	B	0.10	272	0.24	327
Florence	A	0.13	35	0.02	660
	B	0.05	48	0.00	660
Midwest Minerals Parsons	A	0.28	348	0.05	660
	B	0.12	493	0.01	660
Midwest Minerals Ft. Scott	A	0.28	69	0.10	660
	B	0.76	111	0.02	660
Cornejo	A	0.16	34	0.11	660
	B	0.07	48	0.03	660

[a] Testing terminated at 300 cycles in accordance with ASTM C666 requirements
[b] Samples removed from chamber early to make room for new samples
[c] Invar bar damaged during testing

Table 6-7 lists the aggregate sets that achieved a final expansion less than the maximum specified by KTMR-22.

Table 6-7: Qualified Aggregate Sets for KTMR-22 Expansion

ASTM C666 Test Method	Salt-Treated	No Salt Treatment
A	None	Florence
B	None	Eastern Colorado Bayer Hamm Mid-States - Edgerton Florence Midwest Minerals - Parsons Midwest Minerals - Fort Scott

None of the prims that were subjected to salt treatment met KTMR-22 final expansion requirements. Table 6-3 and Table 6-7 show that only non-salt-treated aggregate sets had acceptable RDME and expansion performance according to KTMR-22. Five of twelve sets met both of these requirements when subjected to ASTM C666 Method B testing, and only one passed after Method A testing.

6.4 Sawcut Sample Forensic Investigation

A visual inspection of sawcut prisms was also conducted to obtain more information on the damage mechanisms occurring during freeze-thaw cycling. The concrete prisms selected for sawcutting were from the Florence aggregate set due to its extremes in performance. With non-salt-treated aggregate, it finished with the highest average relative modulus compared to the other eleven aggregates. However, it performed poorly compared to the other aggregate sets when its aggregate was treated with salt. Figure 6.6 through Figure 6.9 show images of these sawcut samples. Mass loss was observed near the edges of the samples. It is likely that salt diffused out of the aggregates into the paste, causing the paste to adsorb water faster and increase the degree of

saturation. There was some cracking seen in a few coarse aggregate particles in the salt-treated sample tested in Procedure A. This could indicate that some of the coarse aggregate particles were unsound. When close to the surface, they were able to adsorb sufficient water to cause damage. It is likely that this damage occurred quickly, causing those particles to be quickly removed, reducing the number of cracked aggregates seen.

Figure 6.6: Non-salt-treated Florence Sample Subject to Method A Testing

Figure 6.7: Salt-treated Florence Sample Subject to Method A Testing

Figure 6.8: Non-salt-treated Florence Sample Subject to Method B Testing
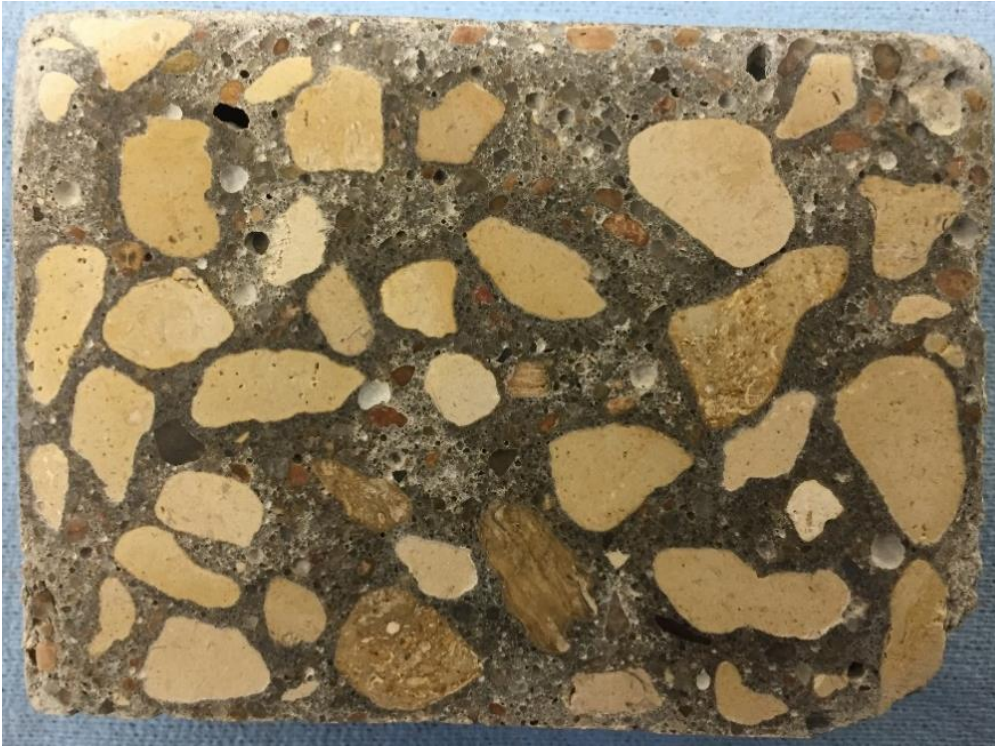
Figure 6.9: Salt-treated Florence Sample Subject to Method B Testing

Chapter 7 - Analysis and Discussion

7.1 Accelerated Curing

The two 30-day curing methods were generally found to yield lower final RDME values than those specified by KTMR-22. The RDME results presented in Table 5-3 are illustrated as scatter plots in Figure 7.1 and Figure 7.2. Each compares one of the 30-day curing methods with KTMR-22 curing. The figures are divided into quadrants with two lines drawn along x = 60 and y = 95, which represent the minimum acceptable RDME values typically used for ASTM C666 and KTMR-22, respectively.
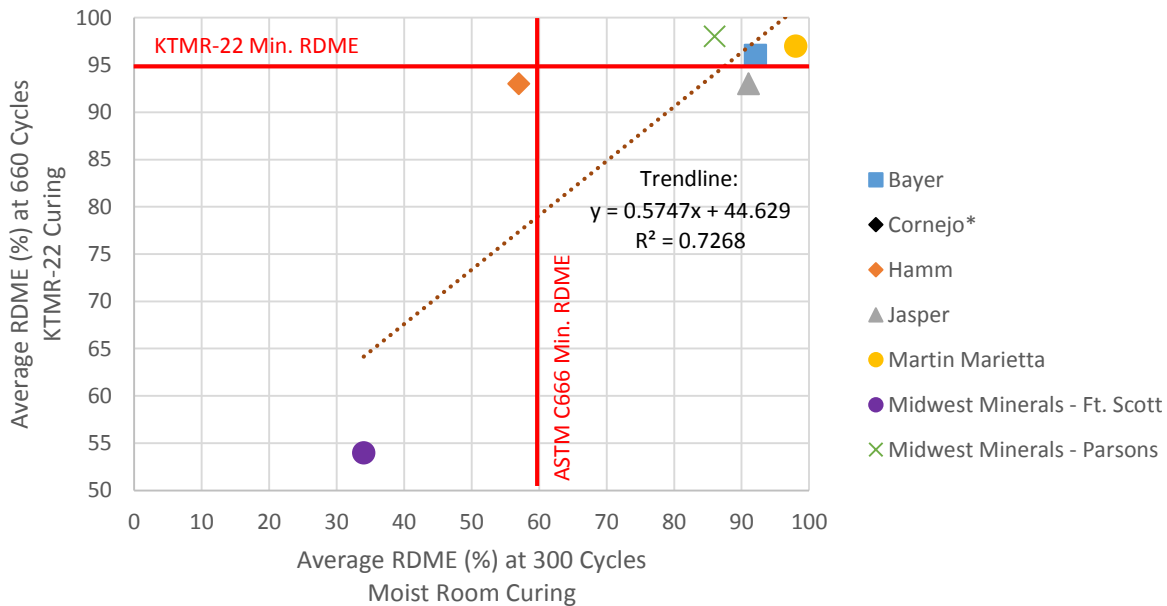
* Excessive deterioration of moist room cured samples prevented measurement of RDME at 300 cycles

Figure 7.1: Comparison of RDME Results for Moist Room- and KTMR-22-cured Samples against ASTM C666 and KTMR-22 Requirements
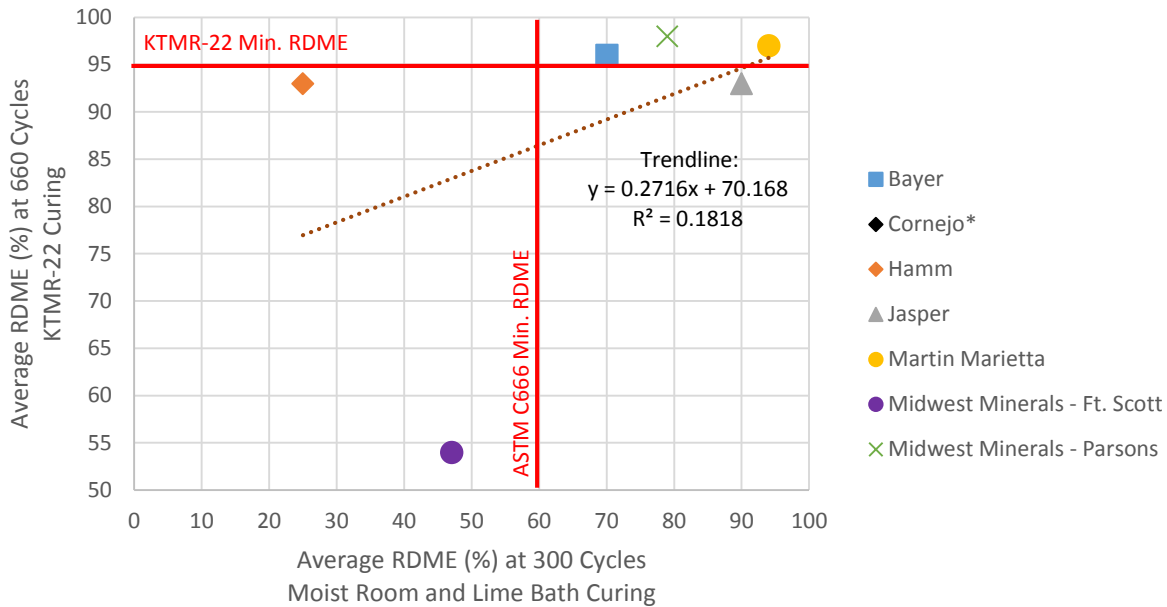
* Excessive deterioration of moist room & lime bath cured samples prevented measurement of RDME at 300 cycles

Figure 7.2: Comparison of RDME Results for Moist Room/Lime Bath- and KTMR-22-cured Samples against ASTM C666 and KTMR-22 Requirements

The trends observed in Figure 7.1 and Figure 7.2 suggest that KDOT's procedure for identifying durable aggregate can be significantly shortened. The upper right quadrant represents the sample sets that meet ASTM C666 RDME requirements after 30 days of curing as well as KTMR-22 requirements after 90 days of curing. The same three sample sets fall in this quadrant for both 30-day curing methods. Two sample sets fall in the lower left quadrant, which represents 30-day-cured samples that failed ASTM C666 and 90-day-cured samples that failed KTMR-22. The Cornejo aggregate set would theoretically also be included in this quadrant. Its KTMR-22 RDME was 76% at 660 cycles and both 30-day-cure RDME values were less than 40% at 119 cycles. The extreme damage of the 30-day-cured samples prevented measurements from being taken at 300 cycles however. Therefore, this data point was excluded from both plots. Only one aggregate set fell in the lower right quadrant, which means it passed the commonly used ASTM C666 acceptance criteria, but failed KTMR-22. However, its final 90-day-cure RDME of 93% shows that it was close to passing and may have done so if tested again. These results suggest that if a given sample set exposed to one of the 30-day cure periods maintains a RDME above 60% after 300 freeze-thaw cycles, it will most likely achieve a RDME above 95% after 660 cycles when

subjected to the KTMR-22 curing method. By switching to 30 days of curing and approximately one month of freeze-thaw cycling, KDOT could reduce the duration of their test procedure by almost four months. Data from more aggregates is needed to verify this trend.

The data displayed in Table 5-4 does not show a clear trend between the final RDME for KTMR-22 curing and the cycle at which the equivalent RDME occurs for the 30-day curing methods. This can be attributed to a significant drop in RDME that typically occurs between cycle 0 and the next cycle at which durability readings were recorded. For many of the 30-day-cured samples, the first RDME reading recorded after cycle 0 was lower than the KTMR-22 RDME at 660 cycles. This drop was not always an accurate representation of their overall freeze-thaw performance. The RDME typically either decreased at a slower rate or stabilized immediately after the drop, as is shown in Figure 7.3 and Figure 7.4.
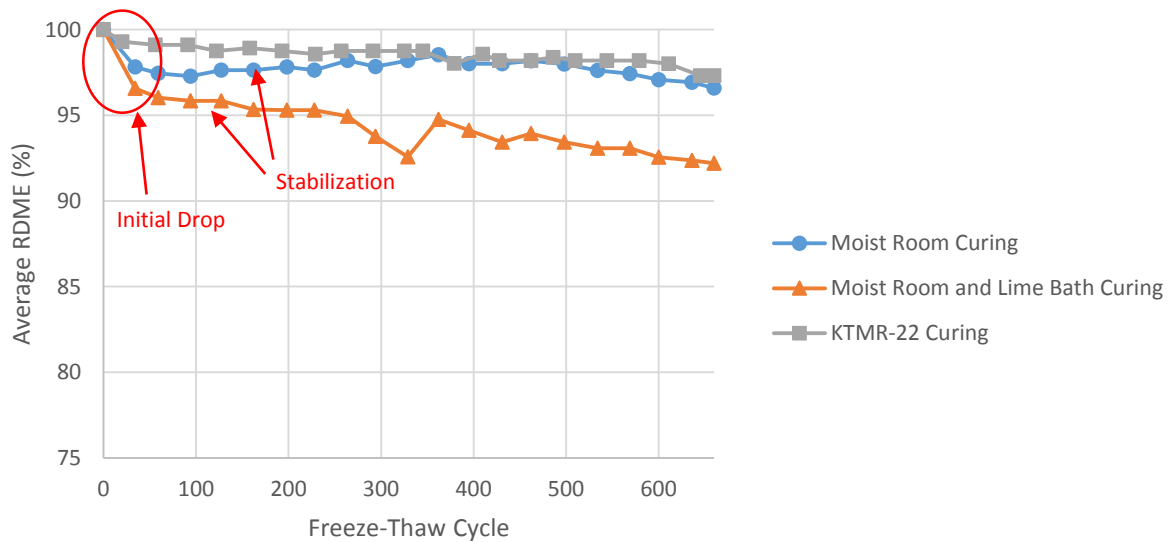
Figure 7.3: Initial Drop in RDME followed by Stabilization
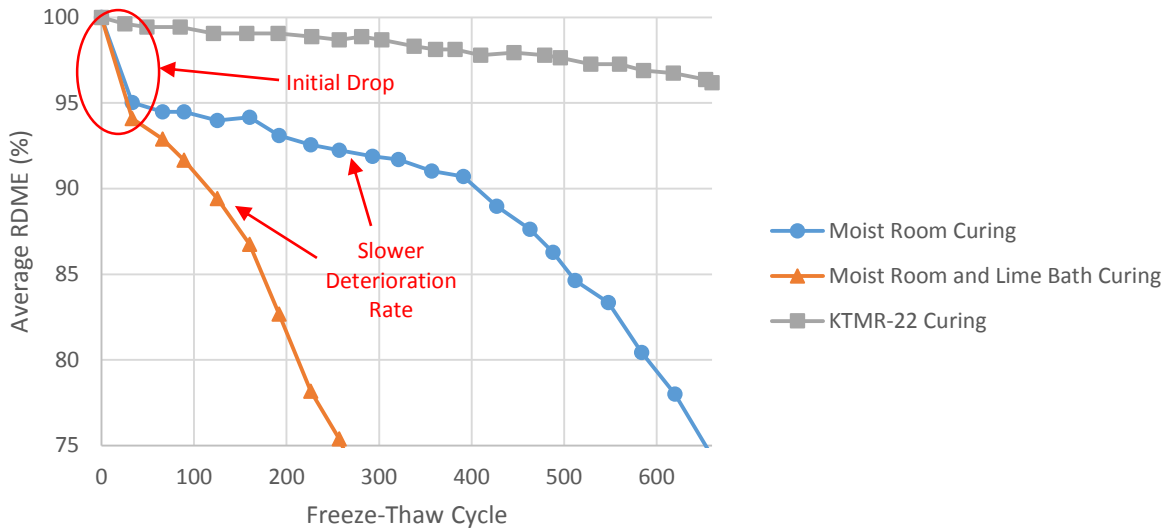
Figure 7.4: Initial Drop in RDME followed by Slower Deterioration Rate

Final expansion values for the 30-day cure methods were typically higher than those of the KTMR-22 curing. The expansion results from Table 5-6 are displayed in Figure 7.5 and Figure 7.6 with boundary lines denoting the expansion limitations commonly used by ASTM C666 and KTMR-22.
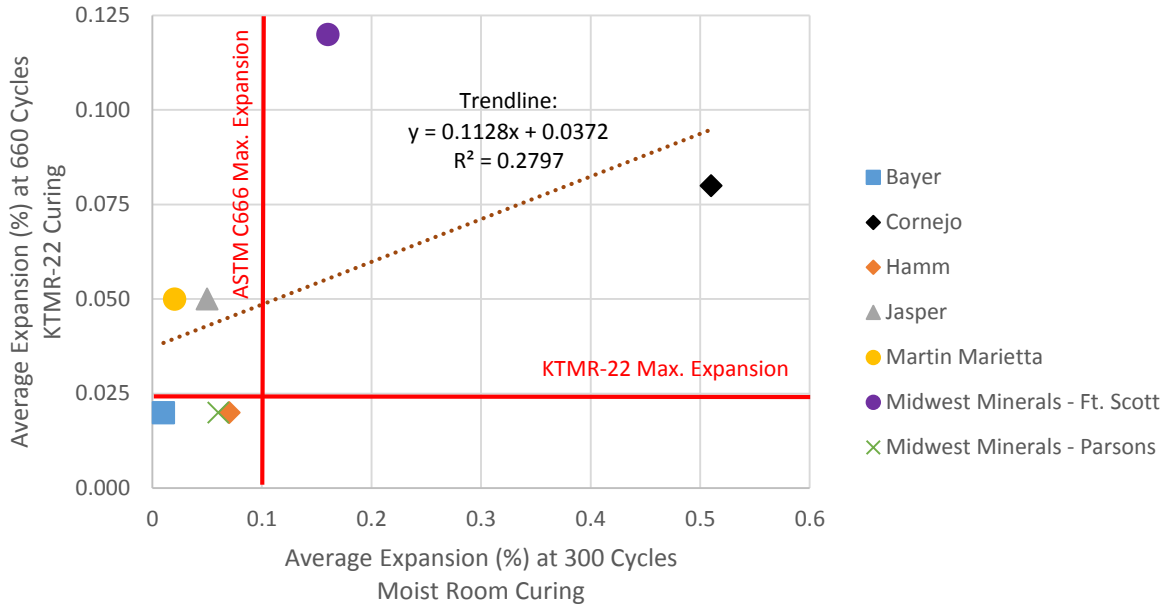
Figure 7.5: Comparison of Expansion Results for Moist Room- and KTMR-22-cured Samples against ASTM C666 and KTMR-22 Requirements
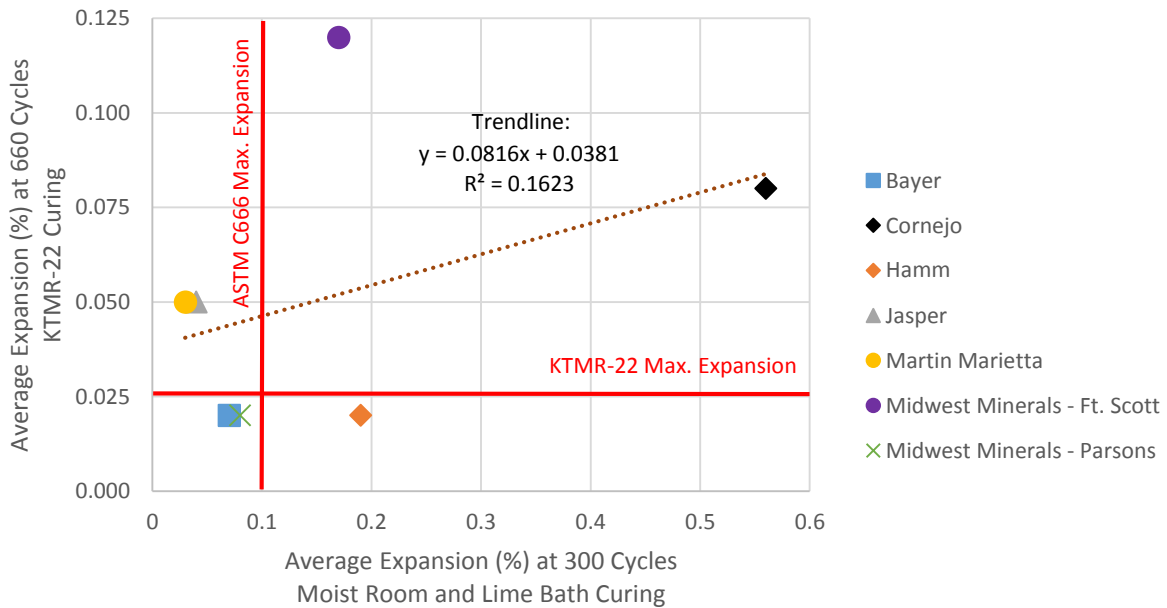
Figure 7.6: Comparison of Expansion Results for Moist Room/Lime Bath- and KTMR-22-cured Samples against ASTM C666 and KTMR-22 Requirements

The expansion results do not show a clear correlation between 30-day-cured samples that pass ASTM C666 and 90-day-cured samples that pass KTMR-22. The Hamm aggregate set met expansion requirements for the moist room and KTMR-22 curing regimes, but not for the moist room plus lime bath method. Martin Marietta, the aggregate set with the highest overall performance in RDME, performed very well in expansion for the accelerated curing methods. However, due to one sample with a 0.11% expansion, the average KTMR-22 expansion was raised to 0.05%. Since this exceeds the maximum limit of 0.025%, the Martin Marietta aggregate set would technically be disqualified from use in pavement according to KTMR-22. Failing KTMR-22 does not seem to be an accurate representation of this aggregate's durability level as it generally performed well, rather than marginally. This suggests that the expansion requirements for aggregate qualification could be adjusted to slightly less stringent values, especially considering that expansion is an optional test in ASTM C666 (2008a).

No significant trends were observed in determining the equivalent freeze-thaw cycles related to final KTMR-22 expansion in Table 5-7. Multiple sample sets cured under the KTMR-22 regime finished with small final expansions. However, the equivalent cycles of the shorter curing methods for these sample sets were as low as cycle 64 and as high as cycle 391. This does not lead to an accurate prediction of the KTMR-22 final expansion based on expansion behavior for the accelerated cure regimes.

7.2 Salt Treatment of Aggregates

Further analysis was conducted on the equivalent cycle data presented in Table 6-4 for non-salt-treated aggregate sets. Figure 7.7 shows a comparison between each sample set's average RDME at its terminal cycle to the difference between final and equivalent cycles of Method A.
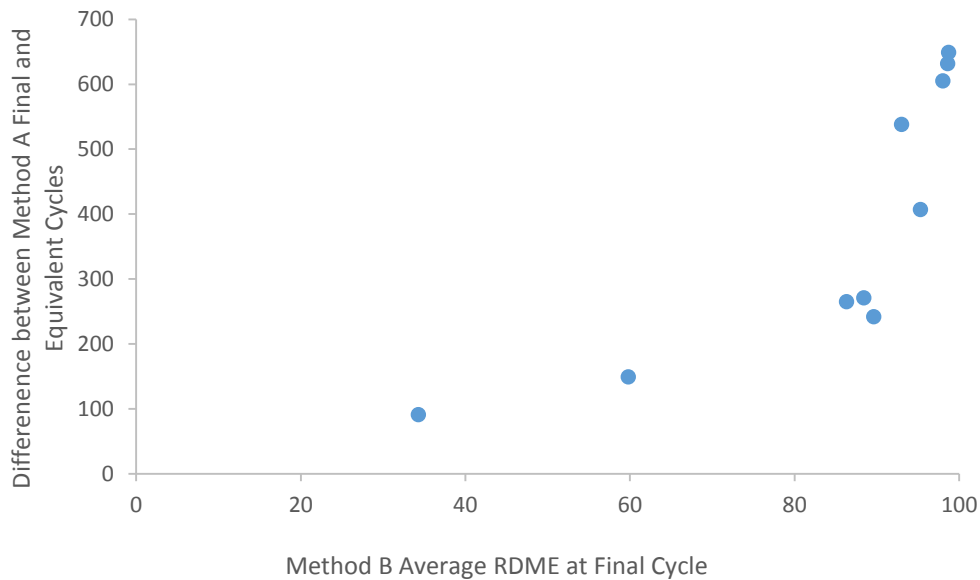
Figure 7.7: Comparison of Method B Final RDME to the Difference between Method A Final and Equivalent Cycles

The difference in final and equivalent cycles increases with increasing final RDME of Method B samples, which can primarily be attributed to a decreasing equivalent cycle with higher Method B performance. This occurred because Method A accelerates deterioration compared to Method B. Additionally, a small difference in RDME of high-performing aggregates can cause a large difference in equivalent cycle number above a RDME of 95%. A similar trend was observed for the salt-treated aggregate sets. In general, as the final cycle decreases, the difference between the final and equivalent cycles decreases as well.

The data presented in Figure 6.5 show that the same aggregate performance requirements can apply to Method A and Method B testing. If this acceptance criteria was implemented for Method A at the completion of 300 freeze-thaw cycles, rather than for Method B at 660, KDOT's aggregate qualification procedures could be reduced by at least one month.

The sawcut sample image presented in Figure 6.7 shows some cracking in coarse aggregate near the edges. The deformed edges of this sample illustrate that severe surface scaling occurred as well. This suggests that the exterior aggregates absorbed some of the water surrounding the prism during Method A testing. These aggregates reached critical saturation in the early stages of freeze-thaw cycling and began to deteriorate quickly. Additionally, some of the salt particles likely

came in contact with the cement paste and accelerated the rate of saturation near the sample edges. As a result, paste and damaged aggregates were removed from the sample's surface.

Method A testing with salt-treated aggregates could be used to replicate and accelerate conditions observed in concrete pavement joints under distress. This may help in determining material vulnerability to joint rot and finding mitigation methods. The extreme contrast in performance of aggregates in the salt-treated test method could help explain differences in performance of pavement joints in concrete made with different aggregates.

Chapter 8 - Conclusions

The KTMR-22 90-day curing regime generally yielded higher durability results compared to those of the two 30-day curing methods examined in the accelerated cure study. The RDME results strongly suggest that a test method consisting of a 30-day curing period followed by 300 freeze-thaw cycles could be used in lieu of 90 days of curing and 660 cycles of testing. By implementing a lower RDME acceptance threshold at 300 cycles for this potential new test method, KDOT aggregate qualification procedures could be reduced by at least three months. More work is needed to test additional aggregates in accelerated curing.

Both salt-treated and non-salt-treated aggregates produced similar trends in freeze-thaw performance when comparing ASTM C666 Method A and Method B test results. Visual inspection of sawcut samples suggests that the salt actually accelerates surface cement paste damage more than D-cracking of the coarse aggregate. Salt treatment of aggregates could indicate a difference in performance of aggregates when exposed to salts in freeze-thaw conditions. However, salt treatment did not appear to predict performance of aggregates when not exposed to salt. The RDME results for non-salt-treated aggregates provide strong evidence that a minimum required RDME of 95% could be used as an acceptance standard for Method A testing after the completion of 300 cycles. This would yield a shorter test duration than 660 cycles of Method B.

8.1 Recommendations for Future Research

Freeze-thaw results for 17 other aggregate sets have yet to be obtained for the accelerated cure study. These results can be used to verify or reject an adjusted test method consisting of a 30-day curing period followed by fewer freeze-thaw cycles.

Further ASTM C666 Method A and Method B testing of non-salt-treated samples should be conducted to validate that the current KTMR-22 acceptance criteria for Method B would also work for Method A at fewer cycles. Salt treatment of aggregates should be used as a future test method for determining the effects of salt exposure on the freeze-thaw resistance of cement paste.

References

Afrani, I., & Rogers, C. (1994). The Effects of Different Cementing Materials and Curing on Concrete Scaling. *Cement, Concrete, and Aggregates*, 132-139.

Akhavan, R., & Malik, M. (1999). *Initial Curing of Portland Cement Concrete Cylinders.* Colorado Department of Transportation, Denver, CO.

Al-Assadi, G., Casati, M., Fernandez, J., & Galvez, J. (2010). Effect of the curing conditions of concrete on the behaviour under freeze-thaw cycles. *Fatigue & Fracture of Engineering Materials & Structures*, pp. 461-469.

ASTM. (2008a). ASTM C666: Standard Test Method for Resistance of Concrete to Rapid Freezing and Thawing. In *Annual Book of ASTM Standards: Volume 4.02: Concrete and Aggregates.* West Conshohocken, PA.

ASTM. (2012a). ASTM C295: Standard Guide for Petrographic Examination of Aggregates for Concrete. In *Annual Book of ASTM Standards: Volume 4.02: Concrete and Aggregates.* West Conshohocken, PA.

ASTM. (2012b). ASTM C457: Standard Test Method for Microscopical Determination of Parameters of the Air-Void System in Hardened Concrete. In *Annual Book of ASTM Standards: Volume 4.02: Concrete and Aggregates.* West Conshohocken, PA.

ASTM. (2012c). ASTM C127: Standard Test Method for Density, Relative Density (Specific Gravity), and Absorption of Coarse Aggregate. In *Annual Book of ASTM Standards: Volume 4.02: Concrete and Aggregates.* West Conshohocken, PA.

ASTM. (2012d). ASTM C128: Standard Test Method for Density, Relative Density (Specific Gravity), and Absorption of Fine Aggregate. In *Annual Book of ASTM Standards: Volume 4.02: Concrete and Aggregates.* West Conshohocken, PA.

ASTM. (2012e). ASTM C1064: Standard Test Method for Temperature of Freshly Mixed Hydraulic-Cement Concrete. In *Annual Book of ASTM Standards: Volume 4.02: Concrete and Aggregates.* West Conshohocken, PA.

ASTM. (2013). ASTM C88: Standard Test Method for Soundness of Aggregates by Use of Sodium Sulfate or Magnesium Sulfate. In *Annual Book of ASTM Standards: Volume 4.02: Concrete and Aggregates.* West Conshohocken, PA.

ASTM. (2014a). ASTM C138: Standard Test Method for Density (Unit Weight), Yield, and Air Content (Gravimetric) of Concrete. In *Annual Book of ASTM Standards: Volume 4.02: Concrete and Aggregates.* West Conshohocken, PA.

ASTM. (2014b). ASTM C231: Standard Test Method for Air Content of Freshly Mixed Concrete by the Pressure Method. In *Annual Book of ASTM Standards: Volume 4.02: Concrete and Aggregates.* West Conshohocken, PA.

ASTM. (2015a). ASTM C192: Standard Test Method for Making and Curing Concrete Test Specimens in the Laboratory. In *Annual Book of ASTM Standards: Volume 4.02: Concrete and Aggregates.* West Conshohocken, PA.

ASTM. (2015b). ASTM C143: Standard Test Method for Slump of Hydraulic-Cement Concrete. In *Annual Book of ASTM Standards: Volume 4.02: Concrete and Aggregates.* West Conshohocken, PA.

Clowers, K. A. (1999). *Seventy-five Years of Aggregate Reserach in Kansas.* Kansas Department of Transportation, Topeka, KS.

Distlehorst, J. A., & Kurgan, G. J. (2007). Development of Precision Statement for Determining Air Void Characteristics of Fresh Concrete with Use of Air Void Analyzer. *Transportation Research Record*, 45-49.

Du, L., & Folliard, K. J. (2005). Mechanisms of air entrainment in concrete. *Cement and Concrete Research*, 1463-1471.

Embacher, R. A., & Snyder, M. B. (2003). *Refinement and Validation of the Hydraulic Fracture Test.* University of Minnesota. St. Paul, MN: Minnesota Department of Transportation.

Hanna, K., Morcous, G., & Tadros, M. K. (2014). Effect of Supplementary Cementitious Materials on Rheological Properties, Bleeding, and Strength of Structural Grout. *Journal of Materials in Civil Engineering*, 789-793.

Hossain, M., & Zurbey, M. H. (1996). *Correlation of KDOT and SHRP's Washington Hydraulic Fracture Index (WHFI) Aggregate Durability Test Methods.* NTIS.

Issa, M. A., Issa, M. A., & Bendok, M. (1999). *Evaluation of Washington Hydraulic Fracture Test (SHRP) for D-Cracking Aggregate.* University of Illinois at Chicago.

Janssen, D. J., & Snyder, M. B. (1994). *Resistance of Concrete to Freezing and Thawing.* Strategic Highway Research Program: Nation Research Council, Washington, DC.

Jonsson, J. A., & Olek, J. (2004). Effect of Temperature-Match-Curing on Freeze-Thaw and Scaling Resistance of High-Strength Concrete. *Cement, Concrete, and Aggregates*, pp. 1-5.

KDOT. (2006). KTMR-22: Resistance of Concrete to Rapid Freezing and Thawing. In *KDOT Standard Specifications for State Road and Bridge Construction.* Topeka, KS.

KDOT. (2007). KT-6: Specific Gravity and Absorption of Aggregates. In *KDOT Construction Manual: Part IV.* Topeka, KS.

Kimbrough, D. (2006, February). Salting Roads: The Solution for Winter Driving. *ChemMatters*, pp. 14-16.

Koubaa, A., & Snyder, M. B. (1996). Evaluation of Frost Resistance Tests for Carbonate Aggregates. *Transportation Research Record*, pp. 35-45.

Lee, M.-G. (2007). Preliminary Study for Strength and Freeze-Thaw Durability of Microwave- and Steam-Cured Concrete. *Journal of Materials in Civil Engineering*, pp. 972-976.

Li, W., Pour-Ghaz, M., Castro, J., & Weiss, J. (2012). Water Absorption and Critical Degree of Saturation Relating to Freeze-Thaw Damage in Concrete Pavement Joints. *Journal of Materials in Civil Engineering*, 299-307.

Mamlouk, M. S., & Zaniewski, J. P. (2011). *Materials for Civil and Construction Engineers.* Upper Saddle River, NJ: Pearson Education, Inc.

Marks, V. J., & Grubb, R. E. (1969). *A Study of Curing Methods and Type II Cements on the Durability of Concrete.* Iowa State Highway Commision, Materials Department.

McLeod, H. A., Welge, J., & Henthorne, R. (2014). *Aggregate Freeze-Thaw Testing and D-Cracking Field Performance: 30 Years Later.* Kansas Department of Transportation, Topeka, KS.

Michigan Department of Transportation. (2015). *Manual for the Michigan Test Methods (MTM's).*

Miller, J. S., & Bellinger, W. Y. (2003). *Distress Identification Manual for the Long-Term Pavement Performance Program.* Federal Highway Administration, McLean, VA.

Moussalli, S. G. (1986). *Evaluation of Fly Ash Concrete Durability Containing Class II Durability Aggregates.* Iowa Department of Transportation, Office of Materials.

NDT James Instruments Inc. (n.d.). *Emodumeter for Resonant Frequency Testing Determining Young's Modulus (E) and Poisson's Ratio*. Retrieved February 2016, from James Instruments Non Destructive Test Equipment: http://www.ndtjames.com/Emodumeter-Resonant-Frequency-Test-Equipment-p/v-e-400.htm

Nebraska Department of Roads. (2008). *Optimized Aggregates Gradations for Portland Cement Concrete Mix Designs Evaluation.*

O'Doherty, J. (1987, May). D-Cracking of Concrete Pavements. *Materials and Technology Engineering and Science*.

Ohio Department of Transportation. (2013). 703: Aggregates. In *Construction and Material Specifications* (pp. 717-718). Columbus, Ohio.

Pigeon, M., Pleau, R., & Aitcin, P.-C. (1986). Freeze-Thaw Durability of Concrete With and Without Silica Fume in ASTM C 666 (Procedure A) Test Method: Internal Cracking Versus Scaling. *Cement, Concrete, and Aggregates*, 76-85.

Riding, K. A., Blackwell, B., Momeni, A. F., & McLeod, H. (2013). *Effects of Curing Methods and Supplementary Cementitious Material Use on Freeze Thaw Durability of Concrete Containing D-Cracking Aggregates.* Kansas State University.

Schwartz, D. R. (1987). *D-Cracking of Concrete Pavements.* Transportation Research Board. Washington, D.C.: National Cooperative Highway Research Program.

Shakoor, A., West, T. R., & Scholer, C. F. (1982). Physical Characteristics of Some Indiana Argillaceous Carbonates Regarding Their Freeze-Thaw Resistance in Concrete. *Bulletin of the Association of Engineering Geologists*, 371-384.

Spragg, R. P., Castro, J., Li, W., Pour-Ghaz, M., Huang, P.-T., & Weiss, J. (2011). Wetting and drying of concrete using aqueous solutions containing deicing salts. *Cement & Concrete Composites*, 535-542.

Stark, D. (1975). Living with Marginal Aggregates. *Annual Meeting of the American Society for Testing and Materials* (p. 48). Montreal, Canada: ASTM.

Tanesi, J., & Meininger, R. (2006). *Freeze-Thaw Resistance of Concrete with Marginal Air Content.* Federal Highway Administration, McLean, VA.

Vogler, R. H., & Grove, G. H. (1989). Freeze-Thaw Testing of Coarse Aggregate in Concrete: Procedures Used by Michigan Department of Transportation and Other Agencies. *Cement, Concrete, and Aggregates*, 57-66.

Wang, K., Lomboy, G., & Steffes, R. (2009). *Investigation into Freezing-Thawing Durability of Low-Permeability Concrete with and without Air Entraining Agent.* Iowa State University.

Whitehurst, E. (1980). D-cracking and aggregate size. *Concrete Construction*, 593-596.

Woodhouse, T. (2005). *Multi-State Coarse Aggregate Freeze-Thaw Comparison.* Michigan Department of Transportation, Construction and Technology Division.

Zemei, W., Caijun, S., Peiwei, G., Wang, D., & Cao, Z. (2015). Effects of Deicing Salts on the Scaling Resistance of Concrete. *Journal of Materials in Civil Engineering*.

Appendix A - Accelerated Cure ASTM C666 Results

Average changes in concrete prism mass for each aggregate set are plotted in Figure A.1 through Figure A.7.
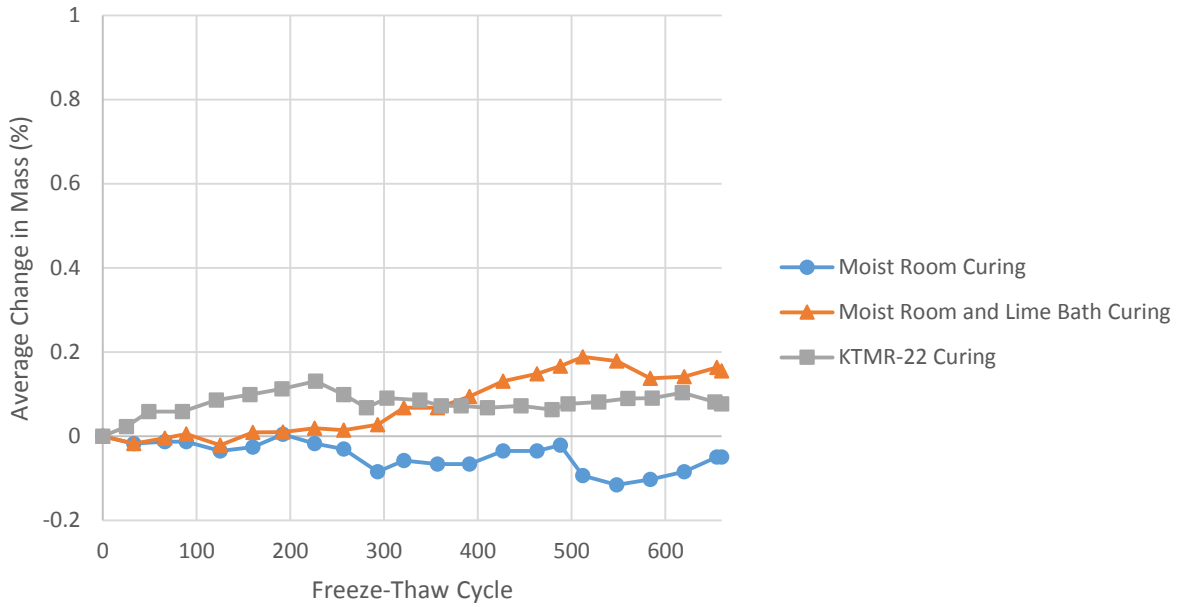
Figure A.1: Average Change in Mass: Bayer Construction Samples
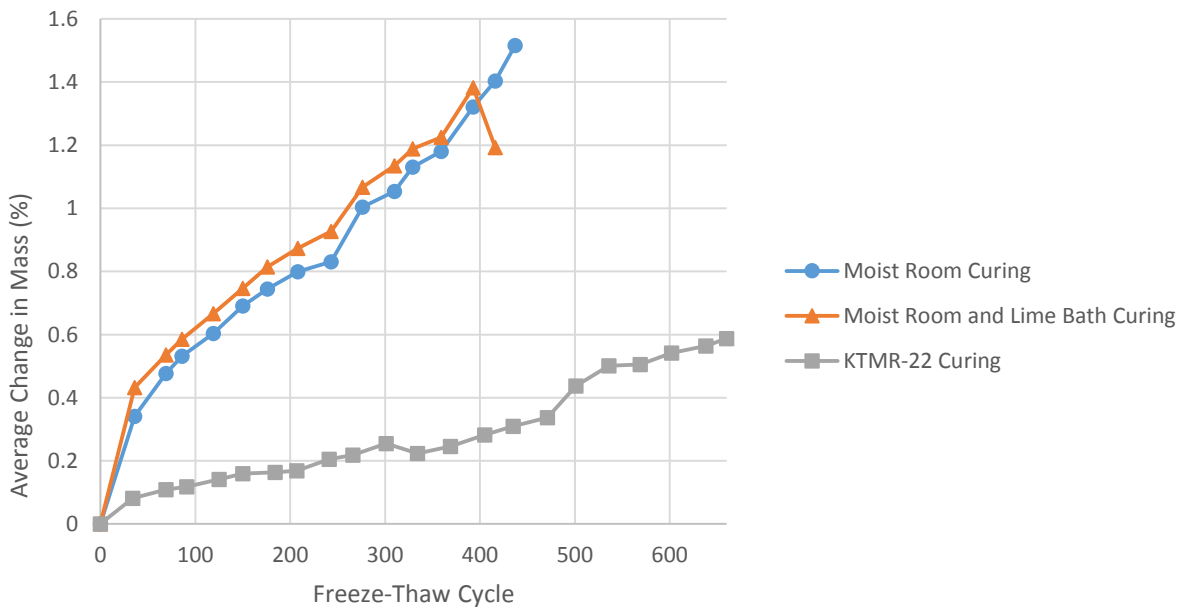
Figure A.2: Average Change in Mass: Cornejo Stone Samples
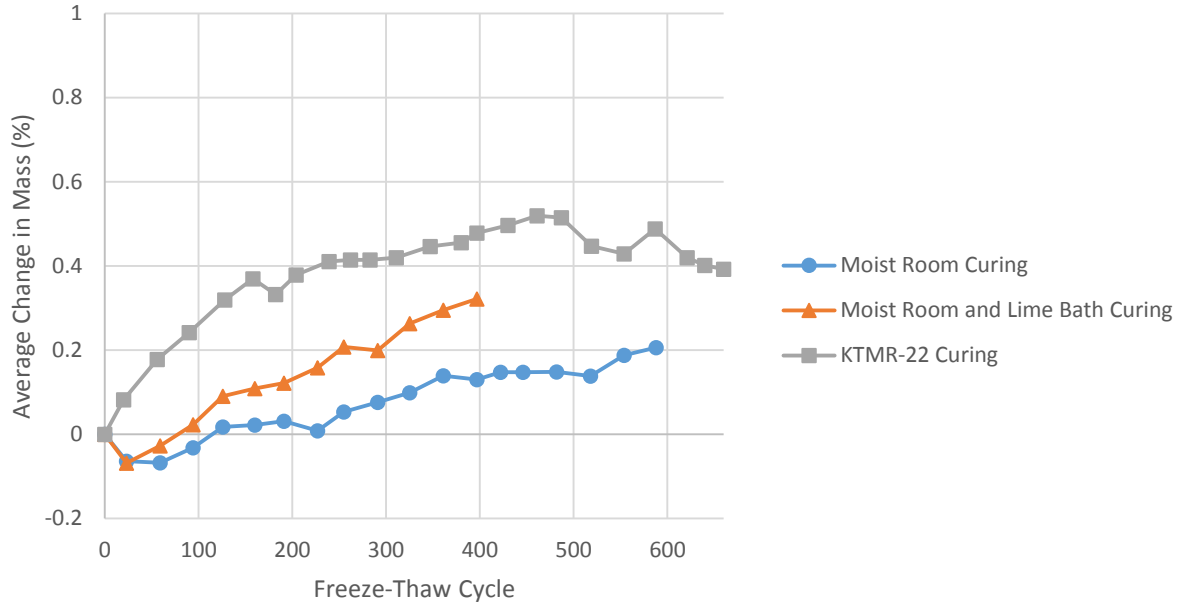
Figure A.3: Average Change in Mass: Hamm WB Samples
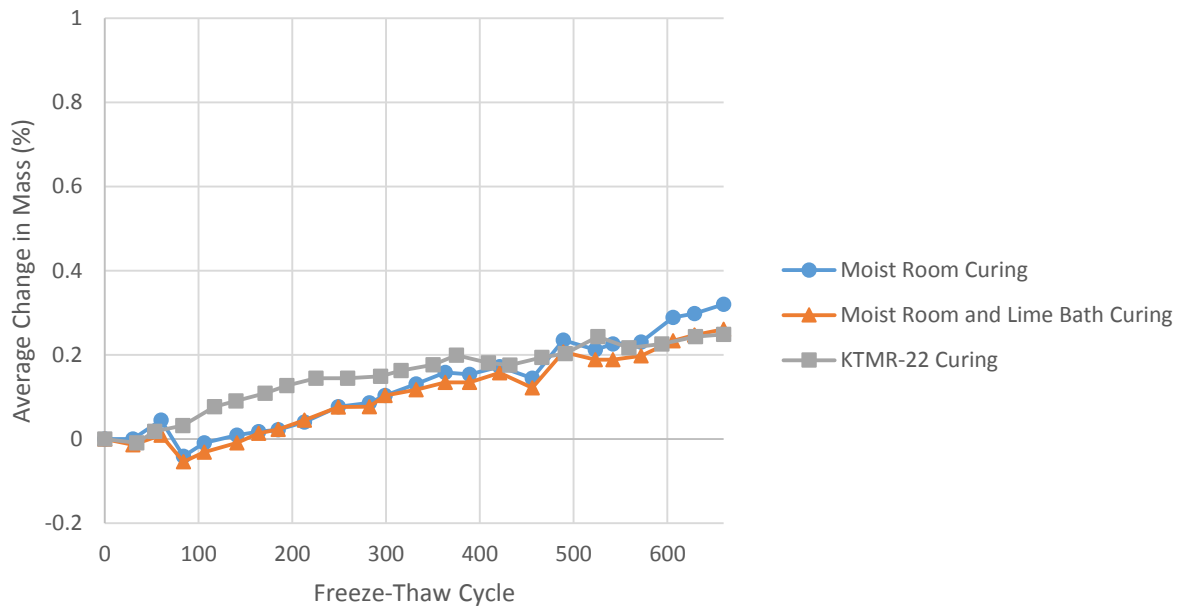
Figure A.4: Average Change in Mass: Jasper Stone Samples
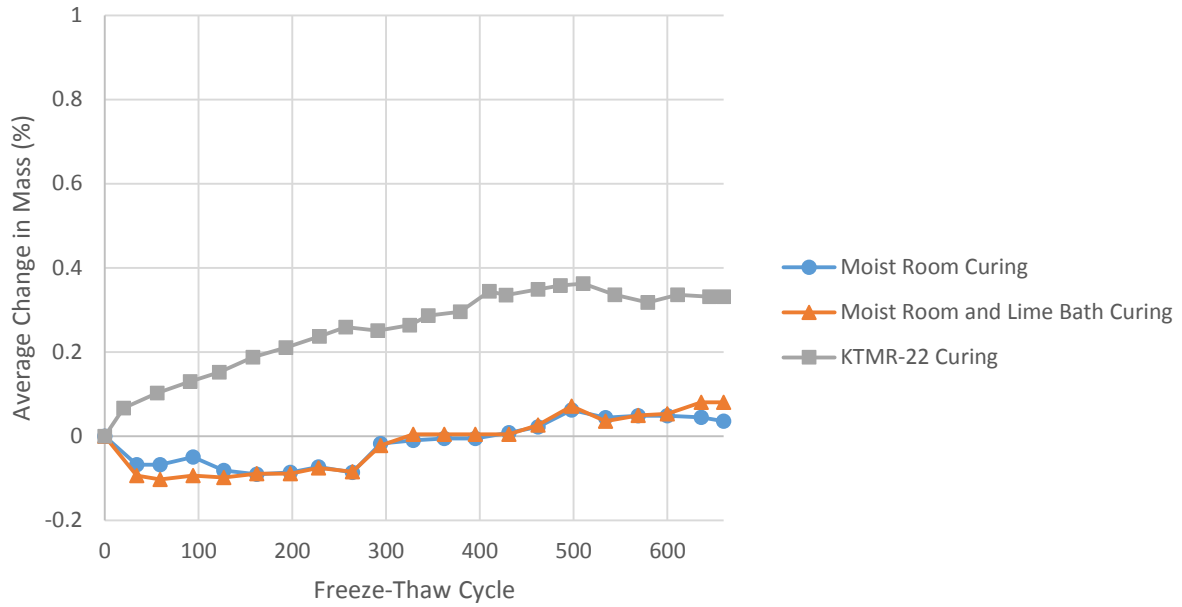
Figure A.5: Average Change in Mass: Martin Marietta Samples
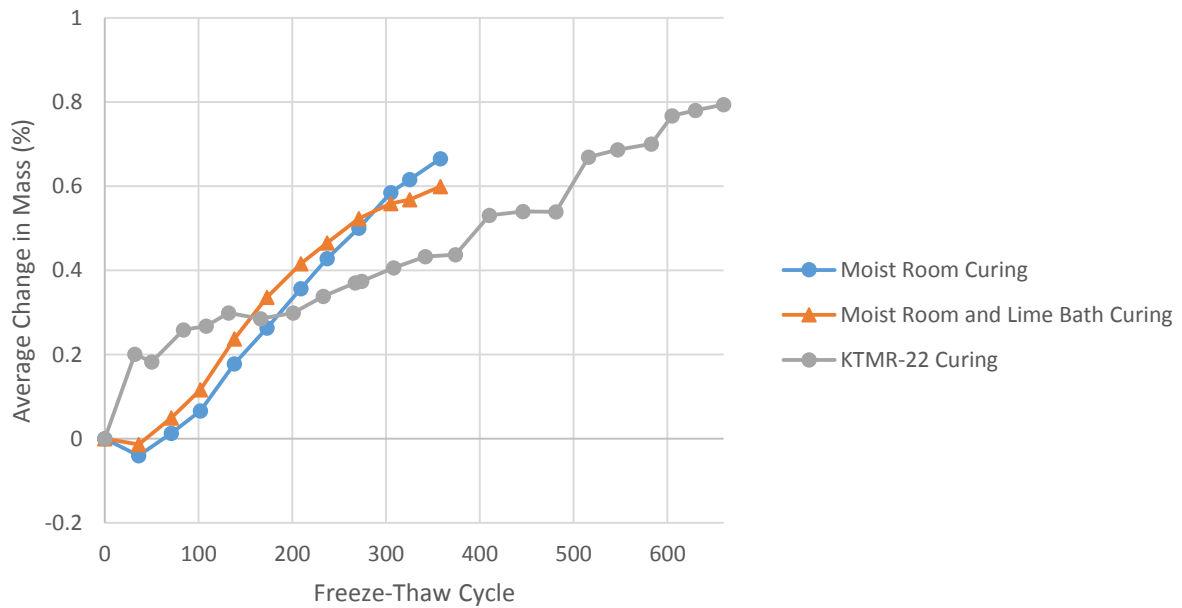
Figure A.6: Average Change in Mass: Midwest Minerals - Fort Scott Samples
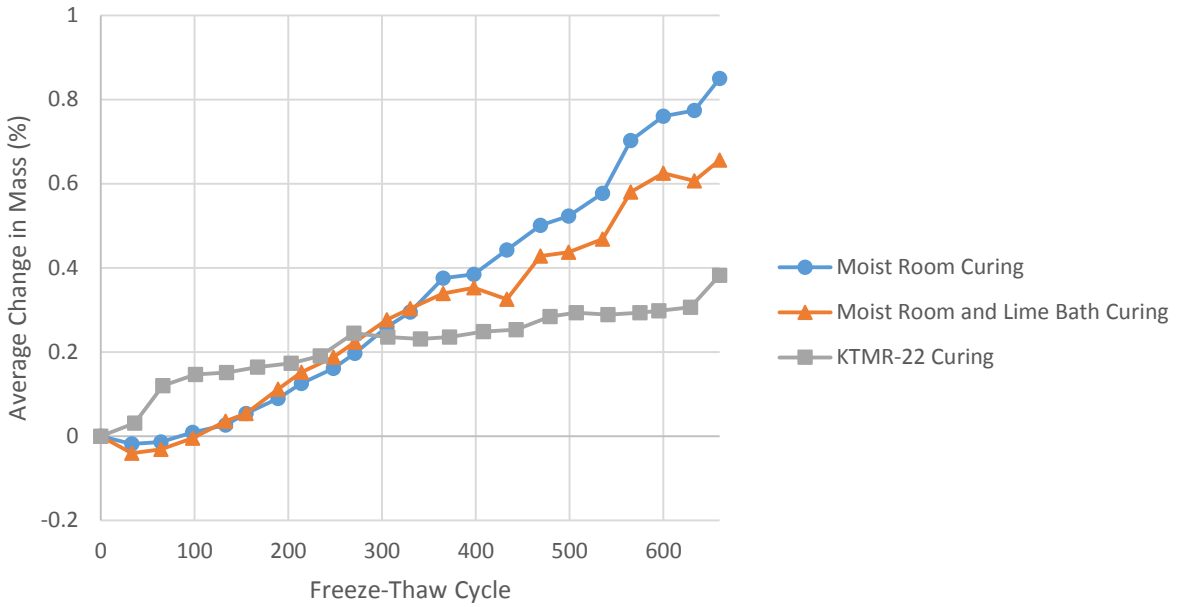
Figure A.7: Average Change in Mass: Midwest Minerals - Parsons Samples

Average concrete prism RDME for each aggregate set is plotted in Figure A.8 through Figure A.14.
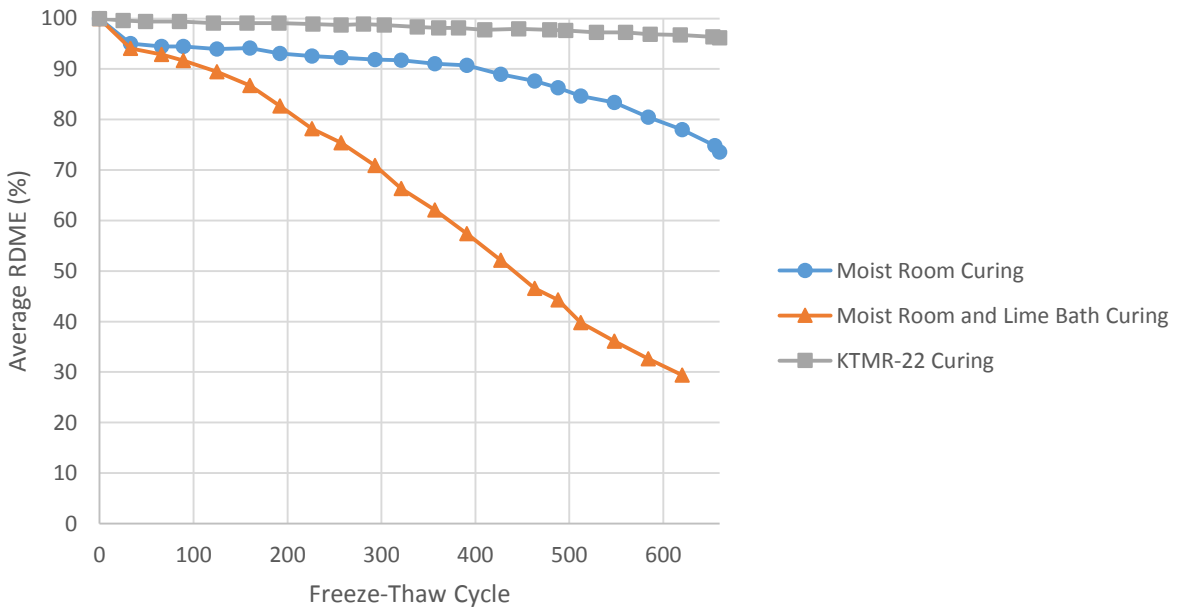
Figure A.8: Average RDME: Bayer Construction Samples
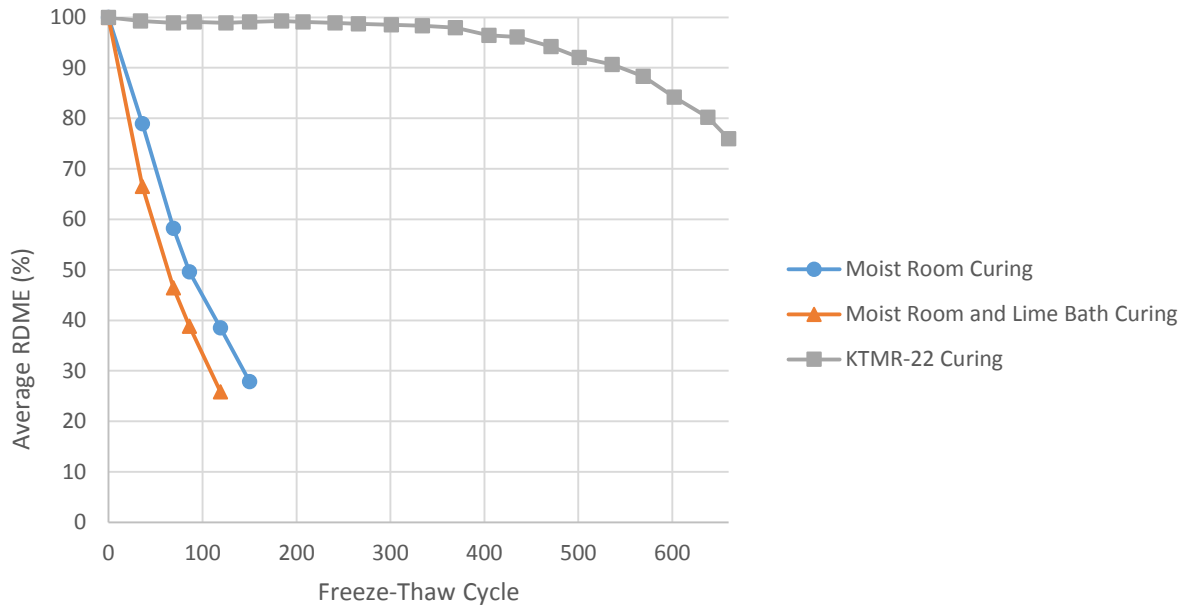
Figure A.9: Average RDME: Cornejo Stone Samples
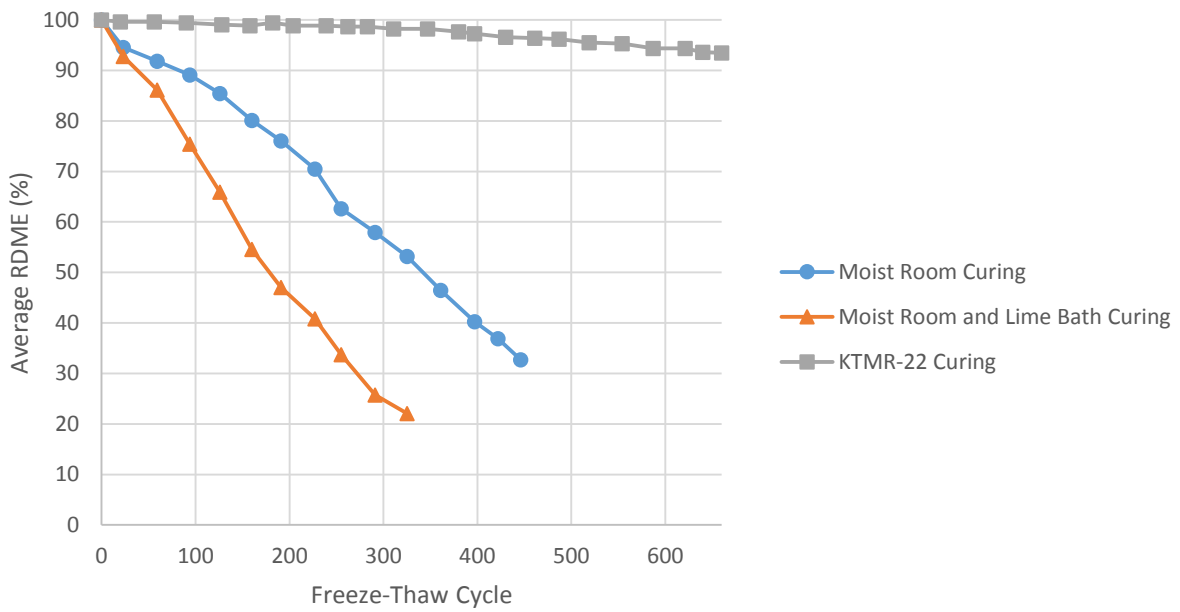
Figure A.10: Average RDME: Hamm WB Samples
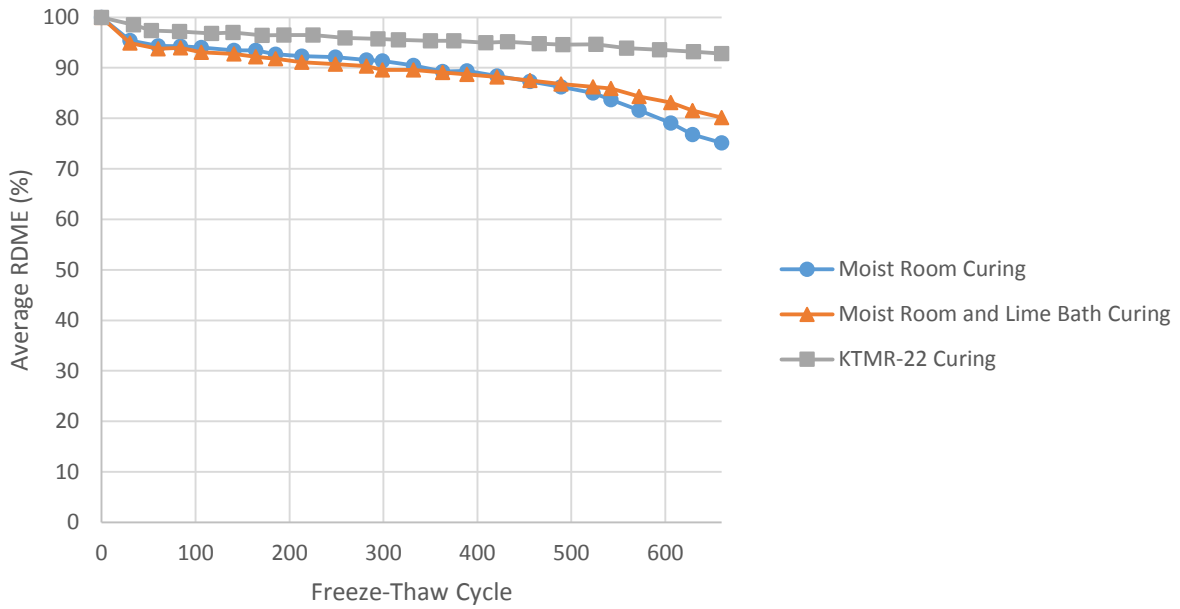
Figure A.11: Average RDME: Jasper Stone Samples
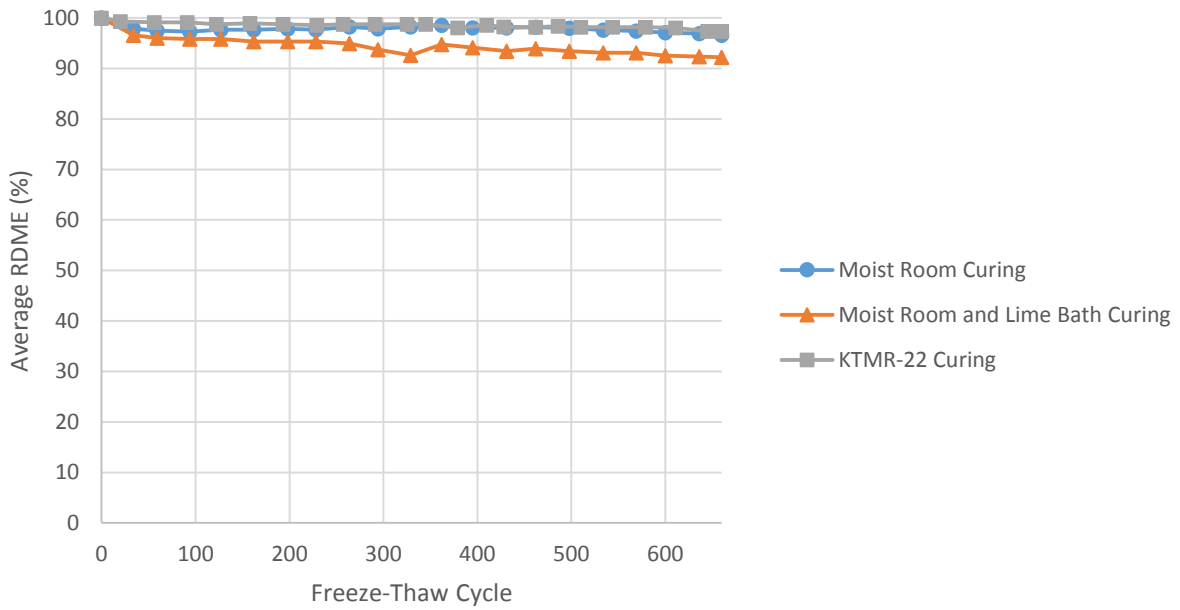
Figure A.12: Average RDME: Martin Marietta Samples
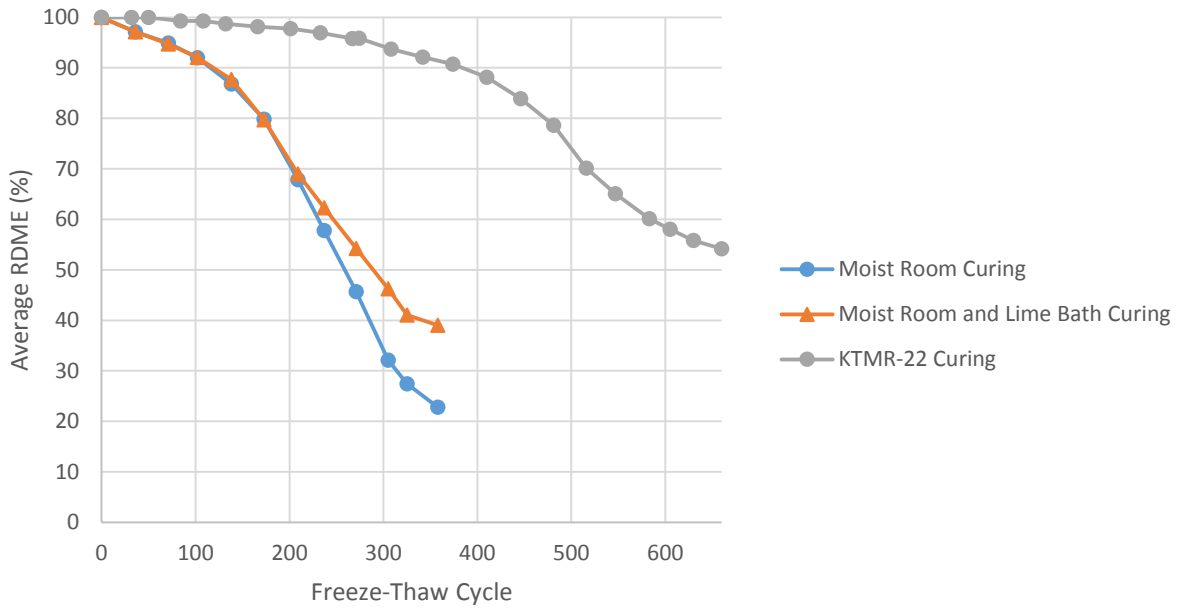
Figure A.13: Average RDME: Midwest Minerals - Fort Scott Samples
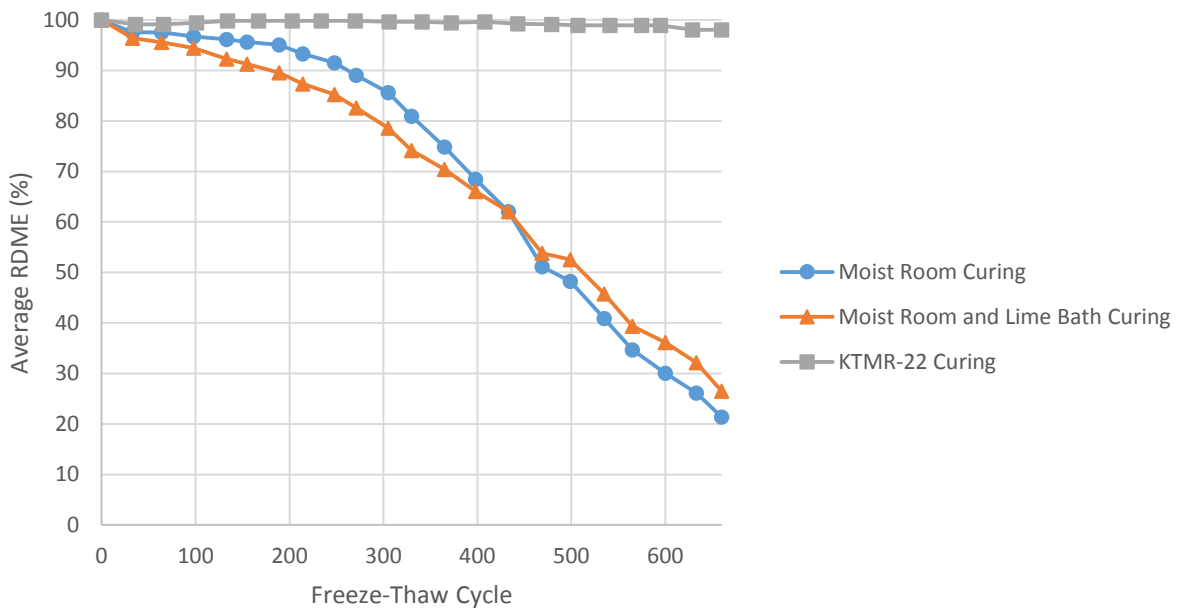
Figure A.14: Average RDME: Midwest Minerals - Parsons Samples

Average concrete prism expansion for each aggregate set is plotted in Figure A.15 through Figure A.21.
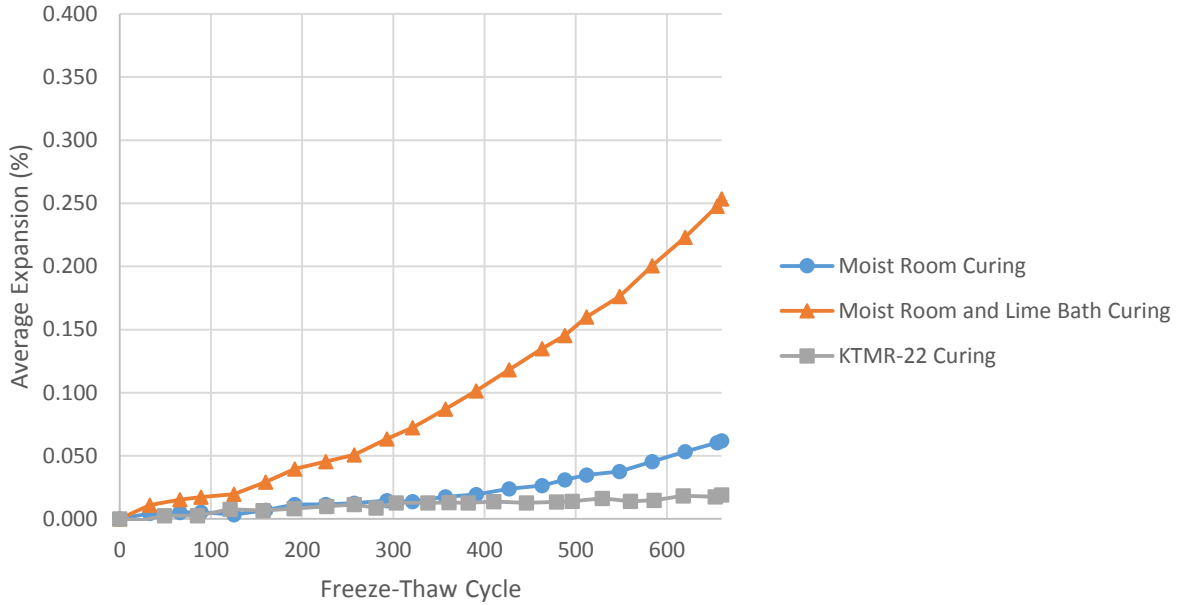
Figure A.15: Average Expansion: Bayer Construction Samples
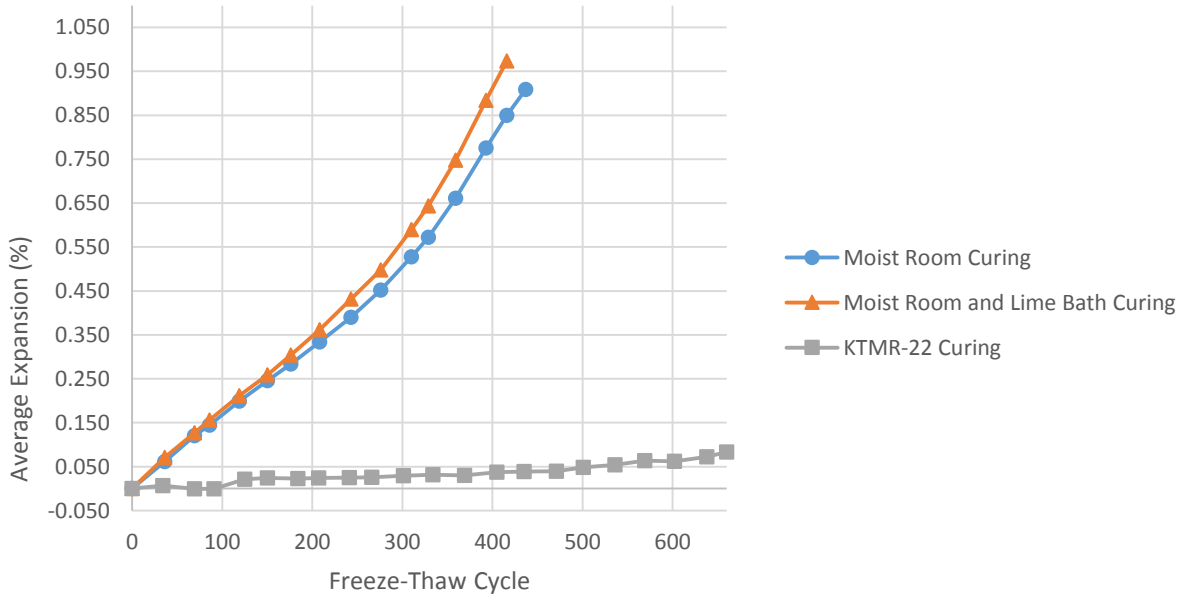
Figure A.16: Average Expansion: Cornejo Stone Samples
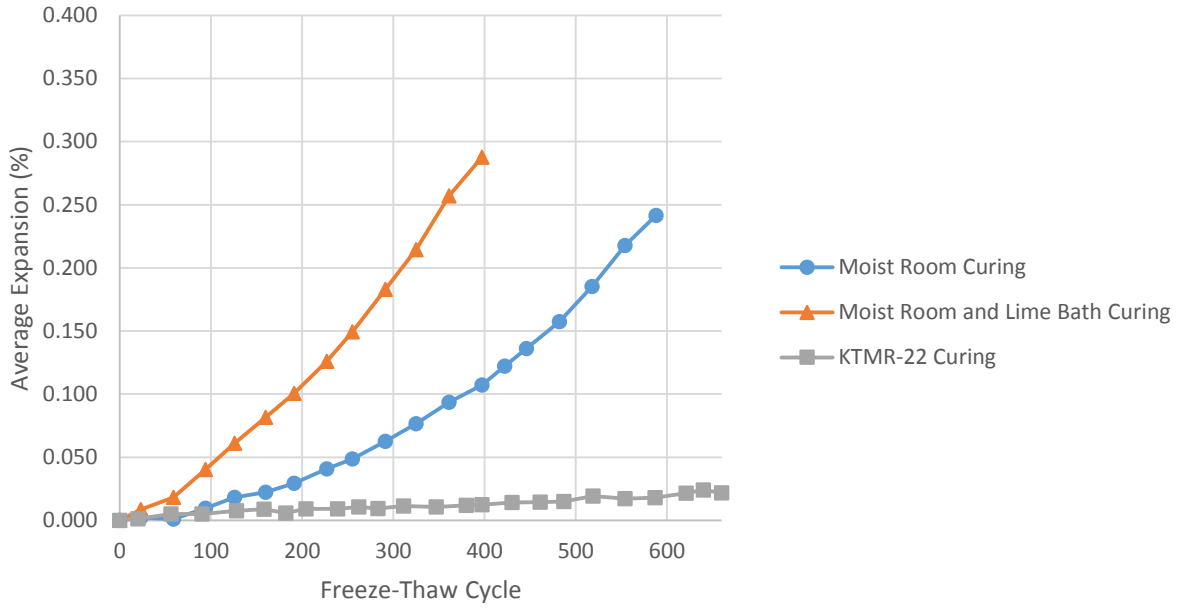
Figure A.17: Average Expansion: Hamm WB Samples
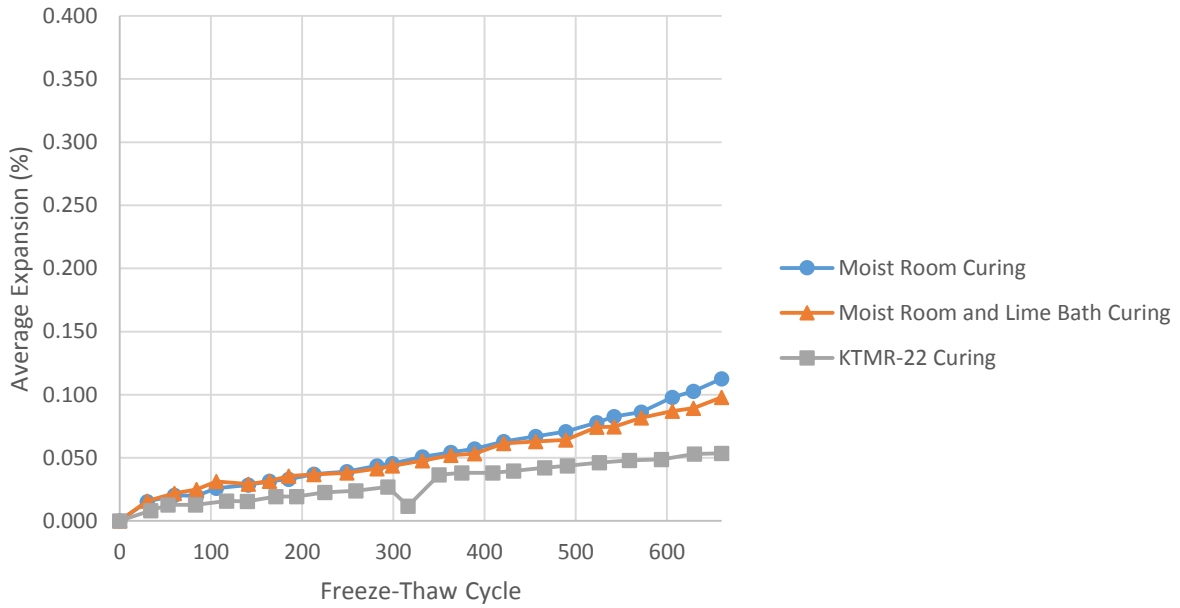
Figure A.18: Average Expansion: Jasper Stone Samples
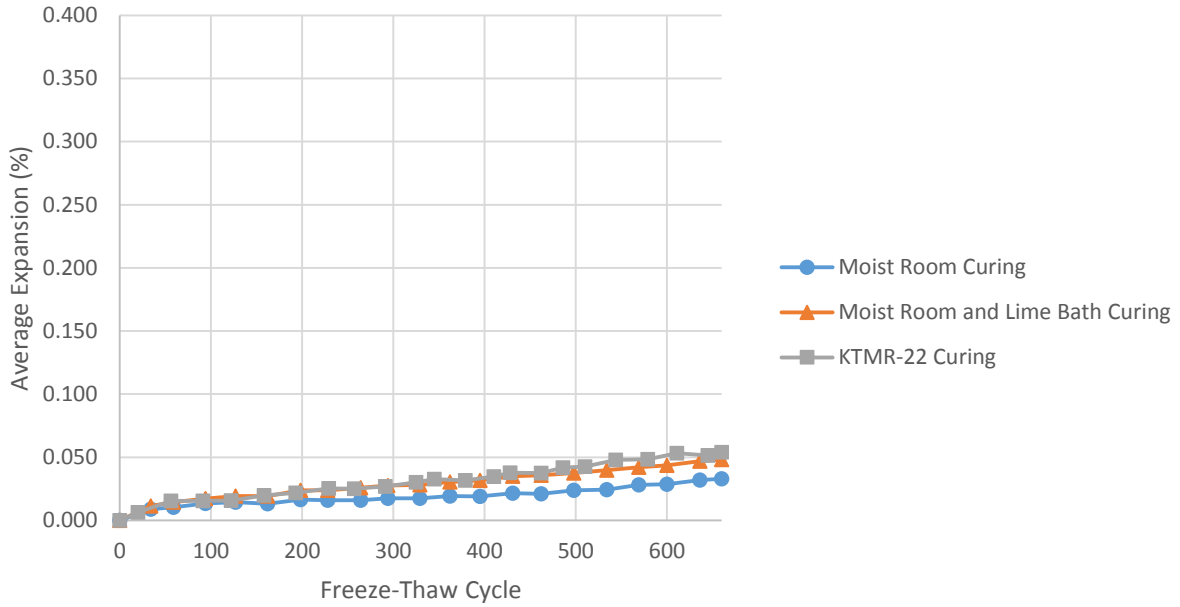
Figure A.19: Average Expansion: Martin Marietta Samples
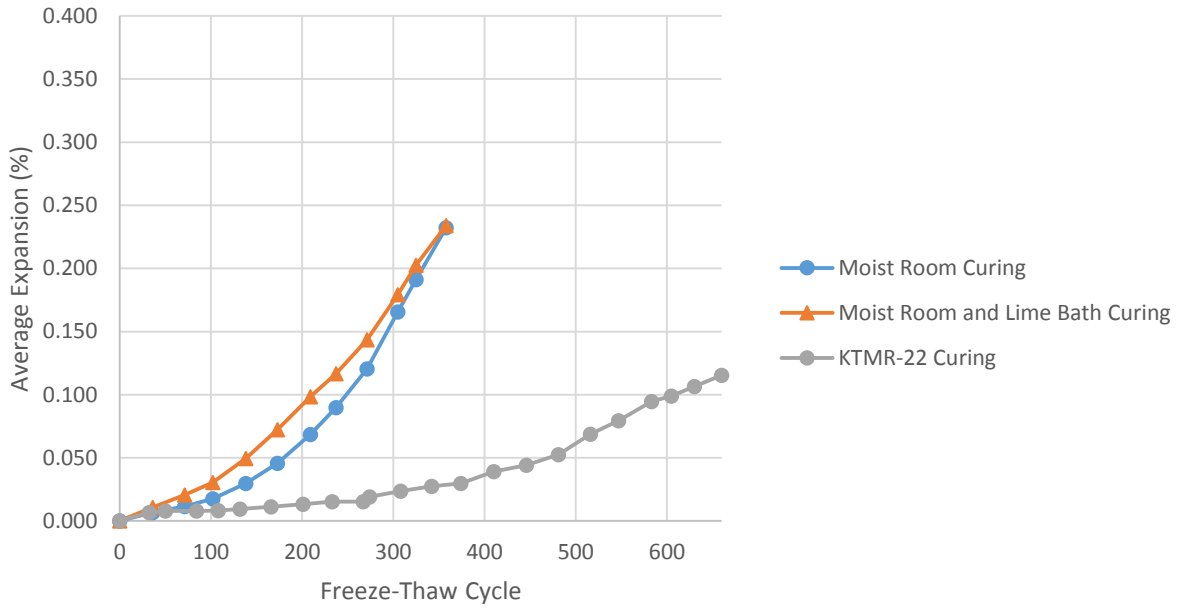
Figure A.20: Average Expansion: Midwest Minerals - Fort Scott Samples
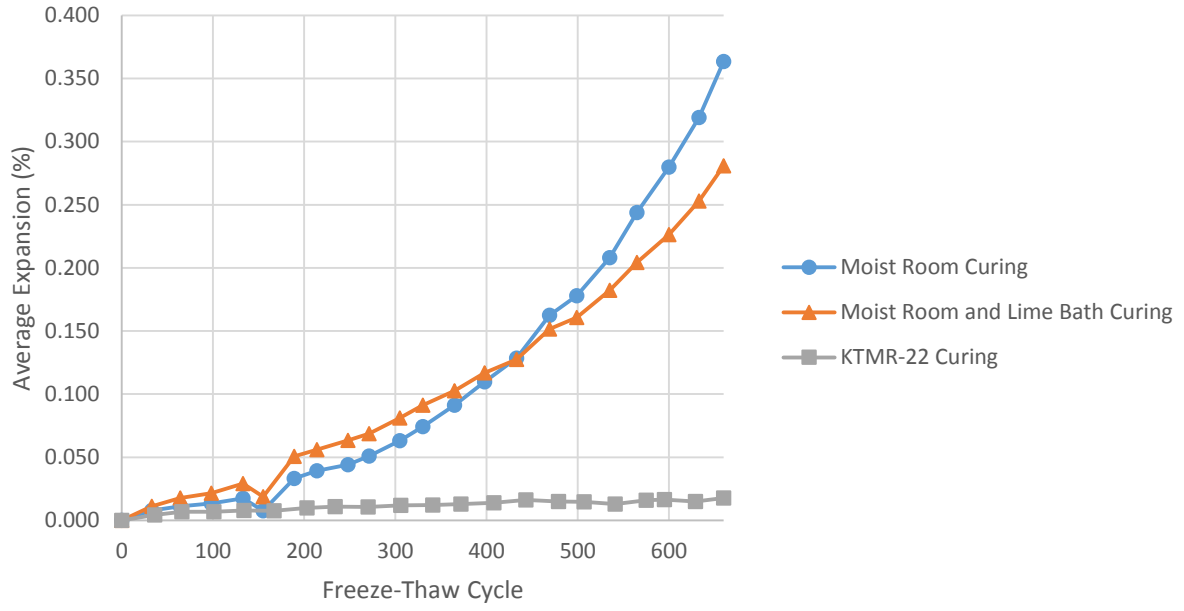
Figure A.21: Average Expansion: Midwest Minerals - Parsons Samples

Appendix B - Salt Brine ASTM C666 Results

Average concrete prism change in mass for each aggregate set is plotted in Figure B.1 through Figure B.12.
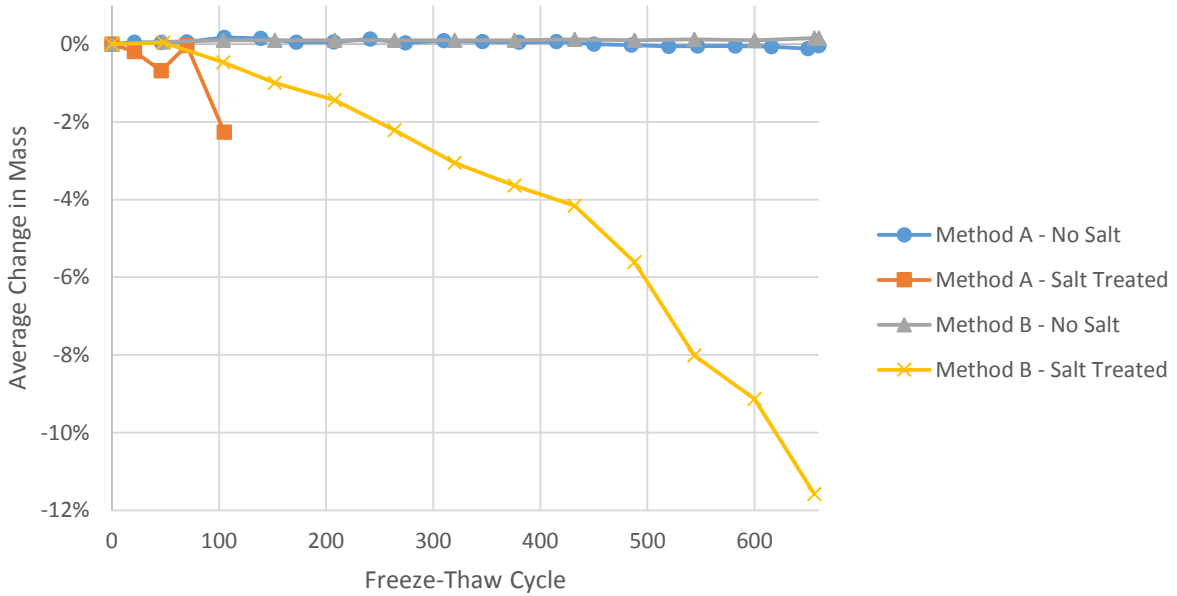
Figure B.1: Average Change in Mass: Bayer Construction Samples
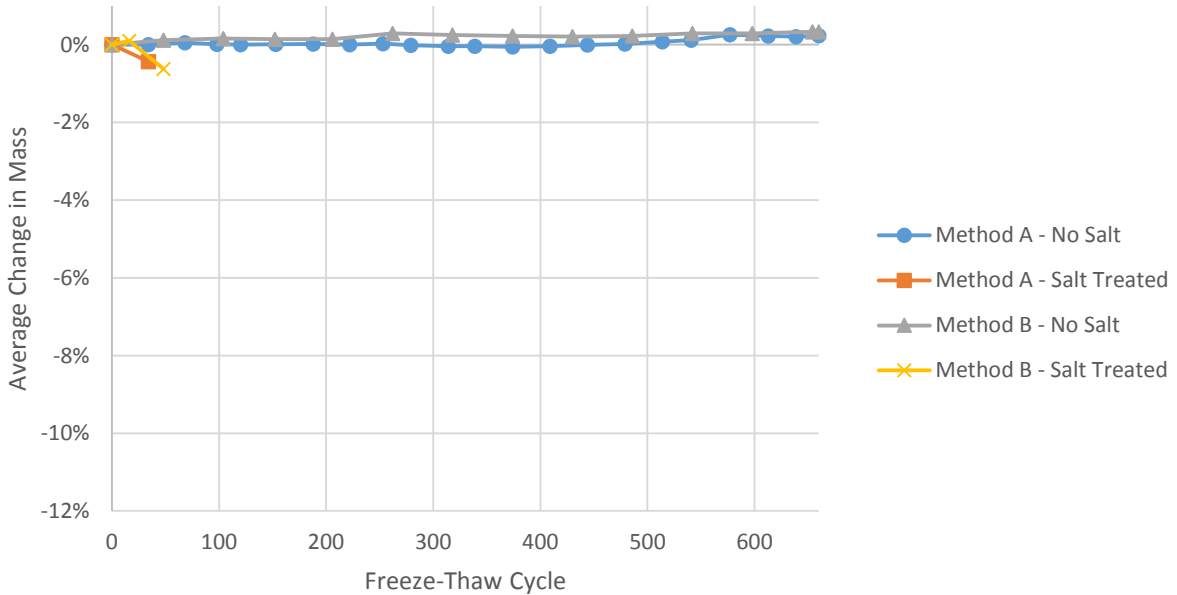
Figure B.2: Average Change in Mass: Cornejo Stone Samples
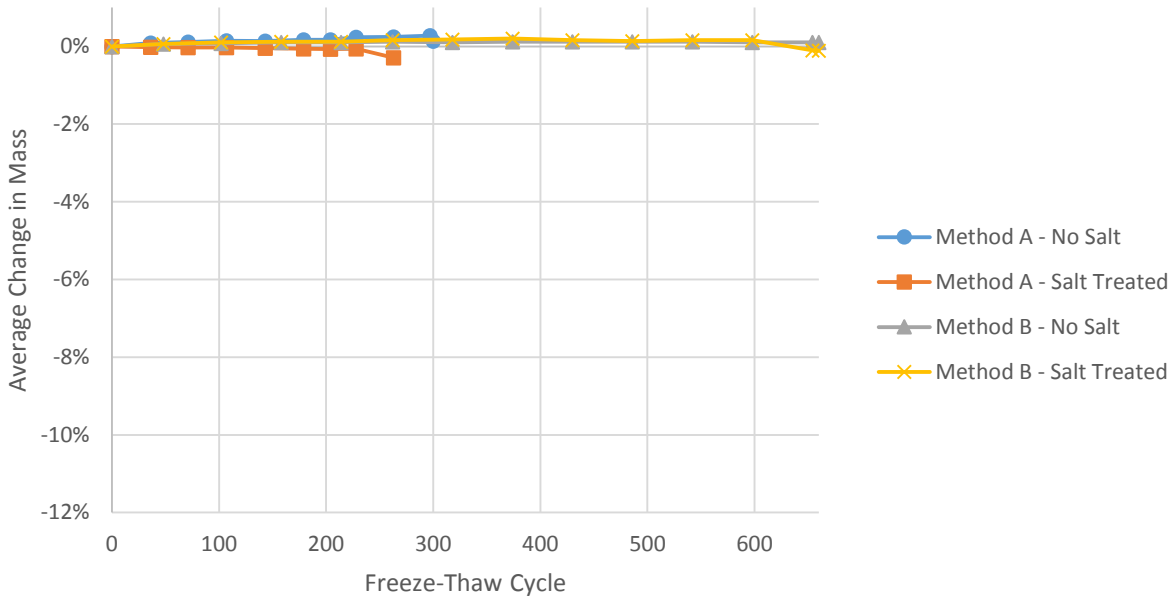
* Method A testing terminated at or before 300 cycles in accordance with ASTM C666 requirements

Figure B.3: Average Change in Mass: Eastern Colorado Aggregates Samples
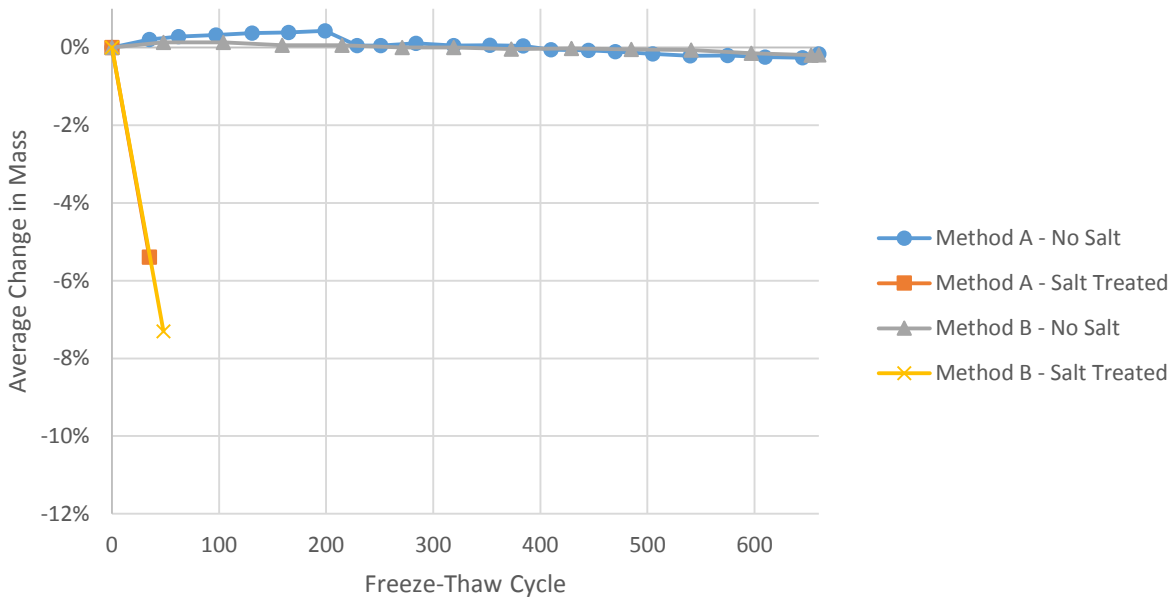
Figure B.4: Average Change in Mass: Florence Rock Samples
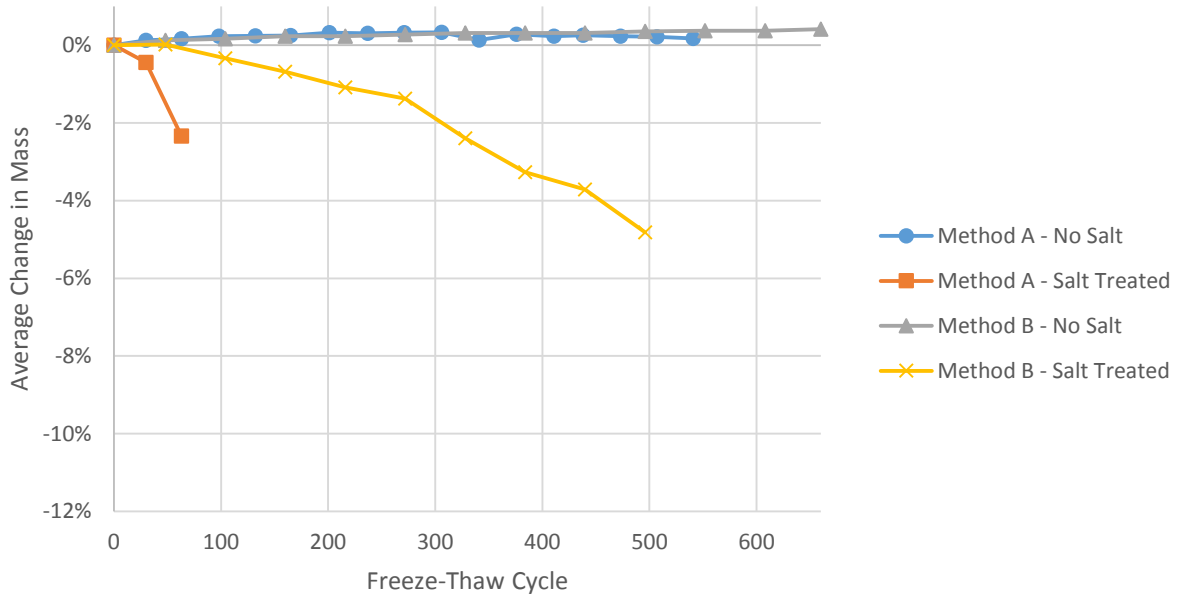
* Non-salt-treated method A samples removed from chamber early to make room for new samples

Figure B.5: Average Change in Mass: Hamm WB Samples
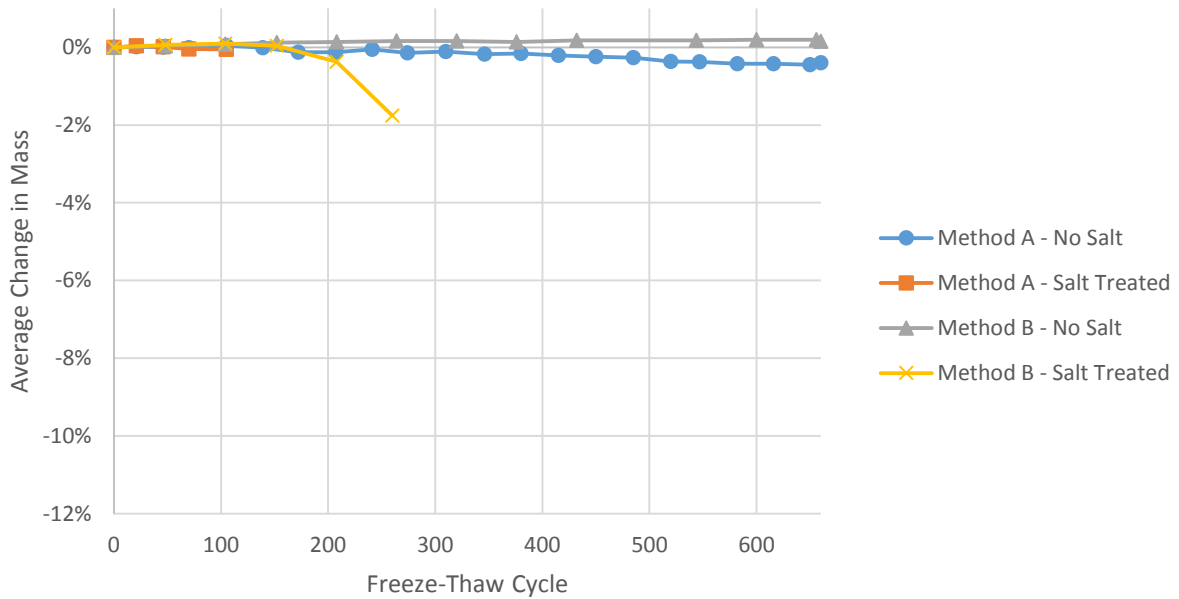
Figure B.6: Average Change in Mass: Jasper Stone Samples
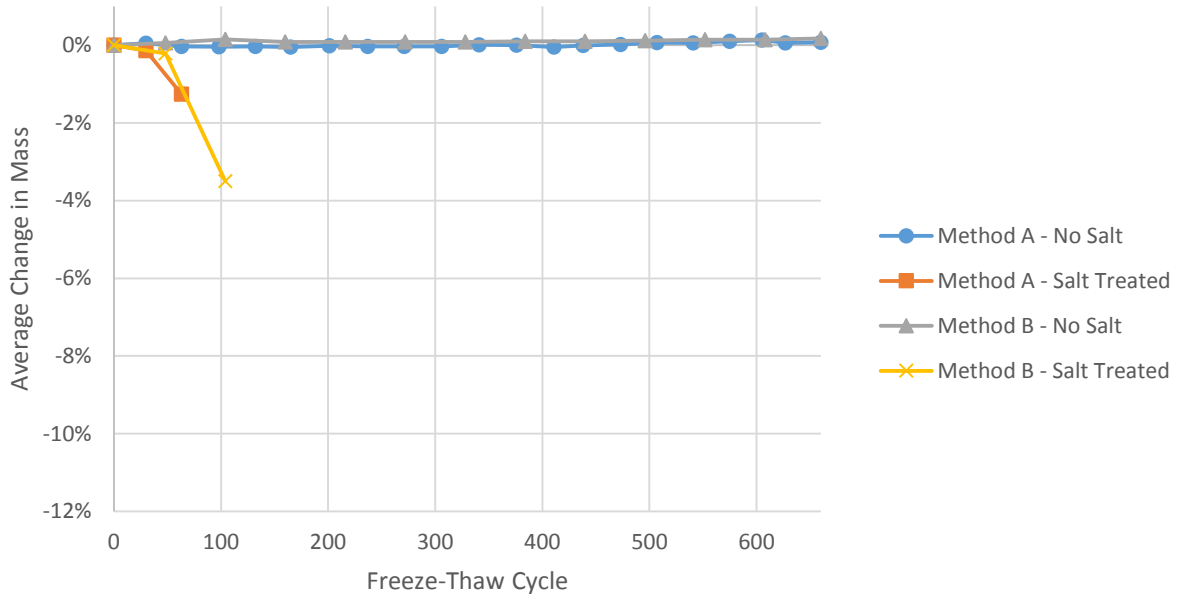
Figure B.7: Average Change in Mass: Mid-States Materials - Edgerton Samples
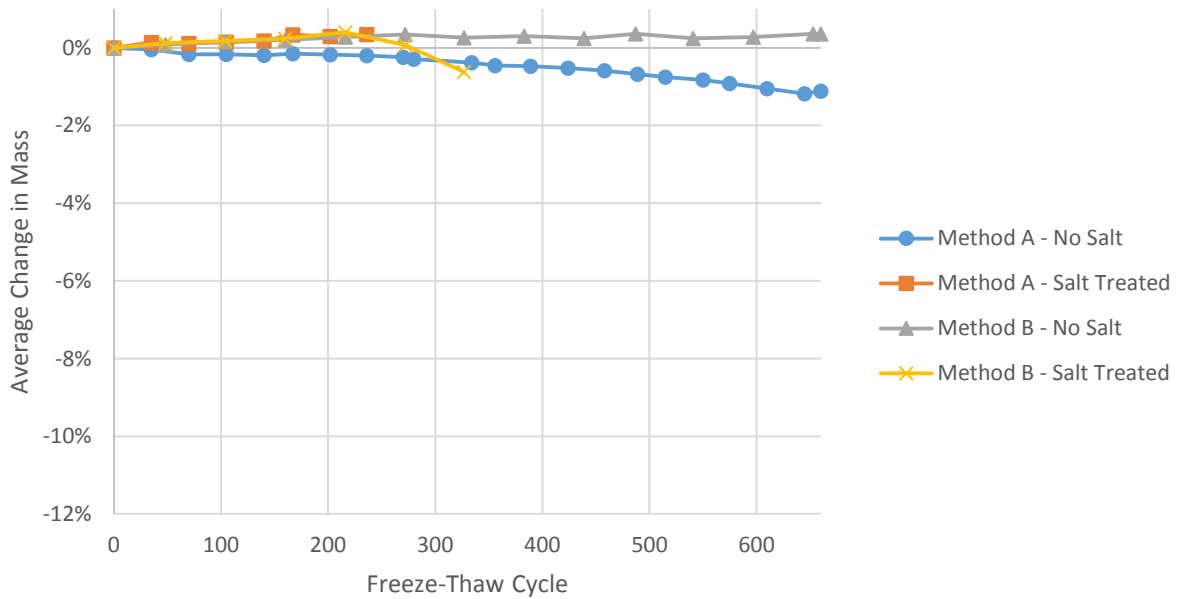
Figure B.8: Average Change in Mass: Mid-States Materials - Osage, Bed 3 Samples
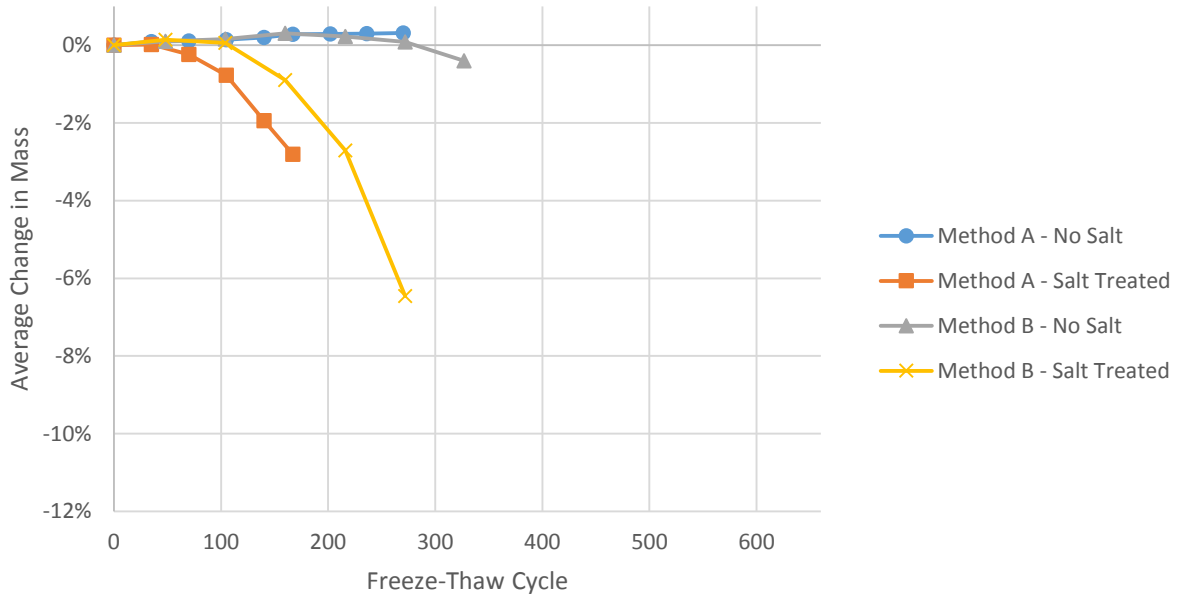
Figure B.9: Average Change in Mass: Mid-States Materials - Osage, Bed 4 Samples
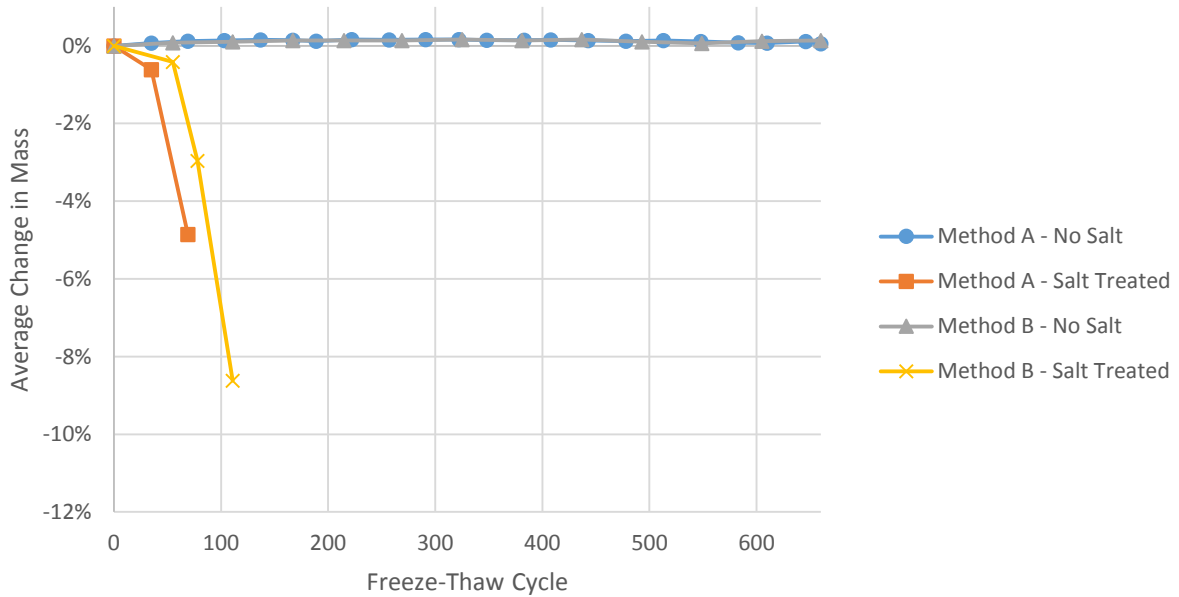
Figure B.10: Average Change in Mass: Midwest Minerals - Fort Scott Samples
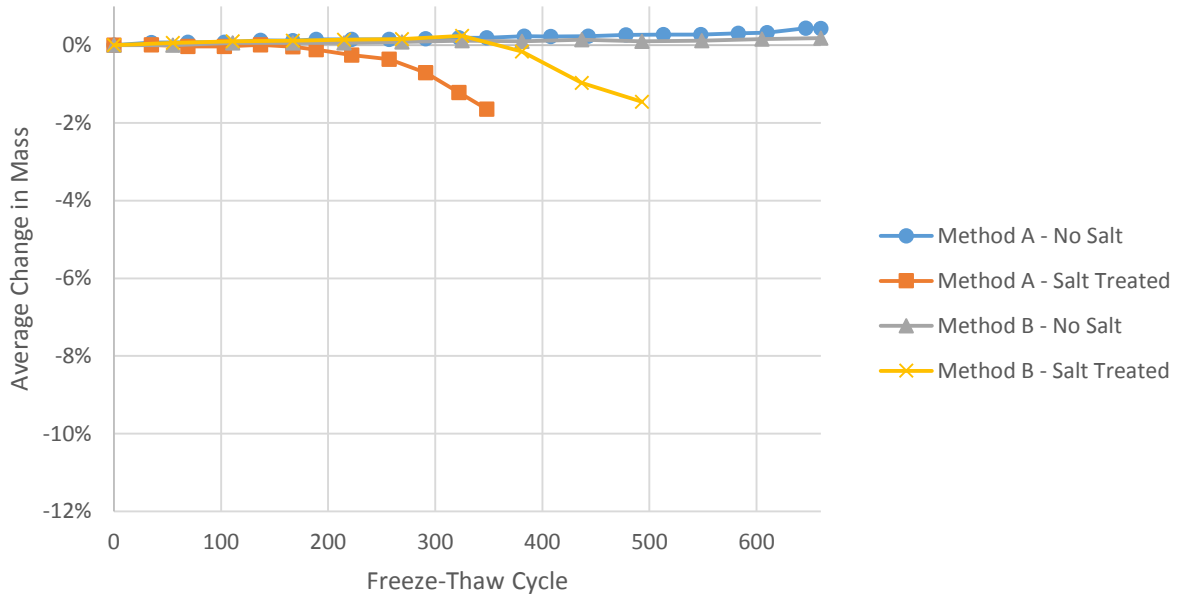
Figure B.11: Average Change in Mass: Midwest Minerals - Parsons Samples
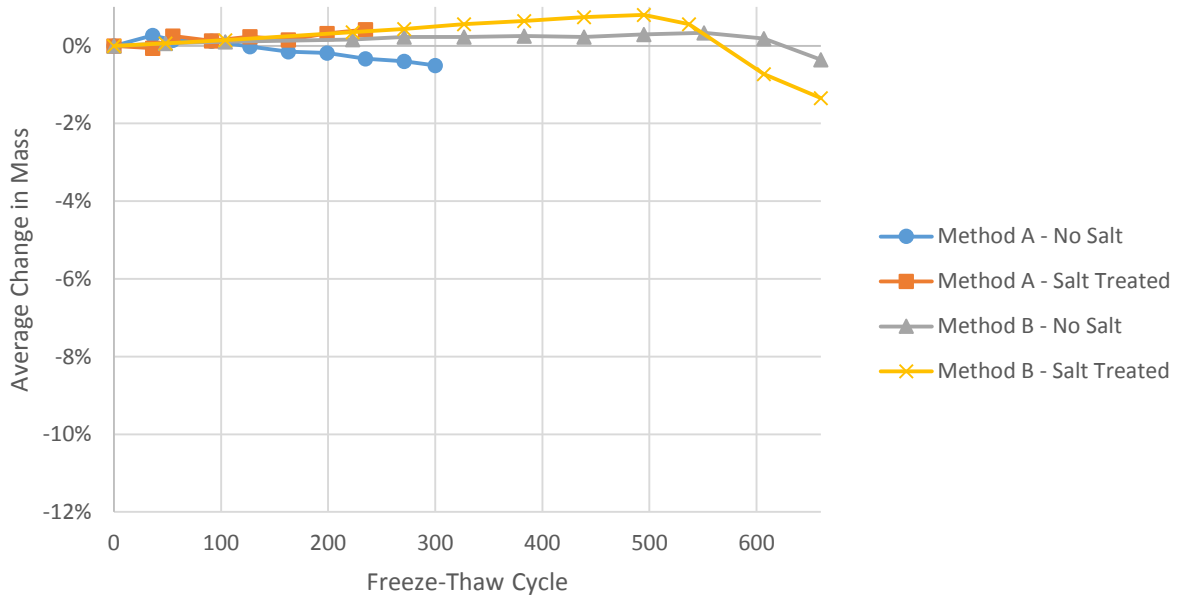
* Method A testing terminated at or before 300 cycles in accordance with ASTM C666 requirements

Figure B.12: Average Change in Mass: Penny's Aggregates Samples

Average concrete prism RDME for each aggregate set is plotted in Figure B.13 through Figure B.24.
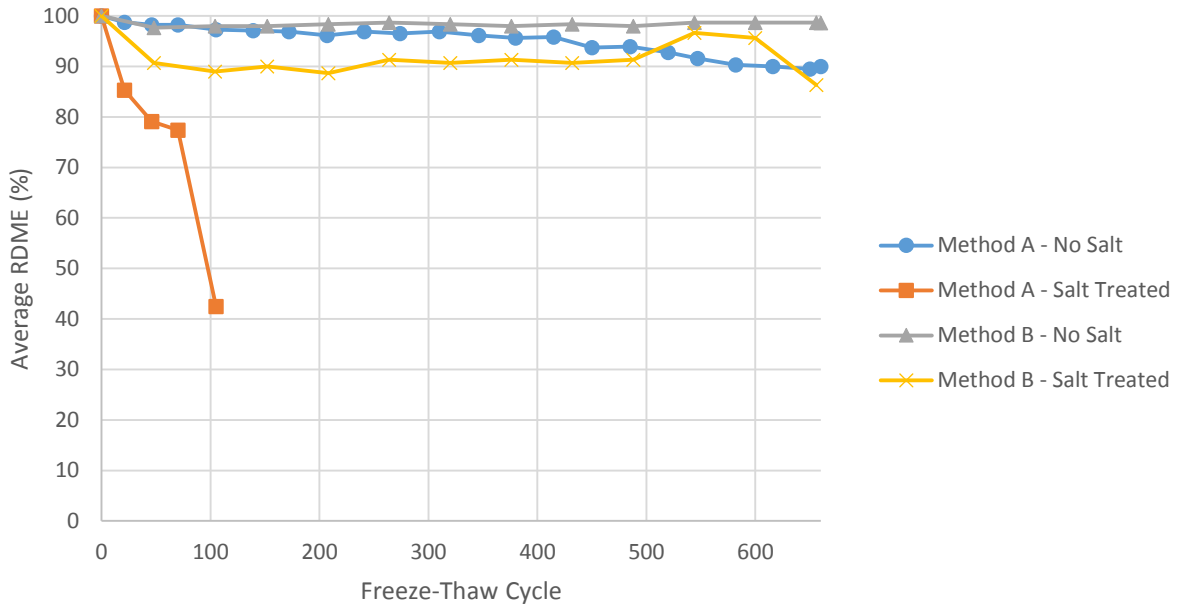
Figure B.13: Average RDME: Bayer Construction Samples
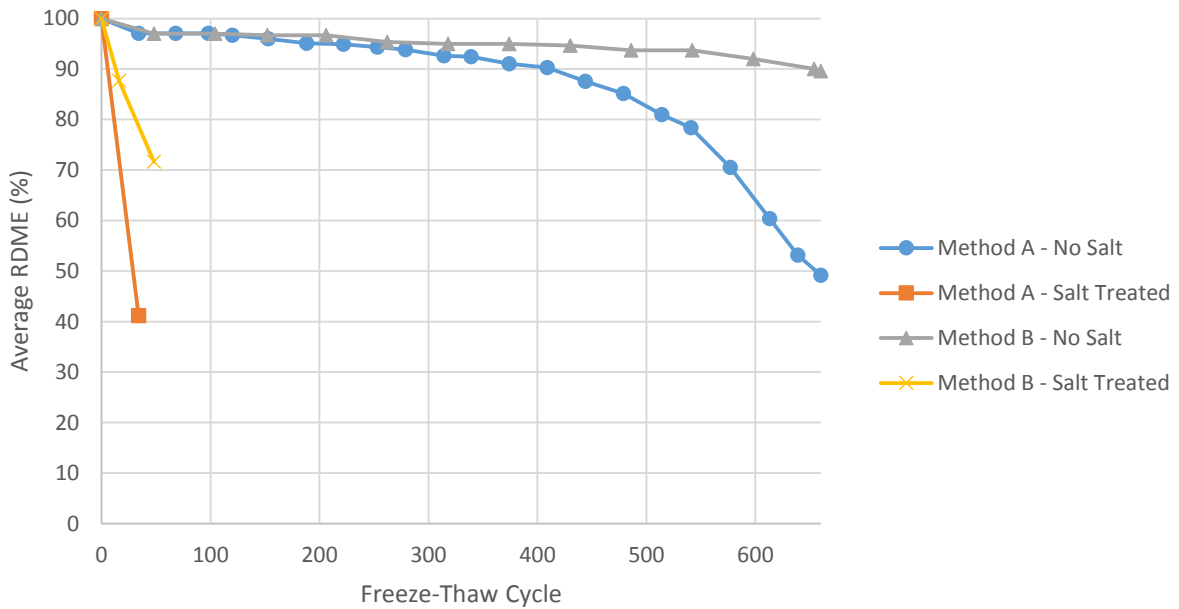
Figure B.14: Average RDME: Cornejo Stone Samples
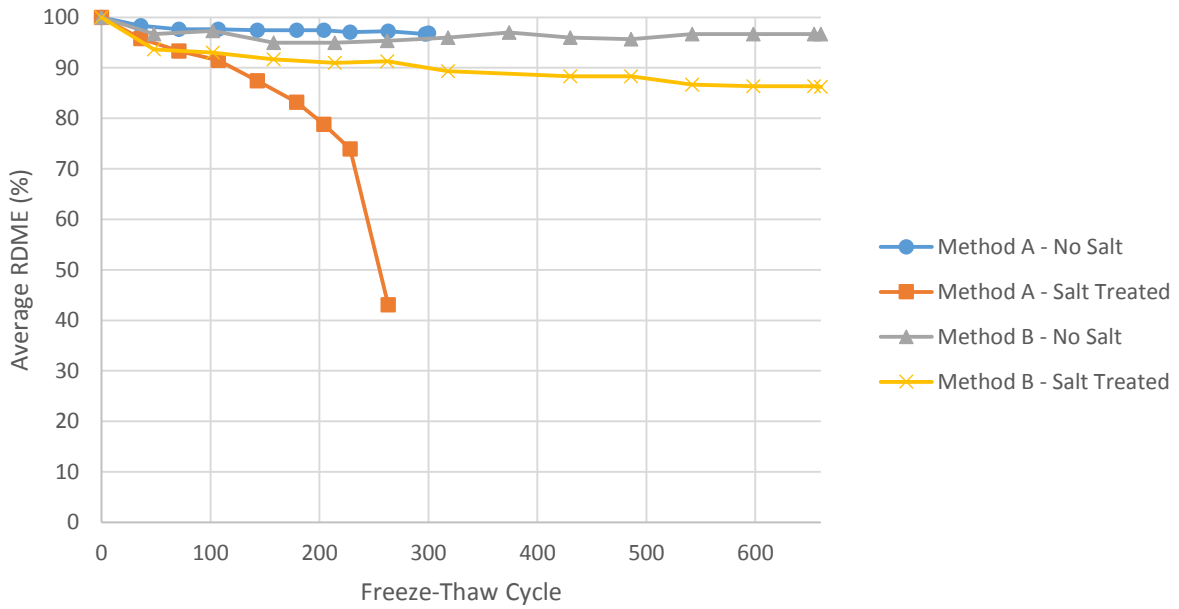
* Method A testing terminated at or before 300 cycles in accordance with ASTM C666 requirements

Figure B.15: Average RDME: Eastern Colorado Aggregates Samples
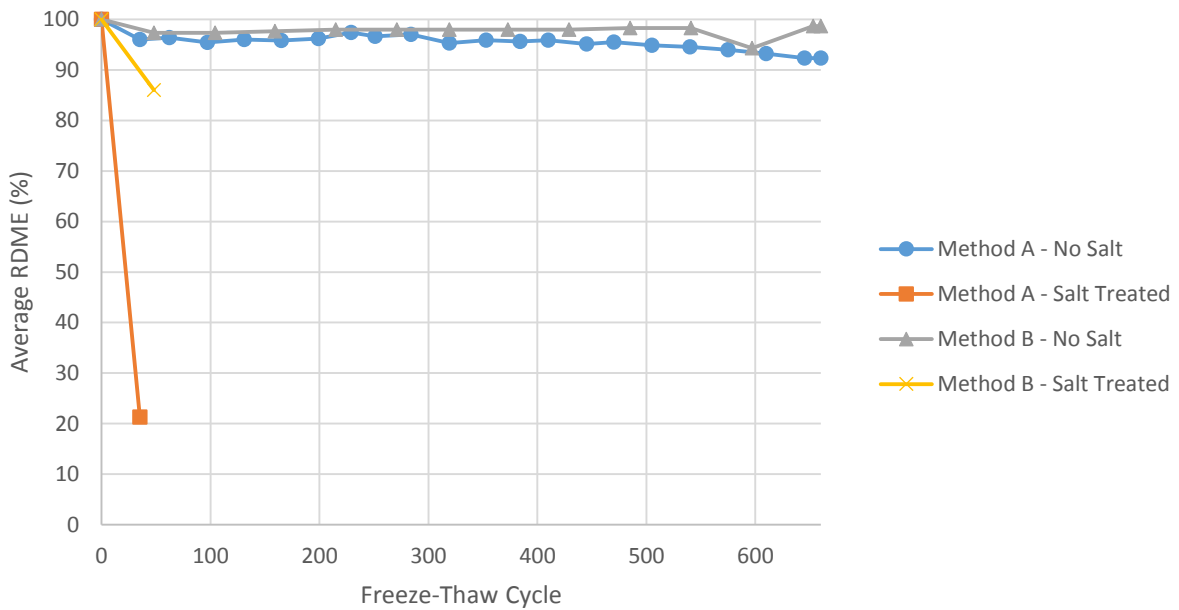
Figure B.16: Average RDME: Florence Rock Samples
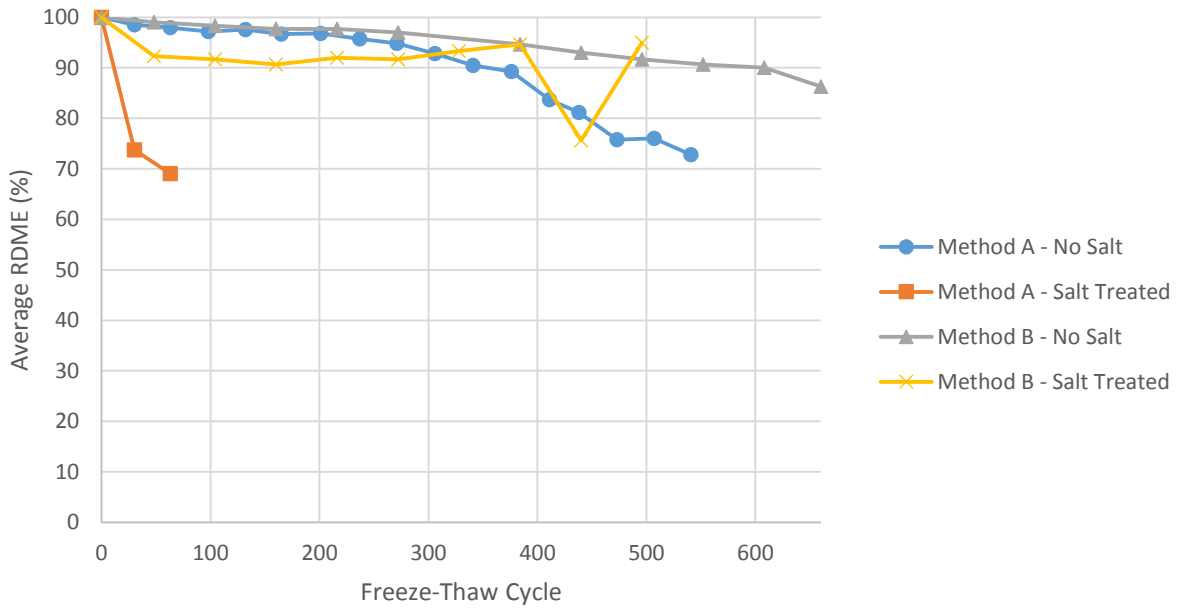
* Non-salt-treated method A samples removed from chamber early to make room for new samples

Figure B.17: Average RDME: Hamm WB Samples
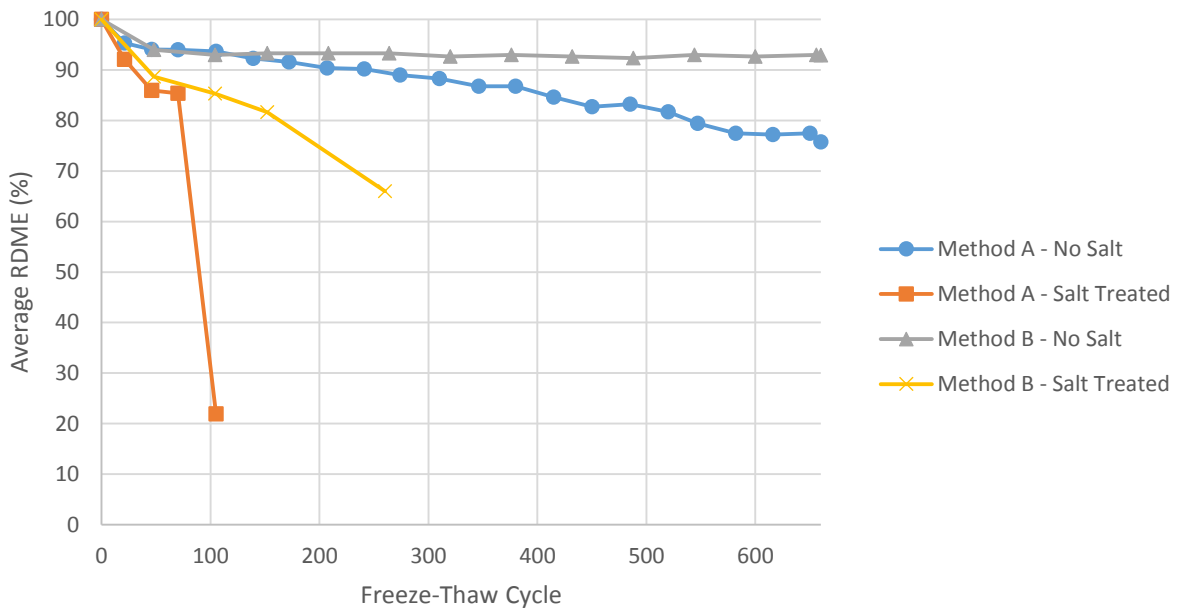
Figure B.18: Average RDME: Jasper Stone Samples
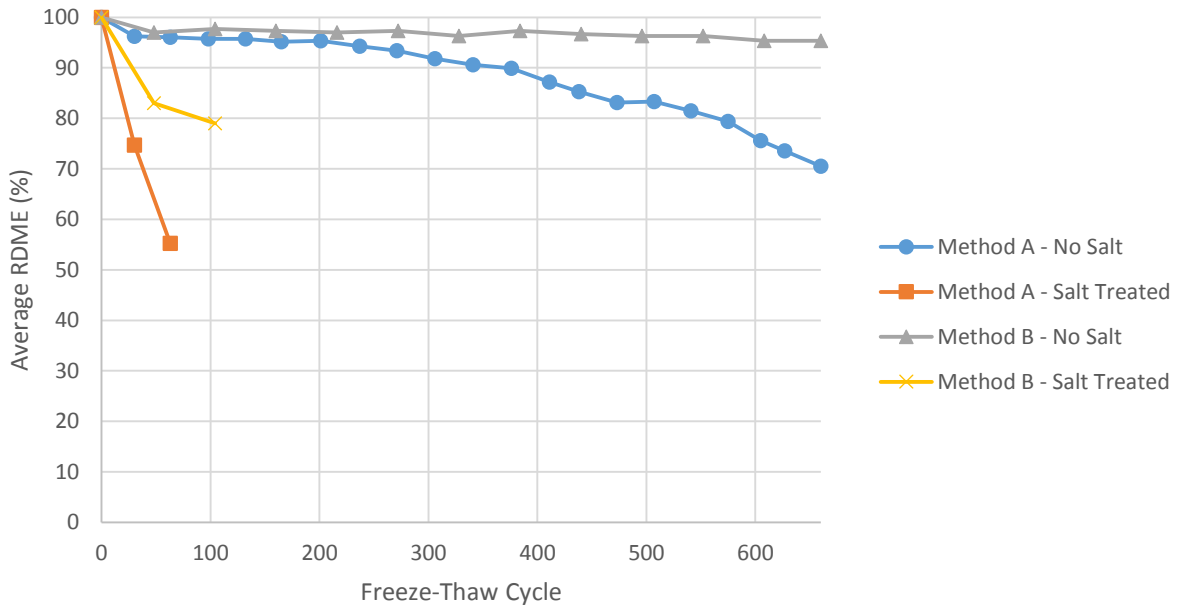
Figure B.19: Average RDME: Mid-States Materials - Edgerton Samples
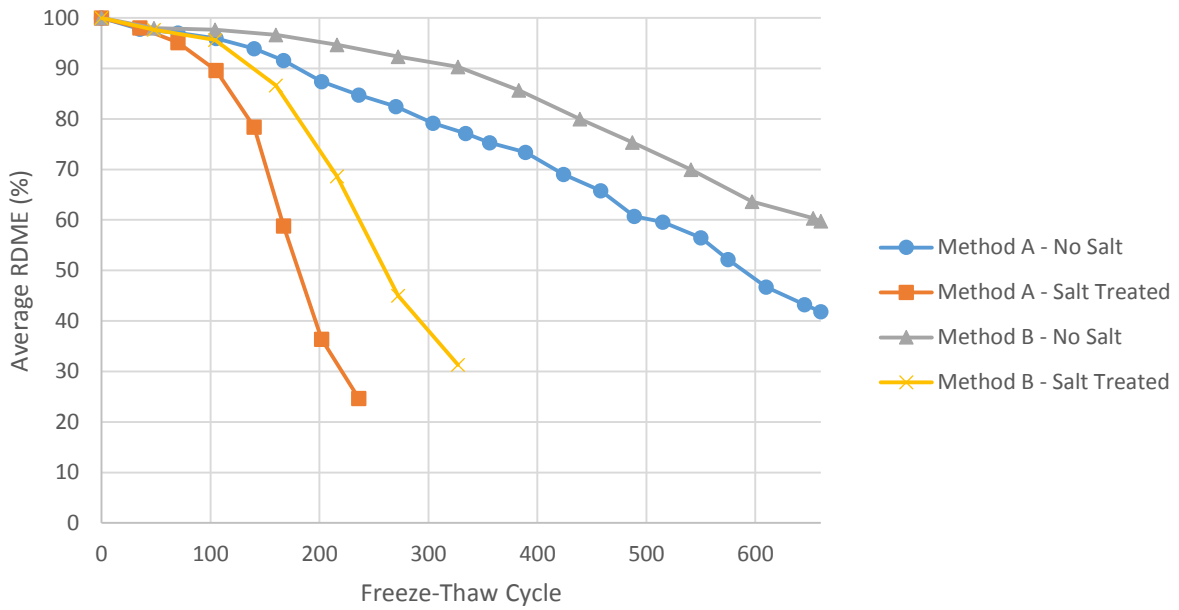
Figure B.20: Average RDME: Mid-States Materials - Osage, Bed 3 Samples
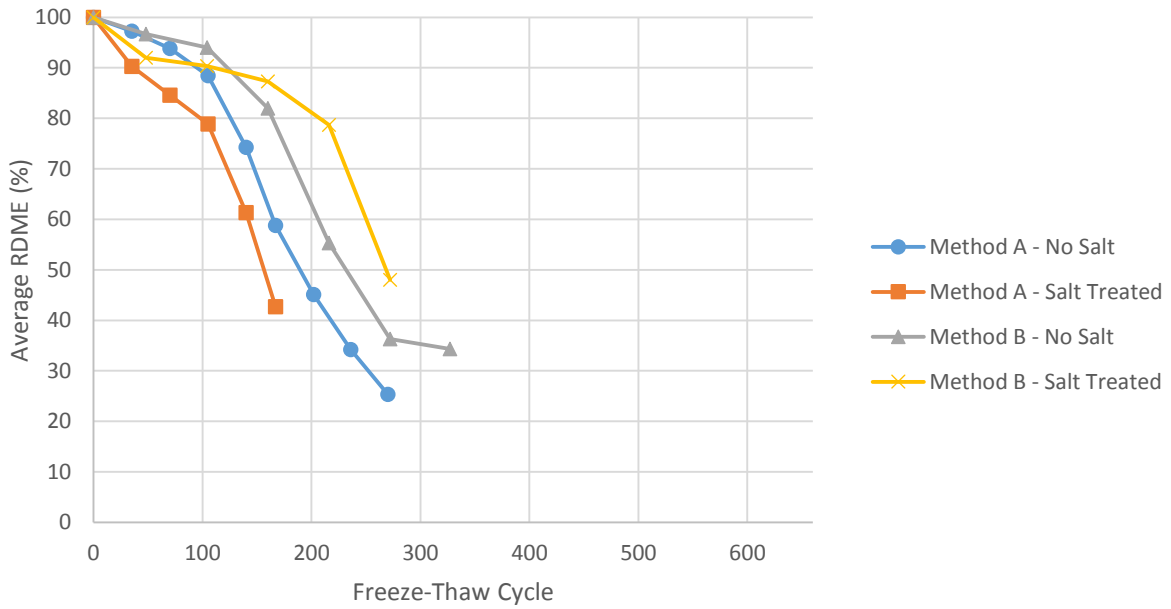
Figure B.21: Average RDME: Mid-States Materials - Osage, Bed 4 Samples
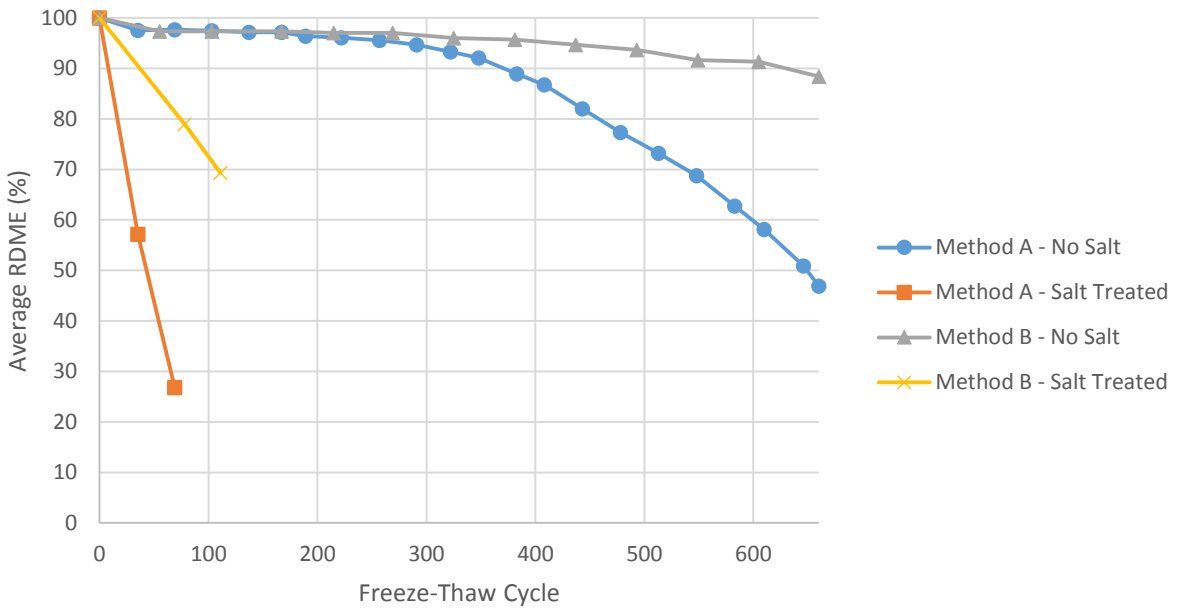
Figure B.22: Average RDME: Midwest Minerals - Fort Scott Samples
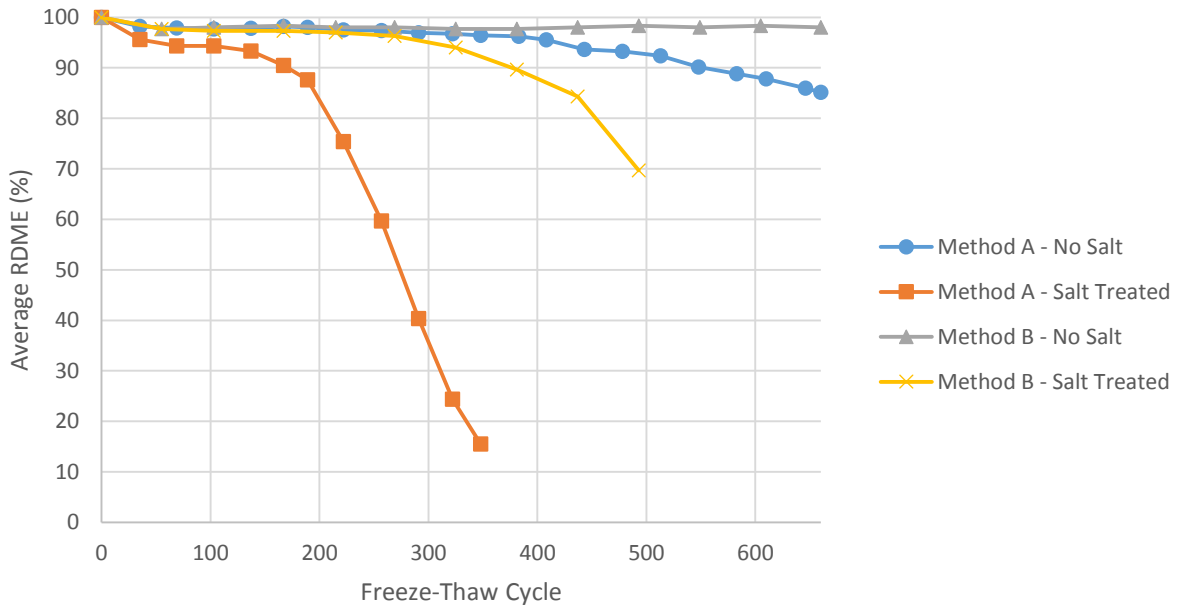
Figure B.23: Average RDME: Midwest Minerals - Parsons Samples
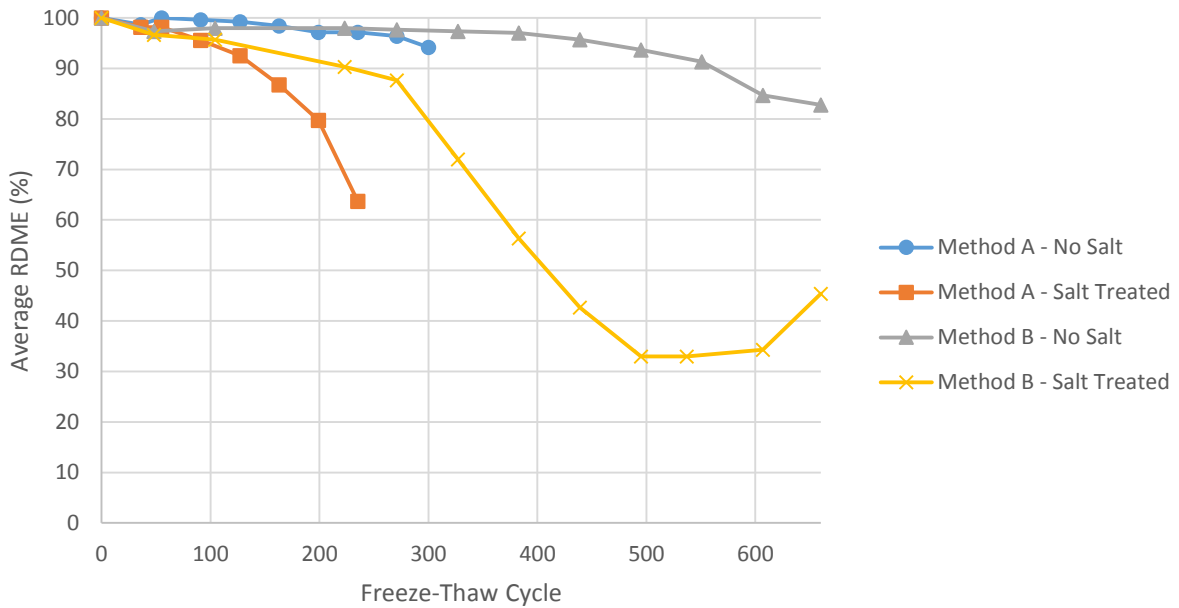
* Method A testing terminated at or before 300 cycles in accordance with ASTM C666 requirements

Figure B.24: Average RDME: Penny's Aggregates Samples

Average concrete prism expansion for each aggregate set is plotted in Figure B.25 through Figure B.36.
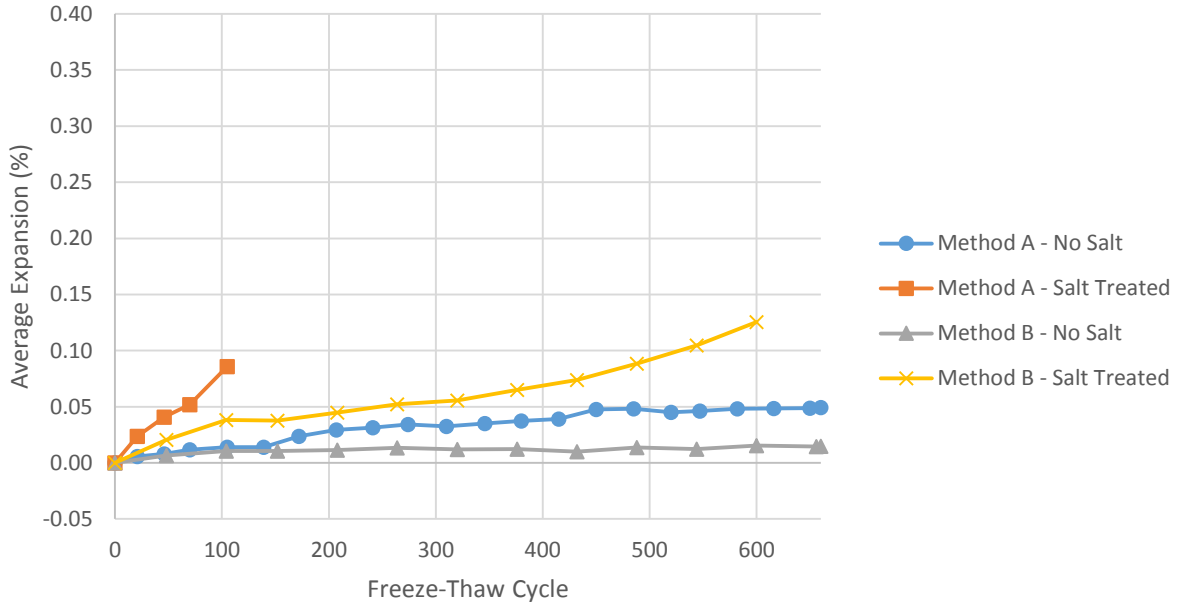
Figure B.25: Average Expansion: Bayer Construction Samples
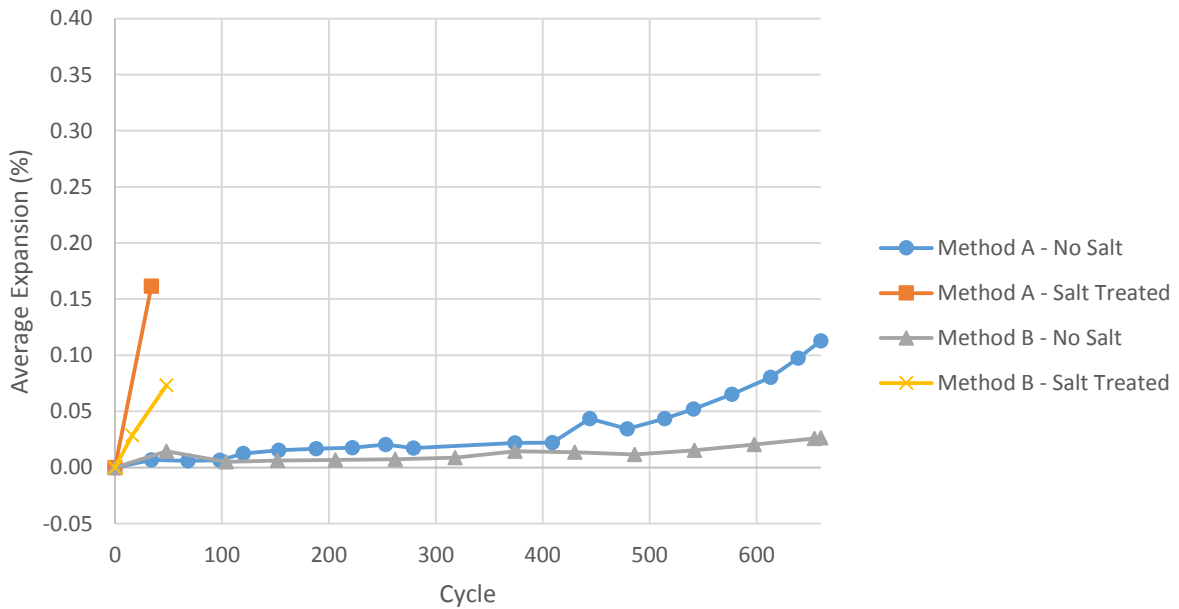
Figure B.26: Average Expansion: Cornejo Stone Samples
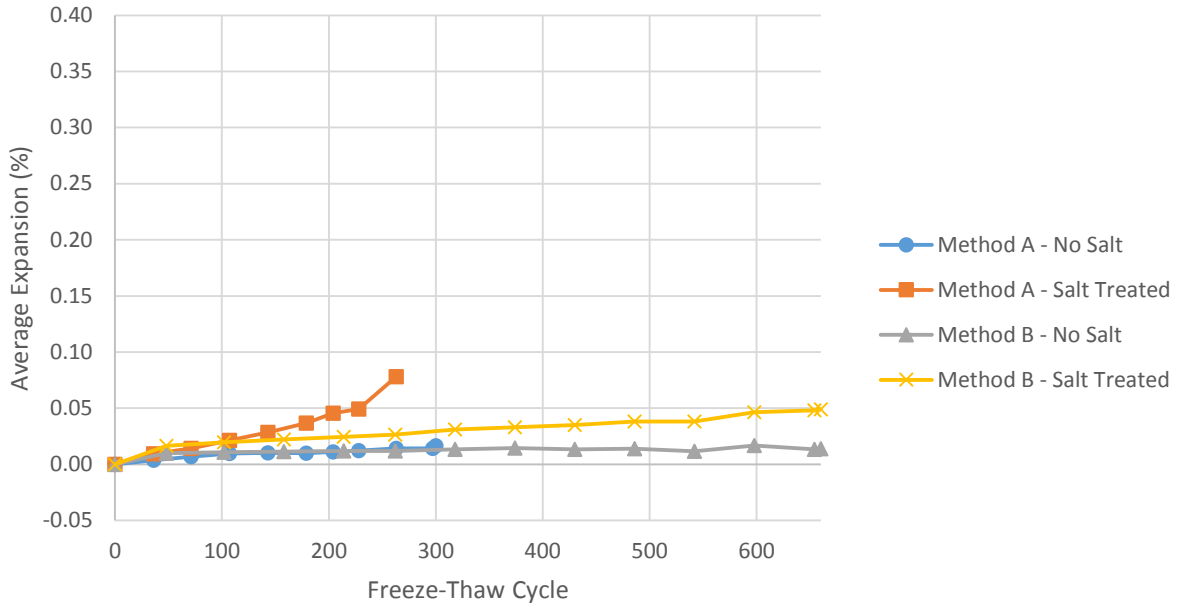
* Method A testing terminated at or before 300 cycles in accordance with ASTM C666 requirements

Figure B.27: Average Expansion: Eastern Colorado Aggregates Samples
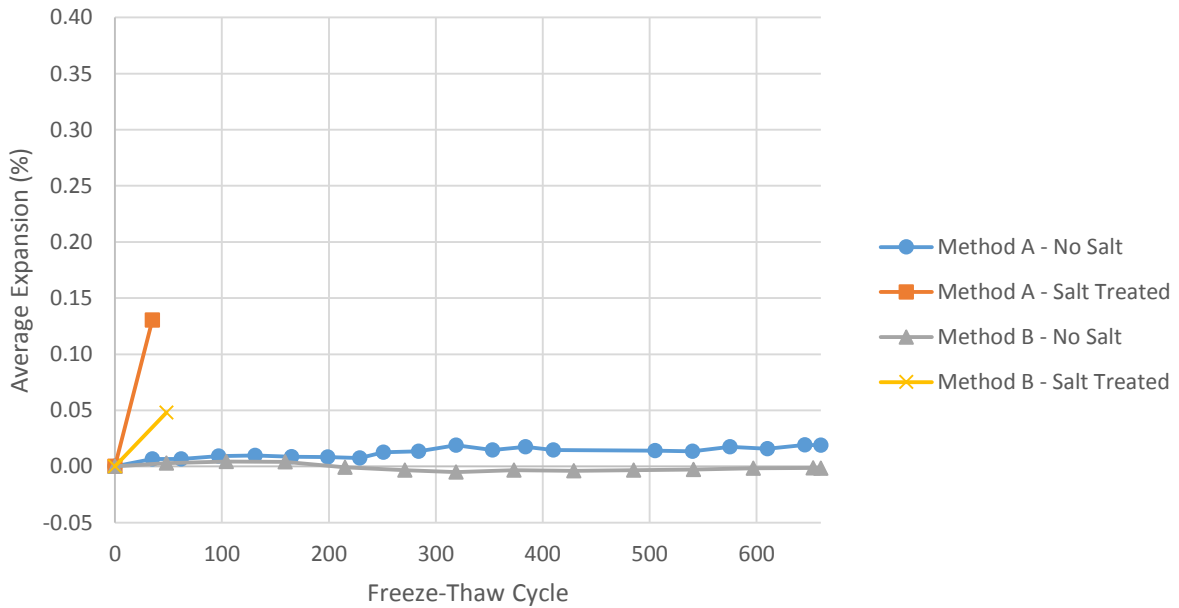
* Salt-treated method B readings recorded and plotted for only one sample

Figure B.28: Average Expansion: Florence Rock Samples
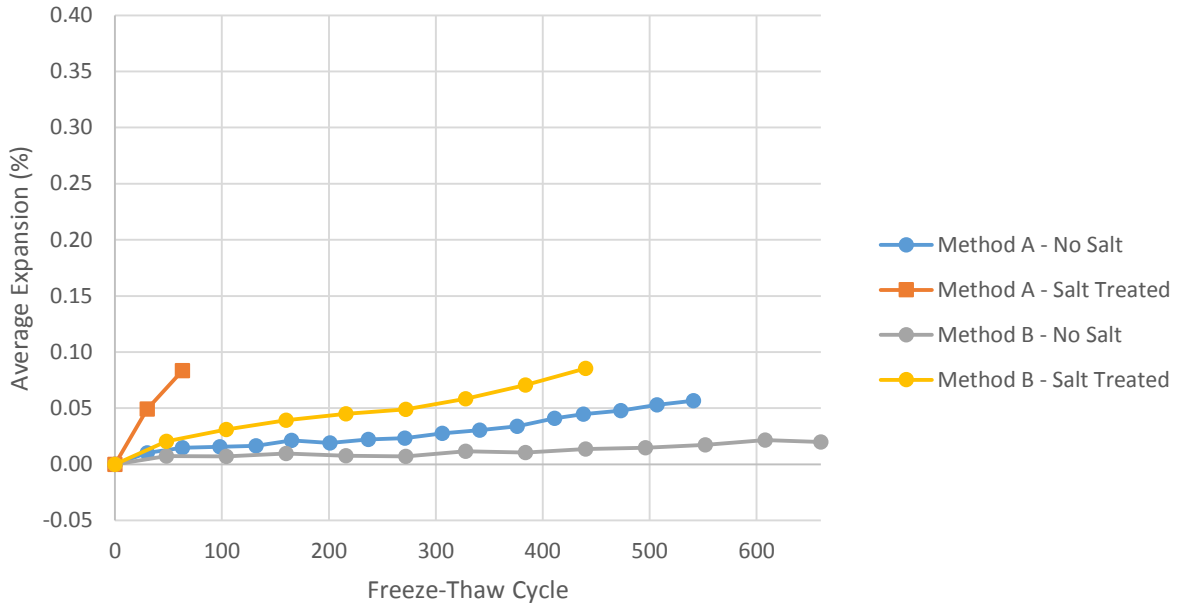
* Non-salt-treated method A samples removed from chamber early to make room for new samples

Figure B.29: Average Expansion: Hamm WB Samples
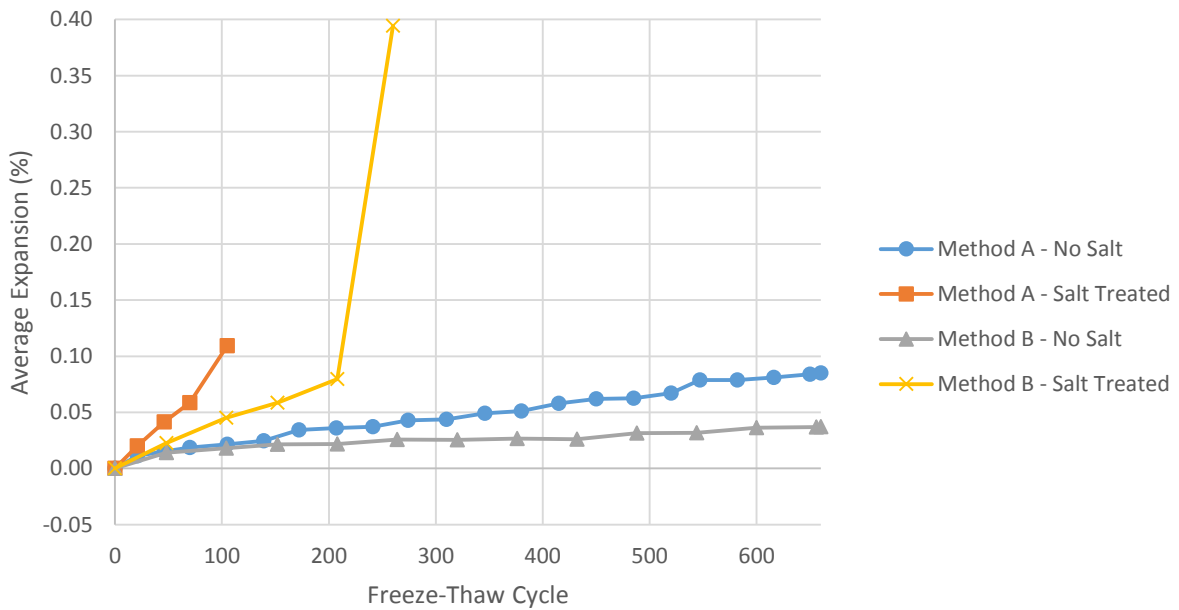
Figure B.30: Average Expansion: Jasper Stone Samples
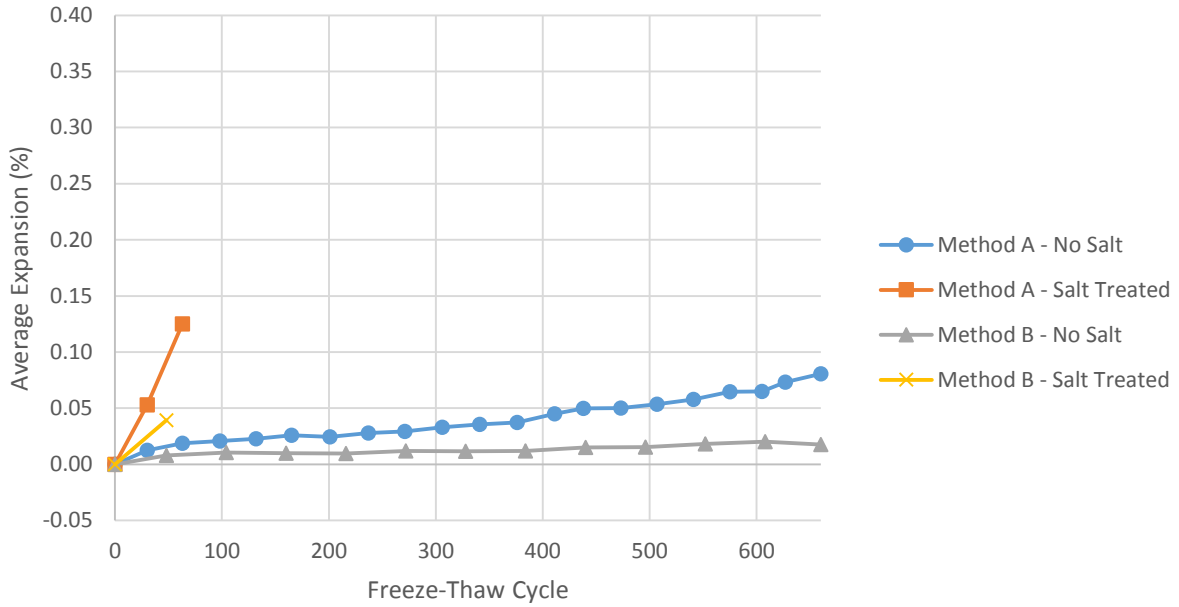
Figure B.31: Average Expansion: Mid-States Materials - Edgerton Samples
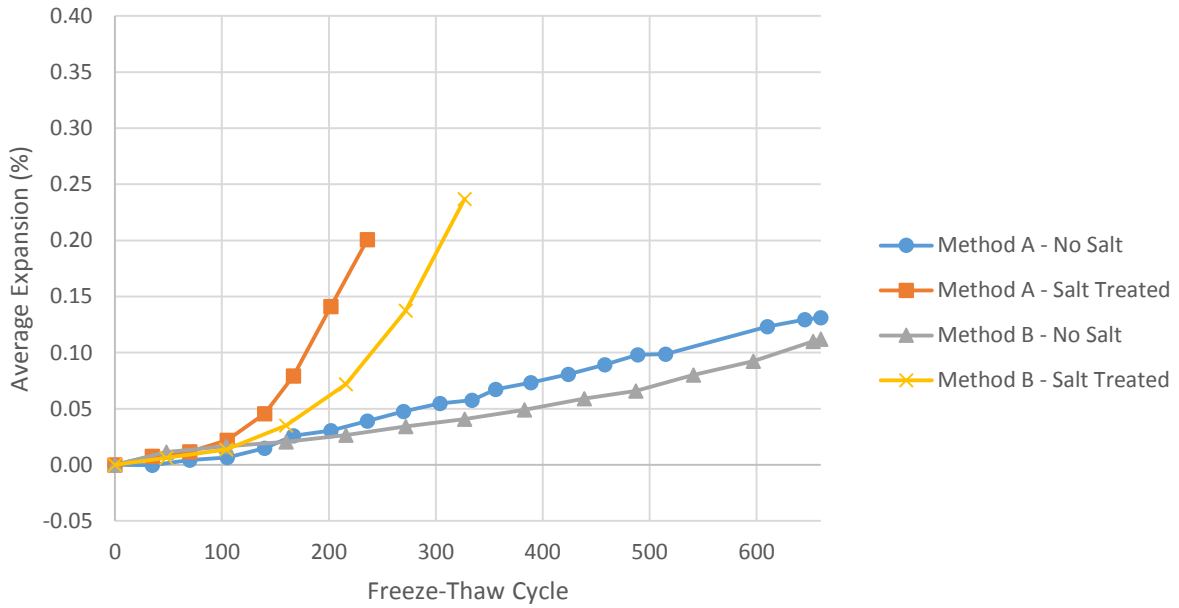
Figure B.32: Average Expansion: Mid-States Materials - Osage, Bed 3 Samples
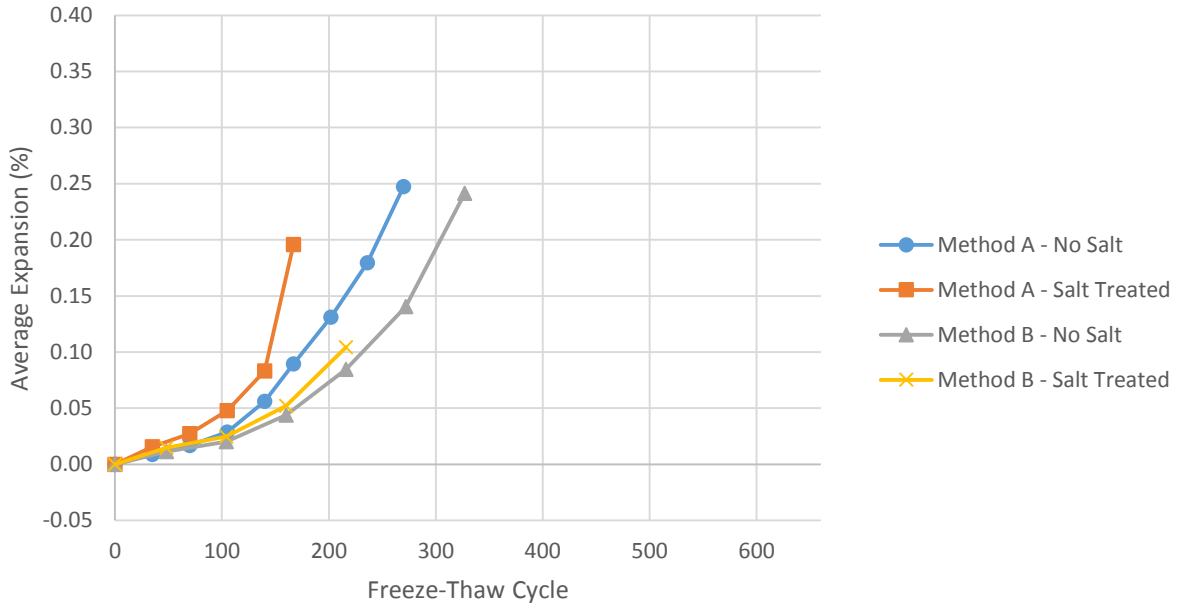
Figure B.33: Average Expansion: Mid-States Materials - Osage, Bed 4 Samples
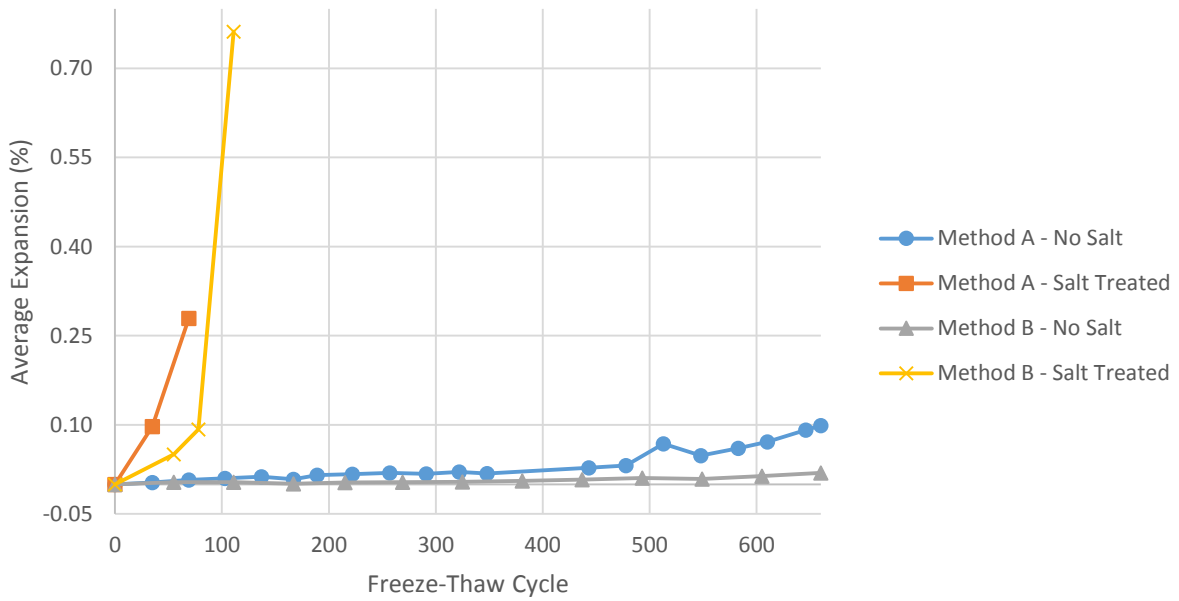
Figure B.34: Average Expansion: Midwest Minerals - Fort Scott Samples
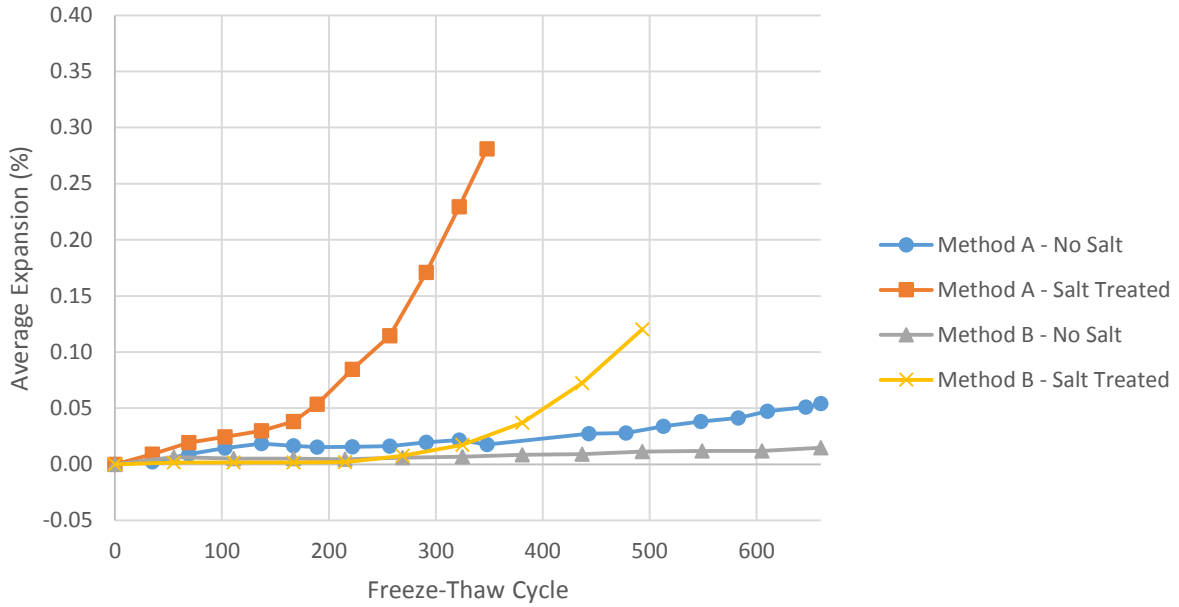
Figure B.35: Average Expansion: Midwest Minerals - Parsons Samples
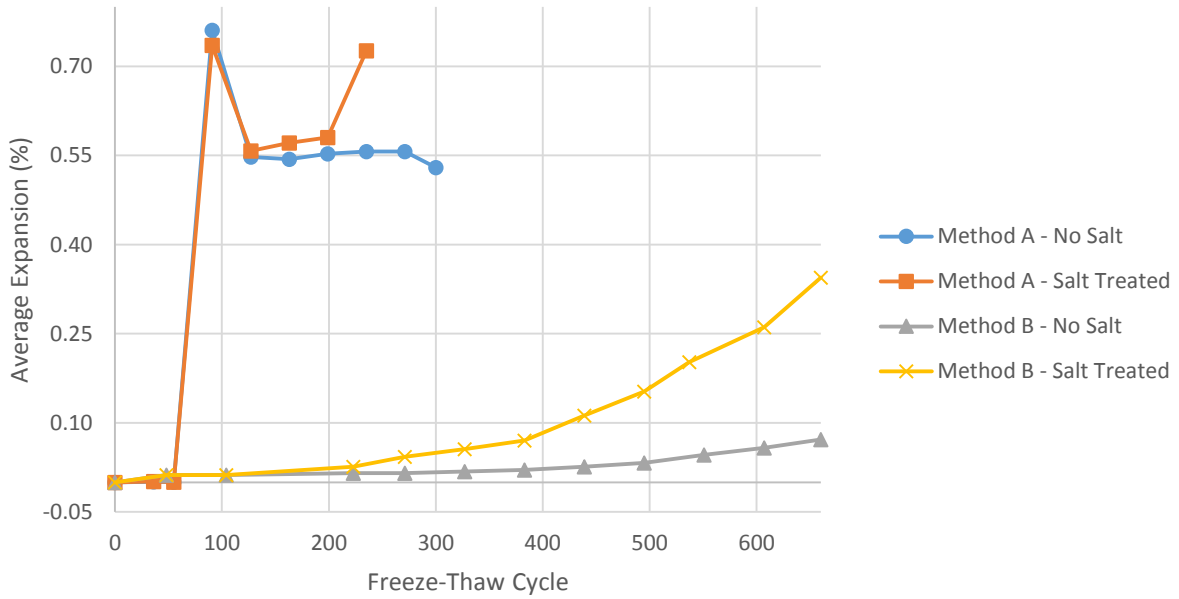
* Method A testing terminated at or before 300 cycles in accordance with ASTM C666 requirements
** Invar bar damaged during Method A testing

Figure B.36: Average Expansion: Penny's Aggregates Samples